3

A short survey of the experimental results from heavy-ion collisions

Rahul Ramachandran Nair

physicsmailofrahulnair@gmail.com

NCBJ

13-12-2021

Online seminar : Selected topics in heavy-ion collisions

Indico page: https://indico.cern.ch/event/1103564/

Few slides inspired from feedbacks & questions

Luminosity measurements in the collisions at the ALICE experiment

Cross-section: $\sigma = N/L_{int}$

1. σ = cross-section of a physical process
2. N = Yield of the physics process
3. $L_{int} = \int L(t)dt$ = integrated luminosity; $L(t)$ = instantaneous luminosity

Measurement methods

1. $L = \dfrac{R_{ref}}{\sigma_{ref}}$: Using the cross-section of a known physical process like Z_0 boson

2. $L = \dfrac{R_{vis}}{\sigma_{vis}} = \dfrac{f_{rev}\mu_{vis}}{\sigma_{vis}}$: Using a visible cross-section σ_{vis} : **This is the method in ALICE**
   - f_{rev} = Accelerator revolution frequency
   - μ_{vis} = Average number of of visible interactions per bunch crossing
   - σ_{vis} = visible cross-section measured experimentally

Luminosity measurements in the collisions at the ALICE experiment

Experimentally: $L = \frac{R_{vis}}{\sigma_{vis}} = \frac{f_{rev}\mu_{vis}}{\sigma_{vis}} = f_{rev}N_1N_2 \bullet \int\int \rho_1(x,y)\rho_2(x,y)dxdy$

1. N_1, N_2 : Bunch intensity
2. ρ = Particle density distribution in transverse plane
3. $\int\int \rho_1(x,y)\rho_2(x,y)dxdy$ = Beam overlap integral

Assuming that factorisation stands

2. $L = \frac{f_{rev}N_1N_2}{h_xh_y}$ where
   - N_1, N_2 : Bunch intensity measured with accelerator instrumentation.
   - $1/h_x = \int \rho_{1,x}(x)\rho_{2,x}(x)dx$, $h_{x,y}$ = effective beam overlap width in x or y direction
   - $h_{x,y}$: **Measured in ALICE with van der Meer (vdM) scans**

Luminosity measurements in the collisions at the ALICE experiment

van der Meer (vdM) scans

It is a dedicated measurement of μ_{vis} vs beam separation

1. Estimate visible rate per bunch crossing
2. Adjust separation distance of each bunch crossing with "Tailored (low μ_{vis} , low intensity, well-spaced bunches " running conditions

- Scan horizontal (x) or vertical (y) direction, while fixing the other direction in the head-on position

3. Usually done couple of times a year.

$$L = \frac{f_{rev} N_1 N_2}{h_x h_y}$$

$h_{x,y}$: The area under the curve normalised by its peak value, obtained during the horizontal (and vertical) scans.

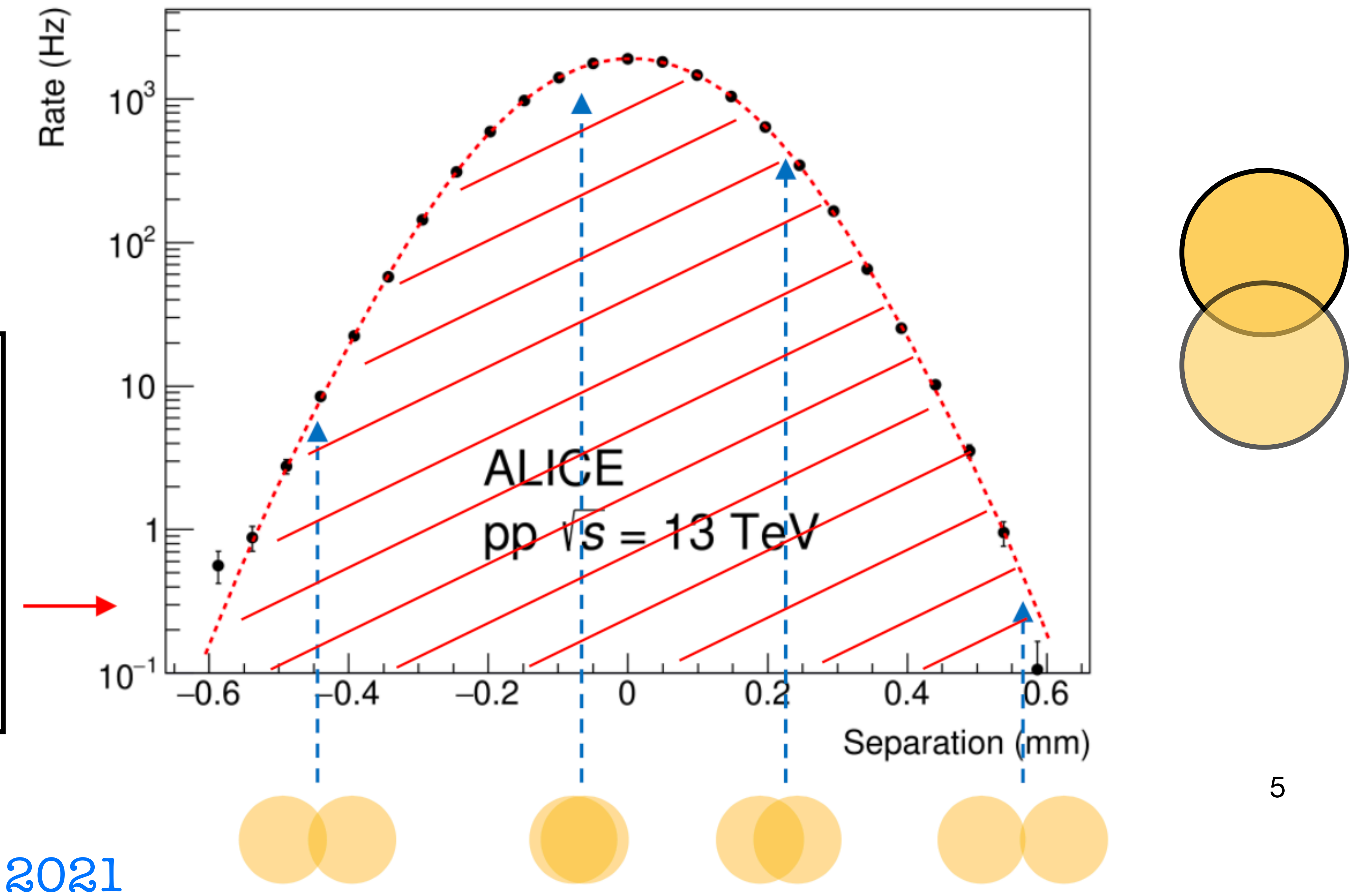

ALICE-PUBLIC-2021-005 Picture Courtesy: Chong Kim in HADRON 2021

LHC Beam status

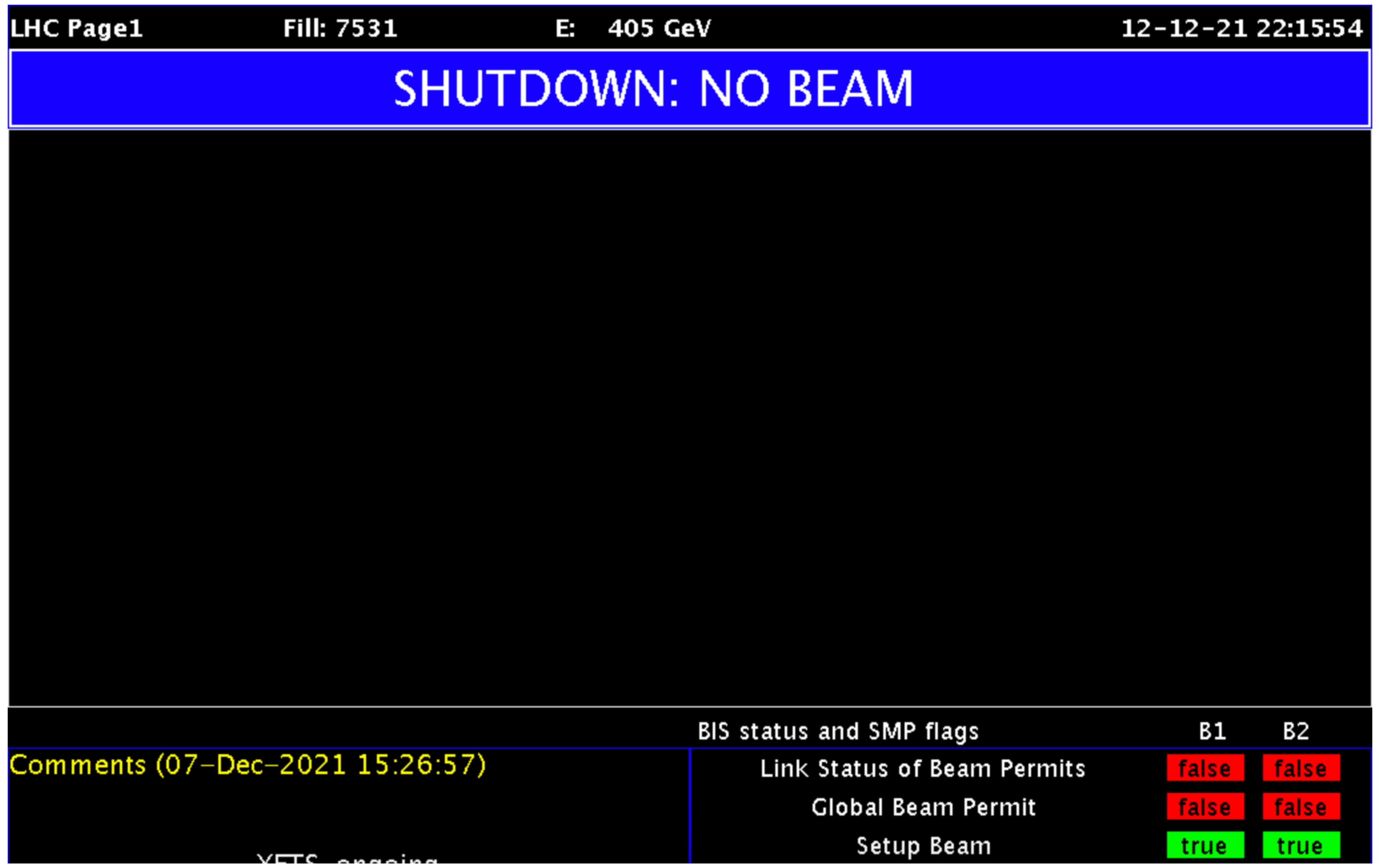

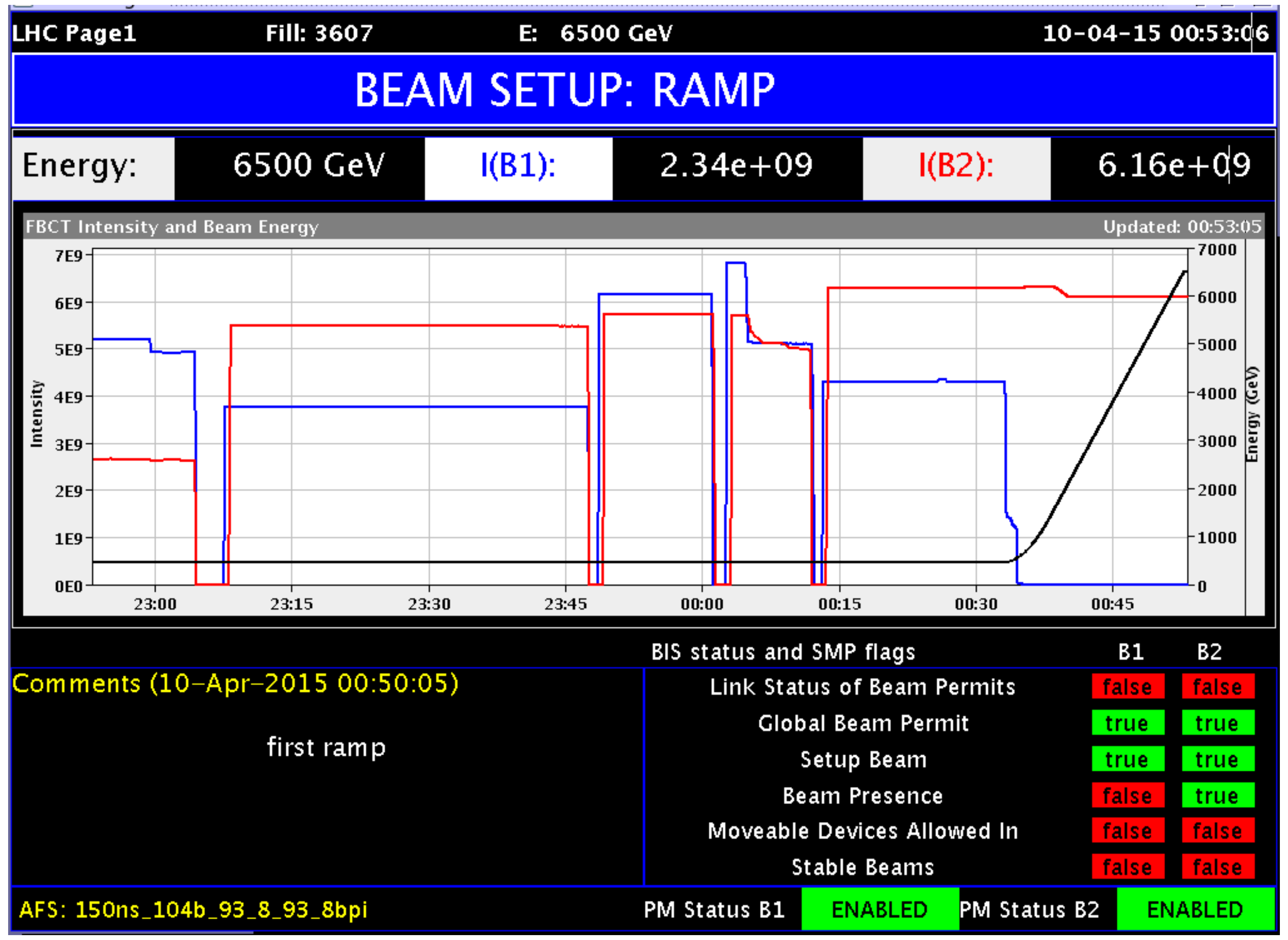

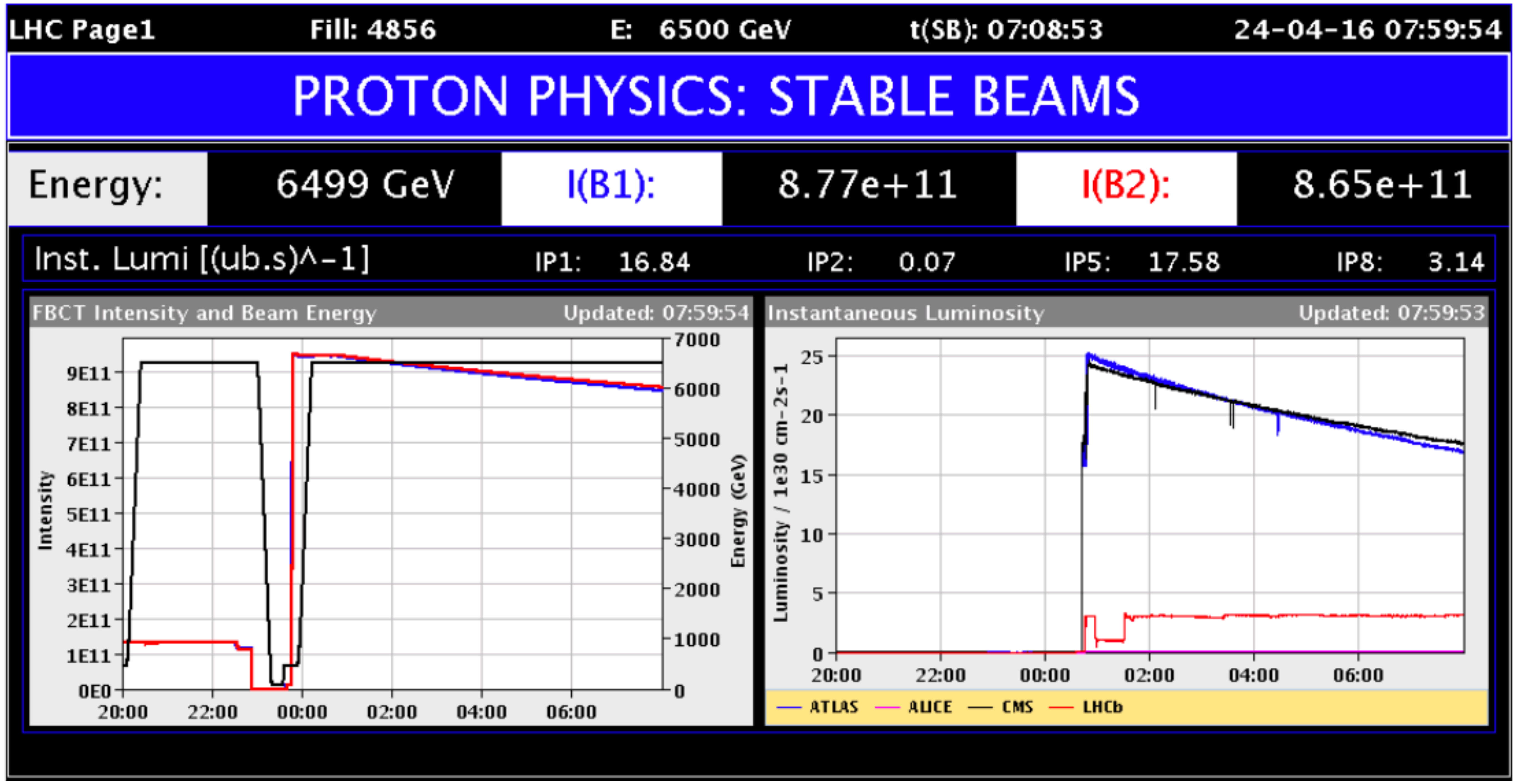

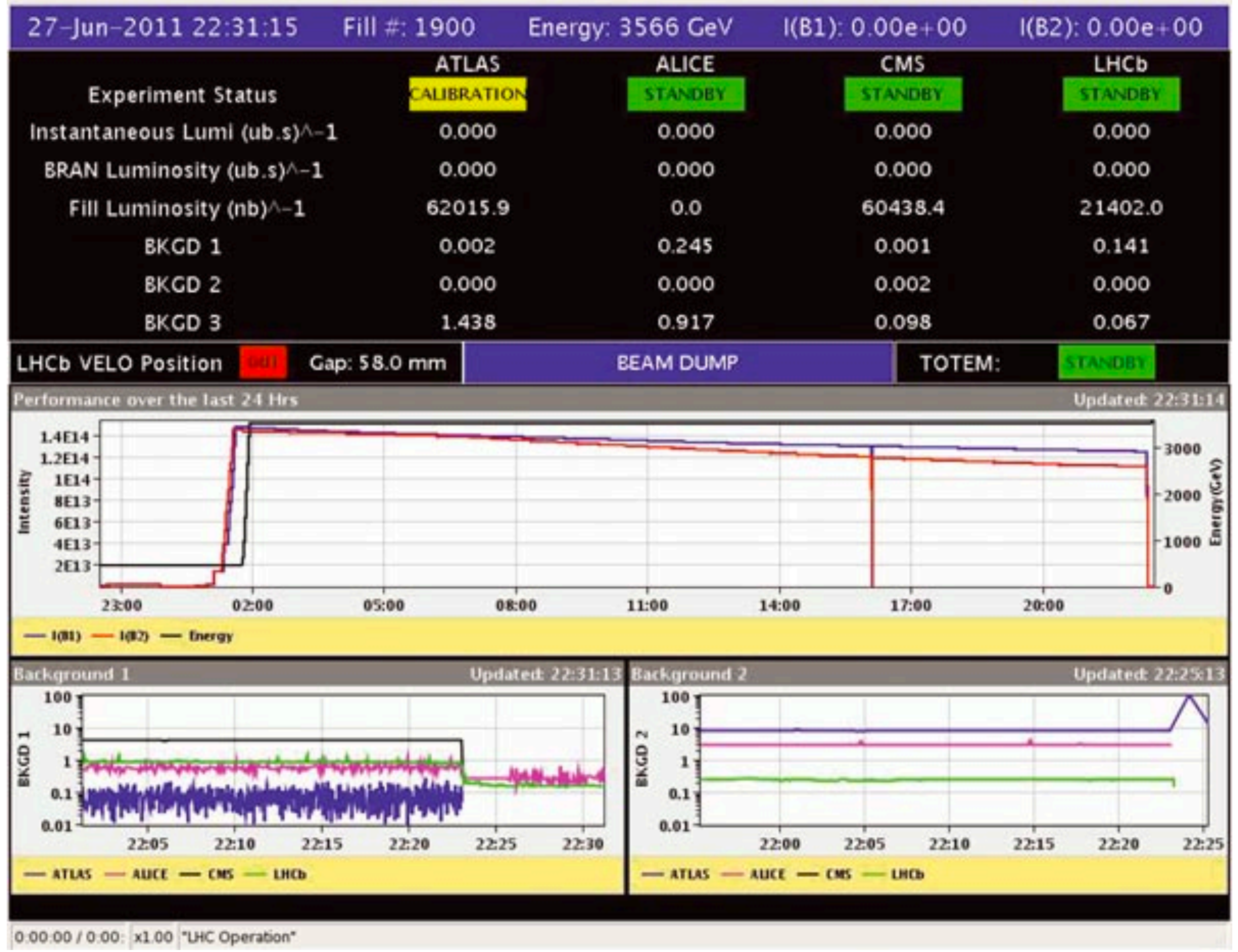

https://op-webtools.web.cern.ch/vistar/vistars.php

Collision systems in Run-1 and Run-2 at LHC

Run Periods

Run 1. : 2010 - 2013

Run 2. : 2015 - 2018

Run 3. : 2021 (Ongoing- started few weeks ago)

Collision systems

Large

1. Pb-Pb collisions : $\sqrt{s_{NN}} =$ 2.76, 5.02 TeV
2. Xe-Xe collisions : $\sqrt{s_{NN}} =$ 5.44 TeV

Small

3. p-Pb collisions : $\sqrt{s_{NN}} =$ 5.02, 8.16 TeV
4. pp collisions : $\sqrt{s} =$ 0.9, 2.76, 5.02, 7, 13 TeV

Proposal for ion running in Run 3-4 from the heavy ion community

Year	Systems, $\sqrt{s_{NN}}$	Time	L_{int}
2021	Pb–Pb 5.5 TeV	3 weeks	2.3 nb^{-1}
	pp 5.5 TeV	1 week	3 pb^{-1} (ALICE), 300 pb^{-1} (ATLAS, CMS), 25 pb^{-1} (LHCb)
2022	Pb–Pb 5.5 TeV	5 weeks	3.9 nb^{-1}
	O–O, p–O	1 week	500 μb^{-1} and 200 μb^{-1}
2023	p–Pb 8.8 TeV	3 weeks	0.6 pb^{-1} (ATLAS, CMS), 0.3 pb^{-1} (ALICE, LHCb)
	pp 8.8 TeV	few days	1.5 pb^{-1} (ALICE), 100 pb^{-1} (ATLAS, CMS, LHCb)
2027	Pb–Pb 5.5 TeV	5 weeks	3.8 nb^{-1}
	pp 5.5 TeV	1 week	3 pb^{-1} (ALICE), 300 pb^{-1} (ATLAS, CMS), 25 pb^{-1} (LHCb)
2028	p–Pb 8.8 TeV	3 weeks	0.6 pb^{-1} (ATLAS, CMS), 0.3 pb^{-1} (ALICE, LHCb)
	pp 8.8 TeV	few days	1.5 pb^{-1} (ALICE), 100 pb^{-1} (ATLAS, CMS, LHCb)
2029	Pb–Pb 5.5 TeV	4 weeks	3 nb^{-1}
Run-5	Intermediate AA	11 weeks	e.g. Ar–Ar 3–9 pb^{-1} (optimal species to be defined)
	pp reference	1 week	

9th LHC Operations Evian Workshop, Evian Les Bains, France, 30 Jan - 1 Feb 2019, pp.267-271

CDS: http://cds.cern.ch/record/2750301

ALSO: arXiv:1812.06772

Goal

Explore the experimental results from heavy-ion collisions and understand their implications

We focus on: LHC Run-1 & Run-2 published results. More recent results are expected to be presented in the coming'Quark Matter 2022' conference.

Brief history from early 2000s

- The relativistic heavy ion collisions in (RHIC) at BNL have shown that a system is created in which particles are produced with a large degree of coherence. (Unlike lot of pp)
- The obtained energy densities exceed those values above which lattice QCD calculations predict the formation of a QGP (which is $\sim 1\mathrm{GeV}/\mathrm{fm}$)
- The measured particle spectra are reproduced by viscous relativistic hydrodynamics:
  1. The hydrodynamic regime is assumed to hold at short times after the collision
  2. The shear viscosity over entropy density ratio is small.

Nucl. Phys. A 750, 30 (2005)

Annu. Rev. Nucl. Part. Sci. 56, 93 (2006)

F. Karsch, Lect. Notes Phys. 583, 209 (2002) (hep-lat/0106019).

Brief history from early 2000s

- The yields and expected back-to-back correlations of high- energy partons are strongly suppressed, compared to expectations from extrapolations from pp collisions& pQCD calculations.

- From these findings, it was argued that a deconfined partonic medium behaves like an almost ideal liquid was formed very shortly after the collision which is very opaque to the high-energy partons(quarks and gluons) passing through it.

At LHC, the available centre of mass energy is large by an order of magnitude. One can expect that the heavy-ion collisions at LHC will to lead to the creation of a denser, hotter, longer-lived medium with a much more abundant rate of various rare particles that can be used to probe it.

Lets go through what we have seen so far in the heavy-ion collisions at LHC.

This talk is largely inspired from the following references

1. Eur. Phys. J. Plus (2016) 131: 52 (Compilation of Run 1 results)

2. Selected ALICE papers (Run 2 results)

3. Presentations by my colleagues, friends and intelligent people who are unknown to me (cited on slides).

Organisation of the results

- Hadron multiplicity and hadrochemistry
- Elliptic and higher harmonic flows
- Correlations and femtoscopy

Soft probes

- Jet physics
- Heavy flavour physics
- Strangeness enhancement
- Charmonium suppression
- Direct photon analysis

Hard & EM probes

- Some of the most recent results
- Future of heavy-ion collision programs

Hadron multiplicity

- Measurements of the charged hadron multiplicity as a function of the centrality of the collision and of the pseudorapidity → Sensitive to the relative contribution from hard and soft processes.

- Hard scattering are expected to be proportional to the number of nucleon-nucleon collisions and soft processes are usually assumed to be proportional to the number of participant nucleons.

- Multiplicity measurements are sensitive to the modelling of the initial state of the collision.

Hadron multiplicity

Observation: A steep rise in the charged hadron multiplicity density per participant pair when moving from top RHIC energy to the LHC. It is understood as an effect due to the significant increase of the contribution of hard processes.

At RHIC energies: The multiplicity per colliding nucleon pair have a mild increase with the collision centrality [1-5].

At LHC energy : [6-8] Similar observation with less than a factor 2 from peripheral (75–80%) to central (0–2%) events.

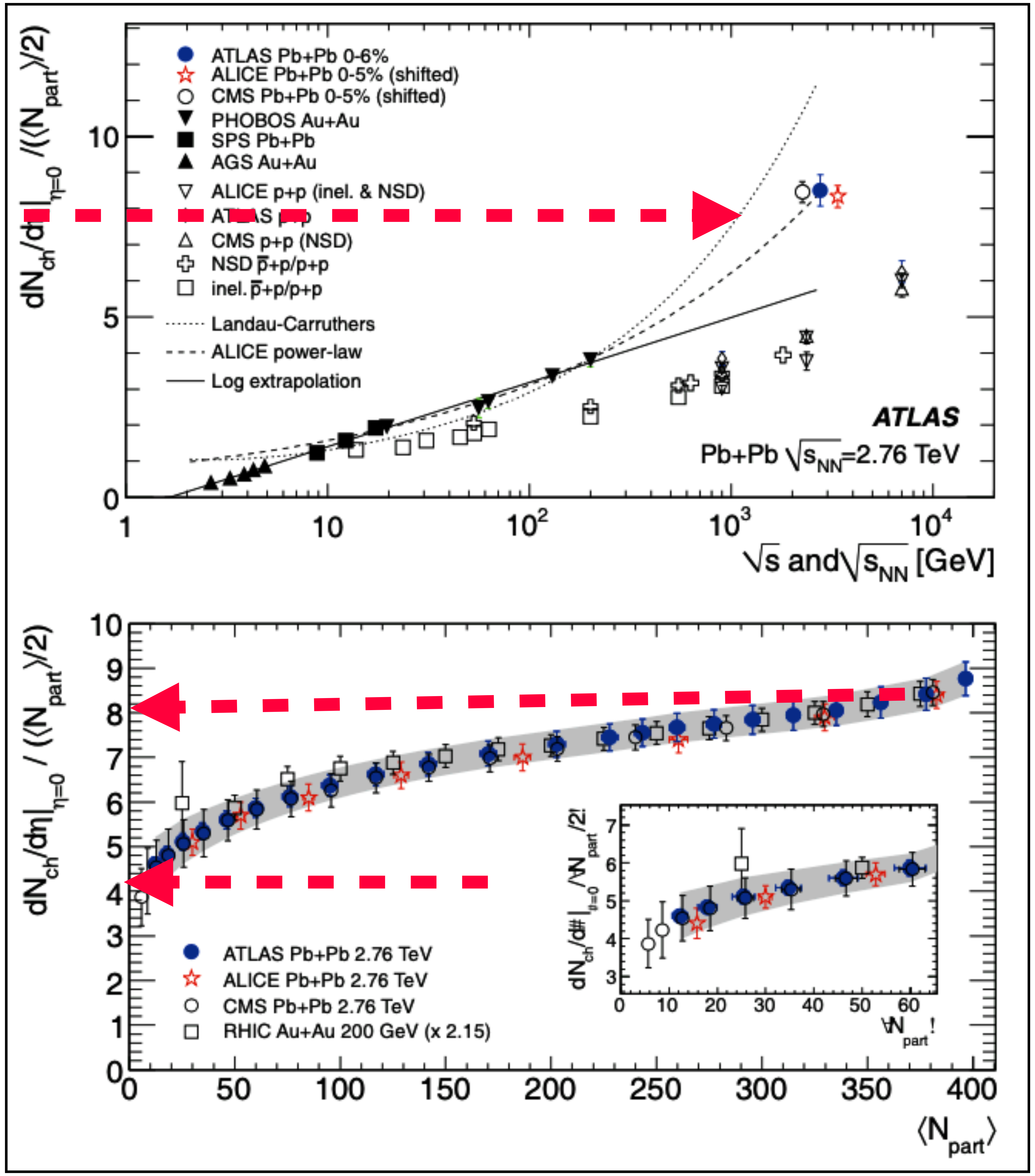

Hadron multiplicity: Comparison with theoretical predications

Two main classes of calculations have been compared to the data:

1. **Two-component models :** Based on a combination of pQCD processes and soft interactions [9-10]

2. **Saturation models :** Includes various parametrisation for the energy and centrality dependence of the saturation scale [11-13].

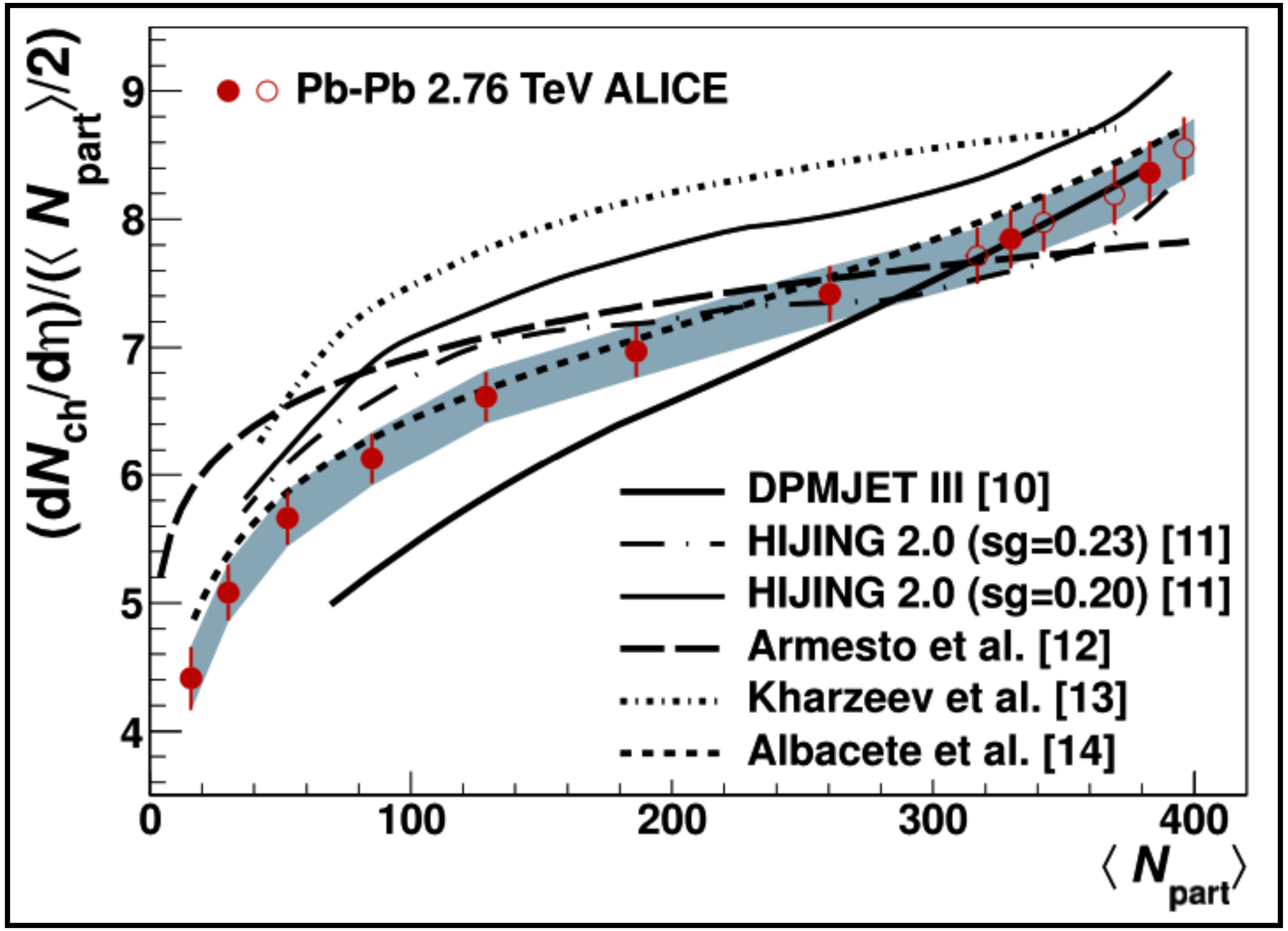

Both classes of models were able to qualitatively predict the observed behaviour.

Hadron multiplicity

η distribution of the transverse energy E_T

~ 2.1 TeV for central Pb-Pb collisions and it has a stronger increase (a factor 3.07 ± 0.24) than the charged-particle multiplicity (2.17 ± 0.15) when moving from RHIC to LHC energy.

This means that there is a significant increase of the $< E_T > / particle$

Invoking Bjorken

We get $\varepsilon = 14$ GeV/fm^3 for a time $\tau_0 = 1$ fm/c. Such a value is **larger by more than one order of magnitude** than the estimated for the critical energy density for the phase transition to a deconfined state

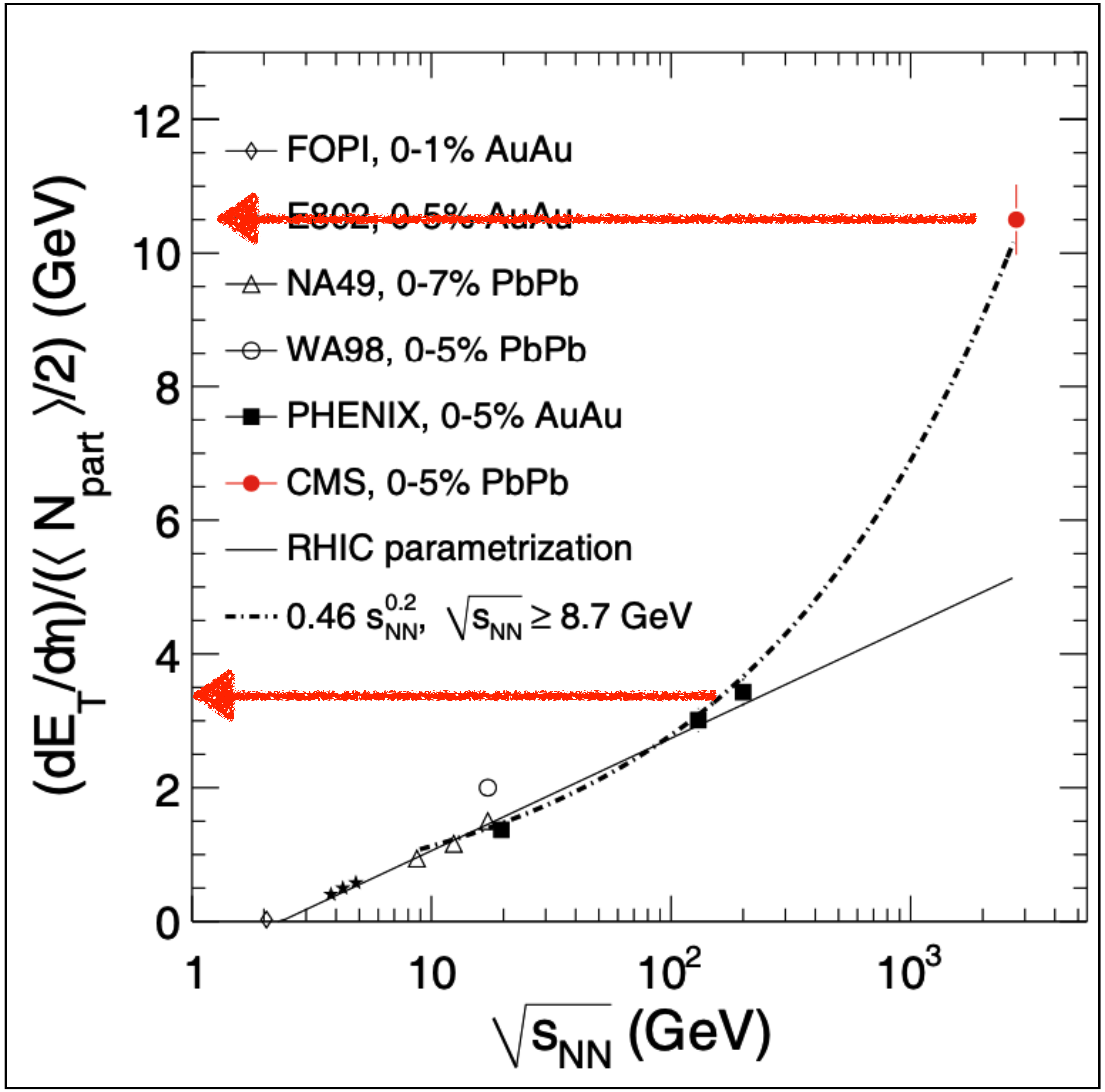

Hadron multiplicity: Centrality dependence of the η density

Range: $-5.0 < \eta < 5.5$ range [14-15]

Model Comparison: The Colour-Glass Condensate (CGC) model well describes the data in its limited domain of applicability, while no model is able to satisfactorily reproduce both shape and absolute values of the yields over the whole η-range.

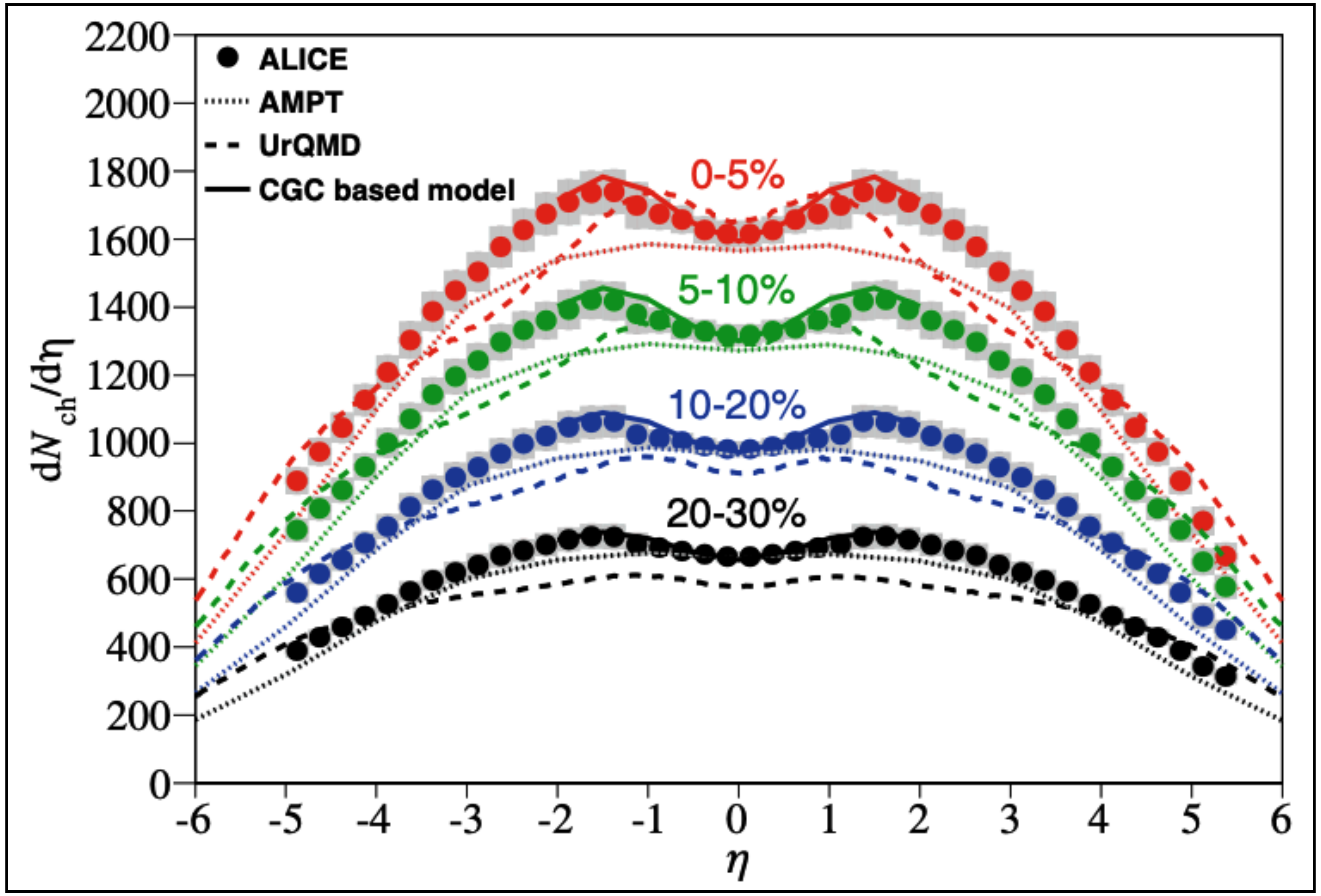

Total integrated charged multiplicity: $N_{ch} = 17165 \pm 772$ for most central collisions

Evolution with centrality is identical to the one observed at RHIC (with 2.67 scaling factor) [103]

Hadrochemistry

Observation: The ϕ mesons exhibit a relative enhancement with respect to pions with increasing pT

It suggests that a mass effect is present as resulting from hydrodynamic calculations.

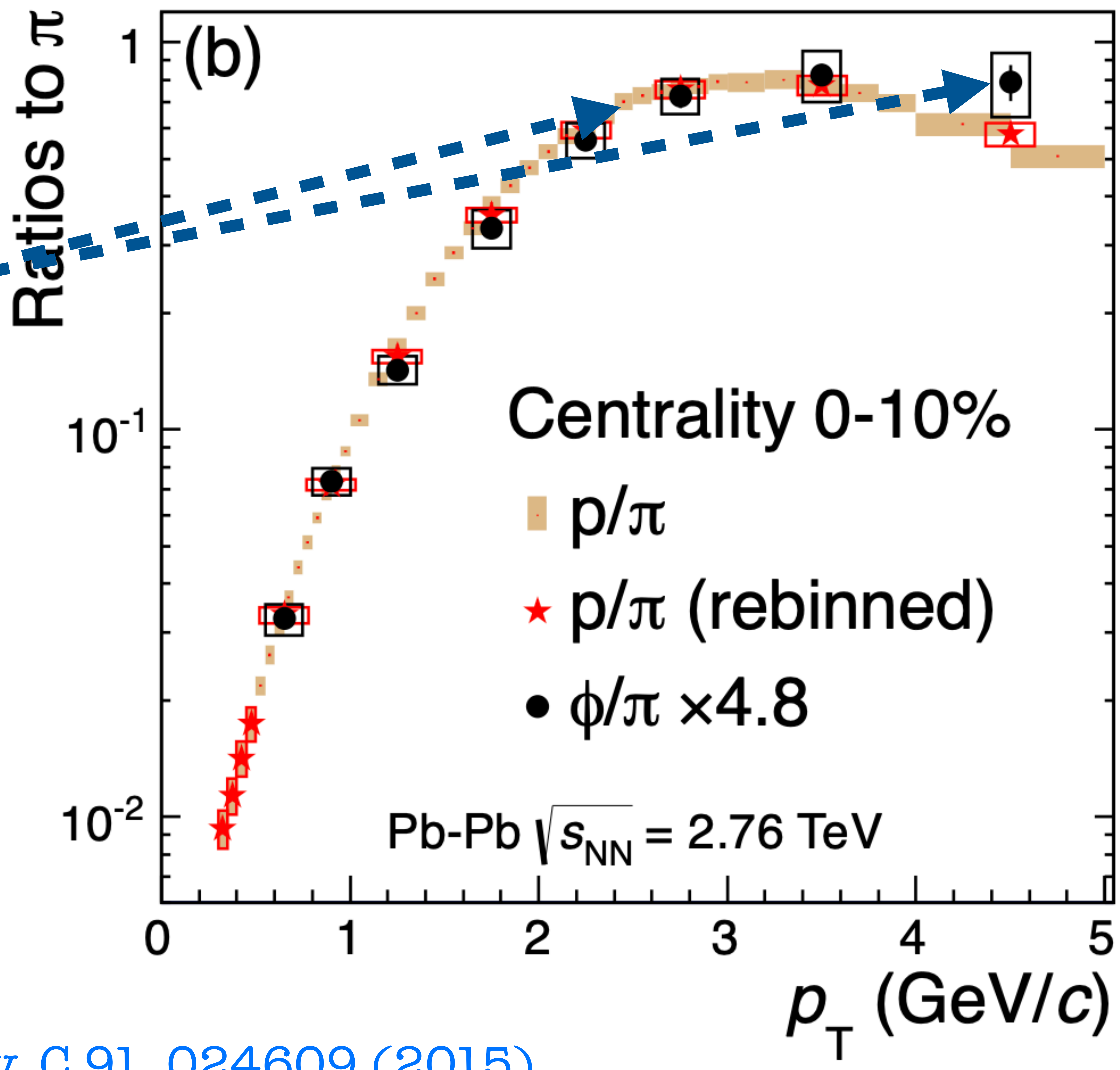

ALICE Collaboration. Phys. Rev. C 91, 024609 (2015)

Hadrochemistry: Nuclear Modification Factor

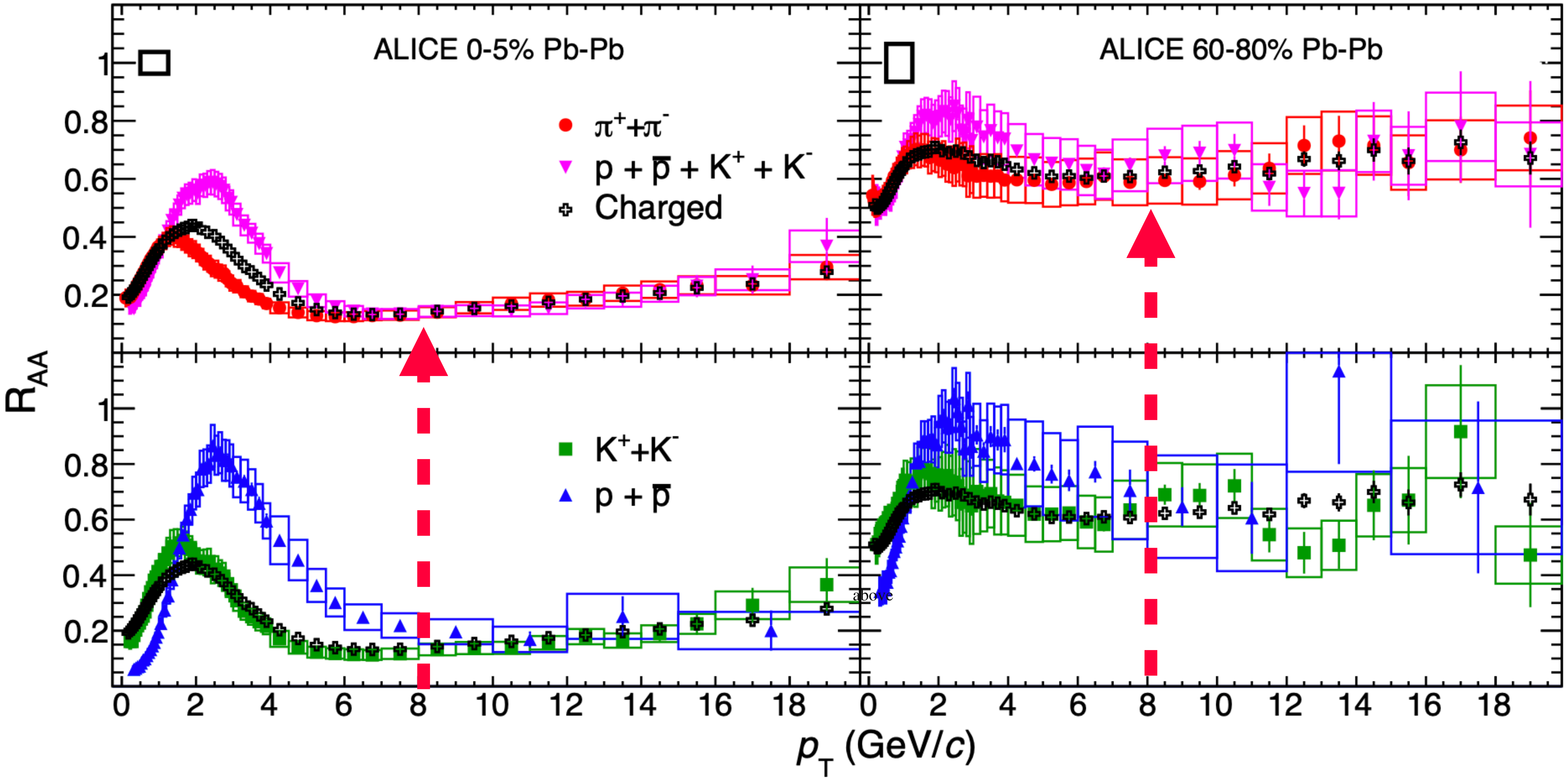

- **Observation:** For all centralities, the nuclear modification factors for all species, and the relative chemical composition in pp and Pb Pb, **become equal above pT ~ 8 GeV/c** [16-17]
- **As at RHIC [18-20]:** It indicates that hadronisation of such particles is not affected by the medium and that the origin of the suppression is partonic.
- Gives strong constrains on ideas that consider non- perturbative [104] or perturbative modifications of hadronisation inside the medium [21].

Elliptic flow

At RHIC [22]: v2 values at low pT in good agreement with ideal hydrodynamic calculations in semi-central and central collisions

Argument: QGP phase behaving as an ideal liquid [23-26].

A hierarchy of v2: was observed for identified particles, with higher values, at a given pT, for lighter particles [27].

Understood in terms of : Radial flow effect

Models including a partonic phase with a harder equation of state (a higher speed of sound) with respect to the hadronic phase, showed quantitative agreement with the results [28].

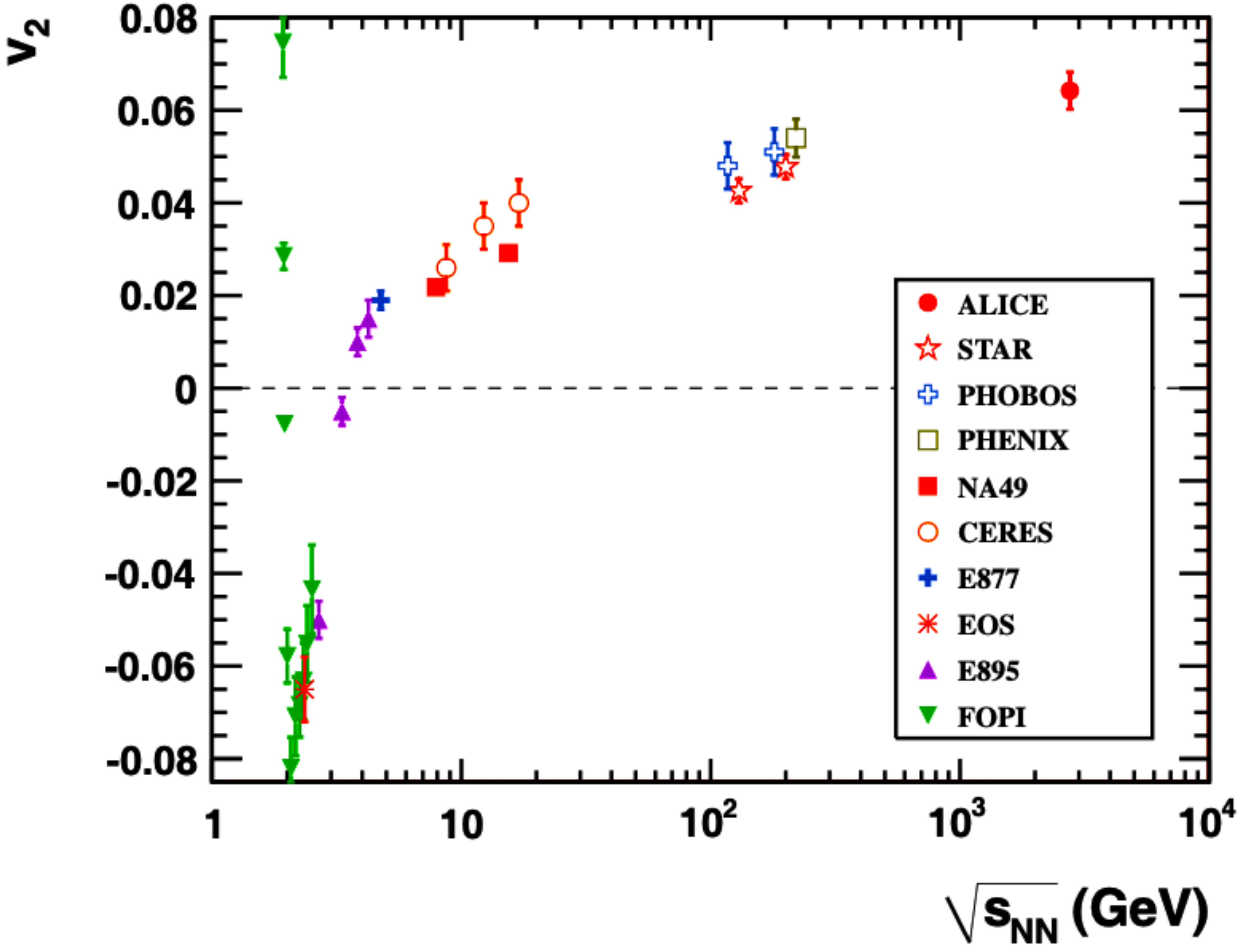

Elliptic flow

At fixed p_T, the observed values of elliptic flow are similar at RHIC and LHC which extends down to low RHIC energies [29-32].

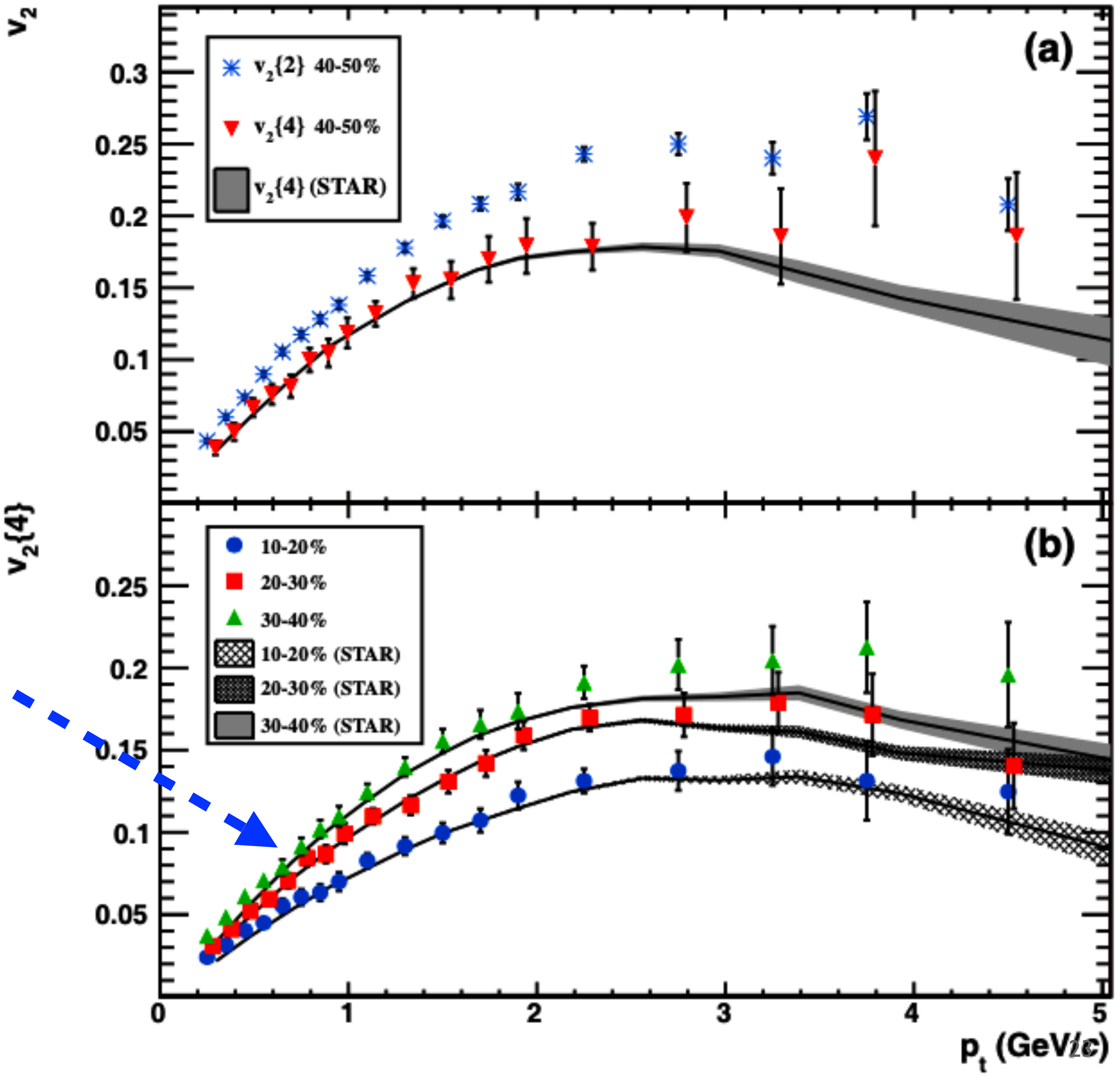

Elliptic flow at high p_T

The interpretation in terms of collective effects does not hold any more

The observed non-zero v_2 : Related to the different path length in the medium for particles emitted in-plane and out-of-plane, which induces a different energy loss.

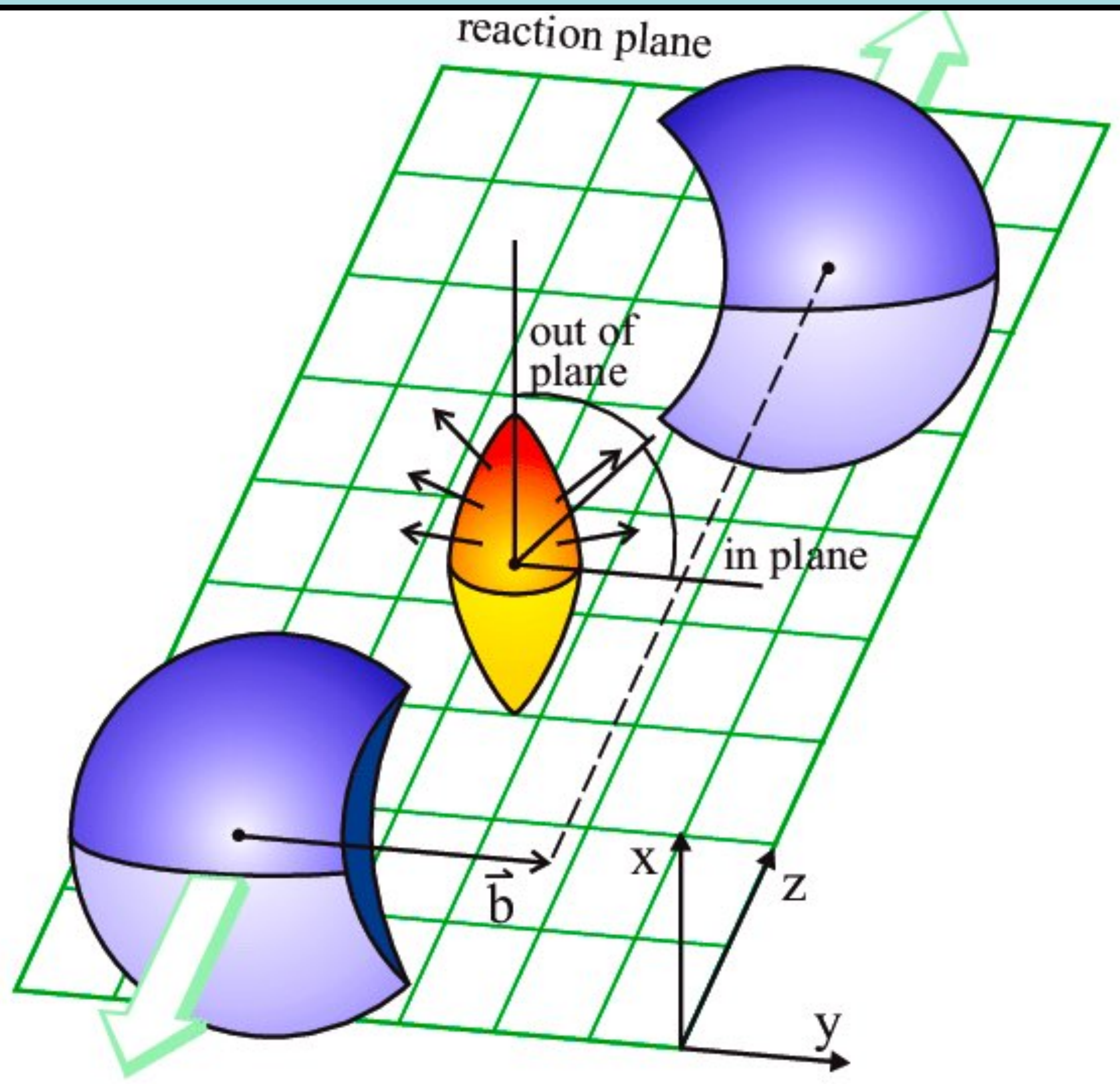

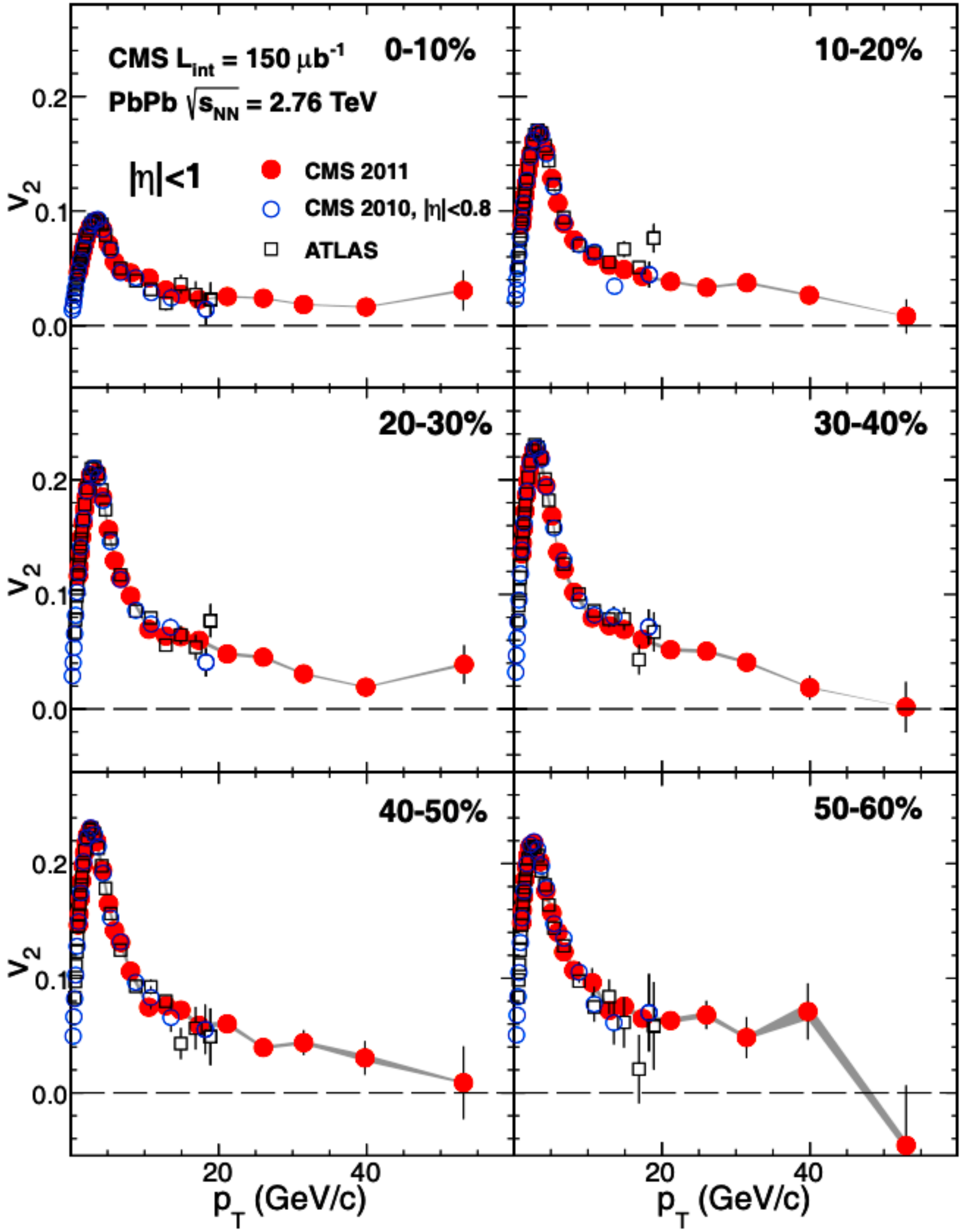

Elliptic flow of identified particles

Detailed studies of the elliptic flow of identified particles have also been carried out in ALICE [33]

v_2 **Mass ordering @ ALICE:** Comparisons with hydrodynamical calculations (VISHNU [34]) shows a similar mass ordering as at RHIC ($\eta/s = 0.16$)

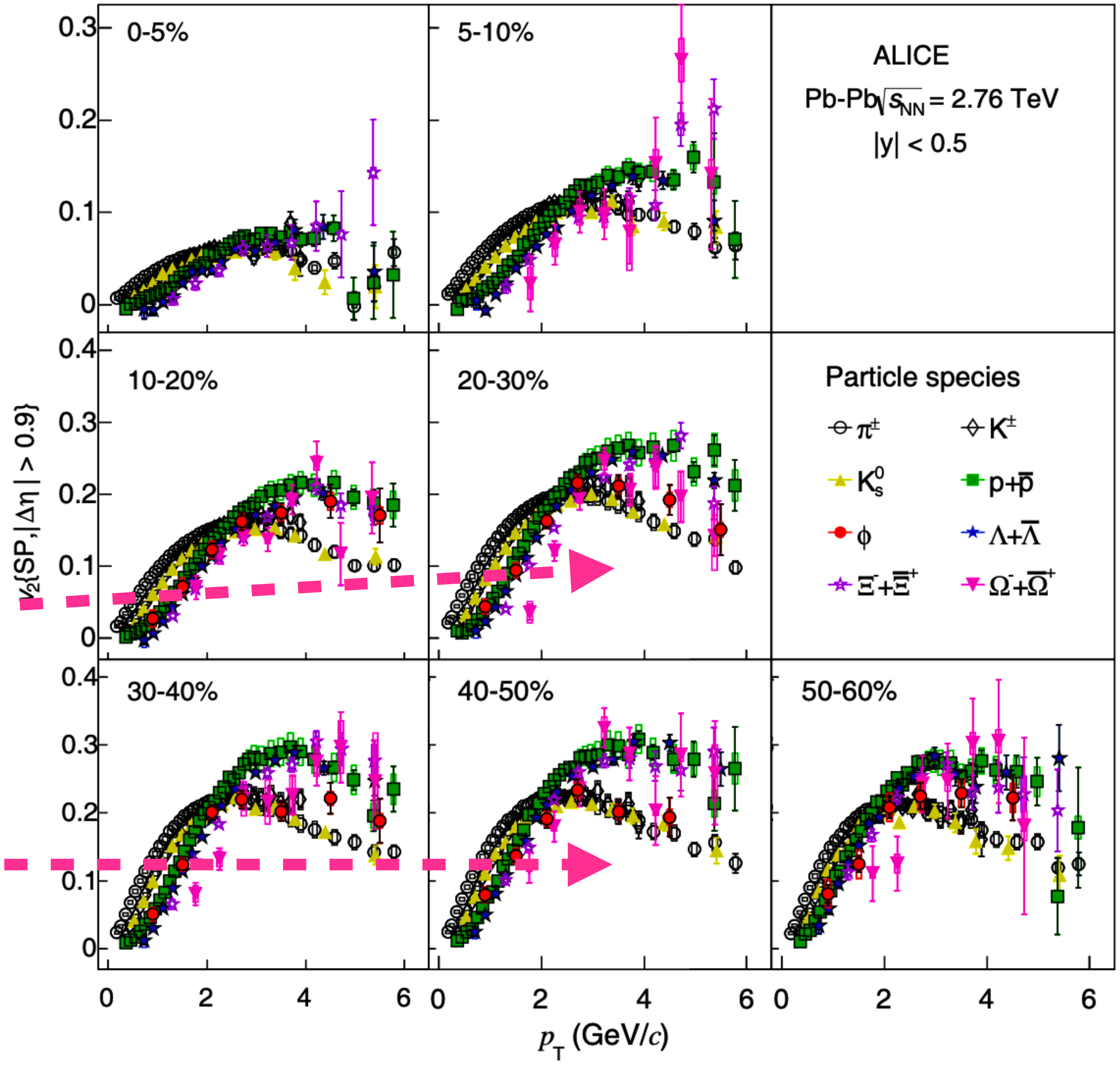

Elliptic flow in small systems

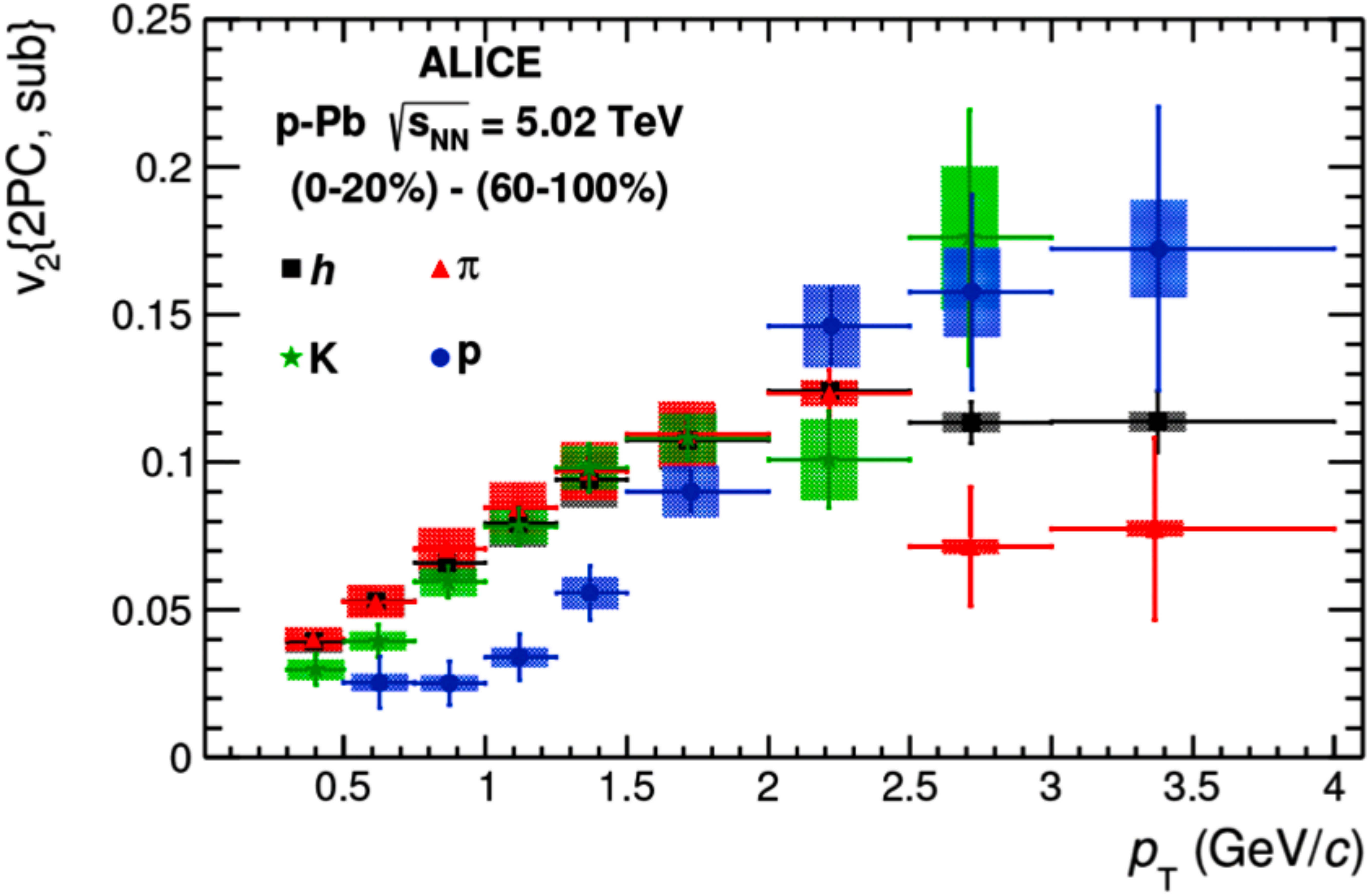

- **Identified particle v2 in pPb collisions:** Here, for high-multiplicity pPb collisions (0–20%) one observes [35] a mass ordering similar to the one seen in PbPb.
- A collective behaviour also in pPb collisions at LHC energies.

Higher harmonic flows

Measurements up to v_6 has been made at ATLAS [36–38].

It can constrain the initial conditions of the collision key to the determination of the viscosity.

The measured flow coefficients is more or less centrality independent → Consistent with an anisotropy primarily associated with fluctuations in the initial geometry.

The approximate scaling $v_n(p_T) \propto v_2(p_T)$: Expected from a hydrodynamic scenario has been observed except for the most central events.

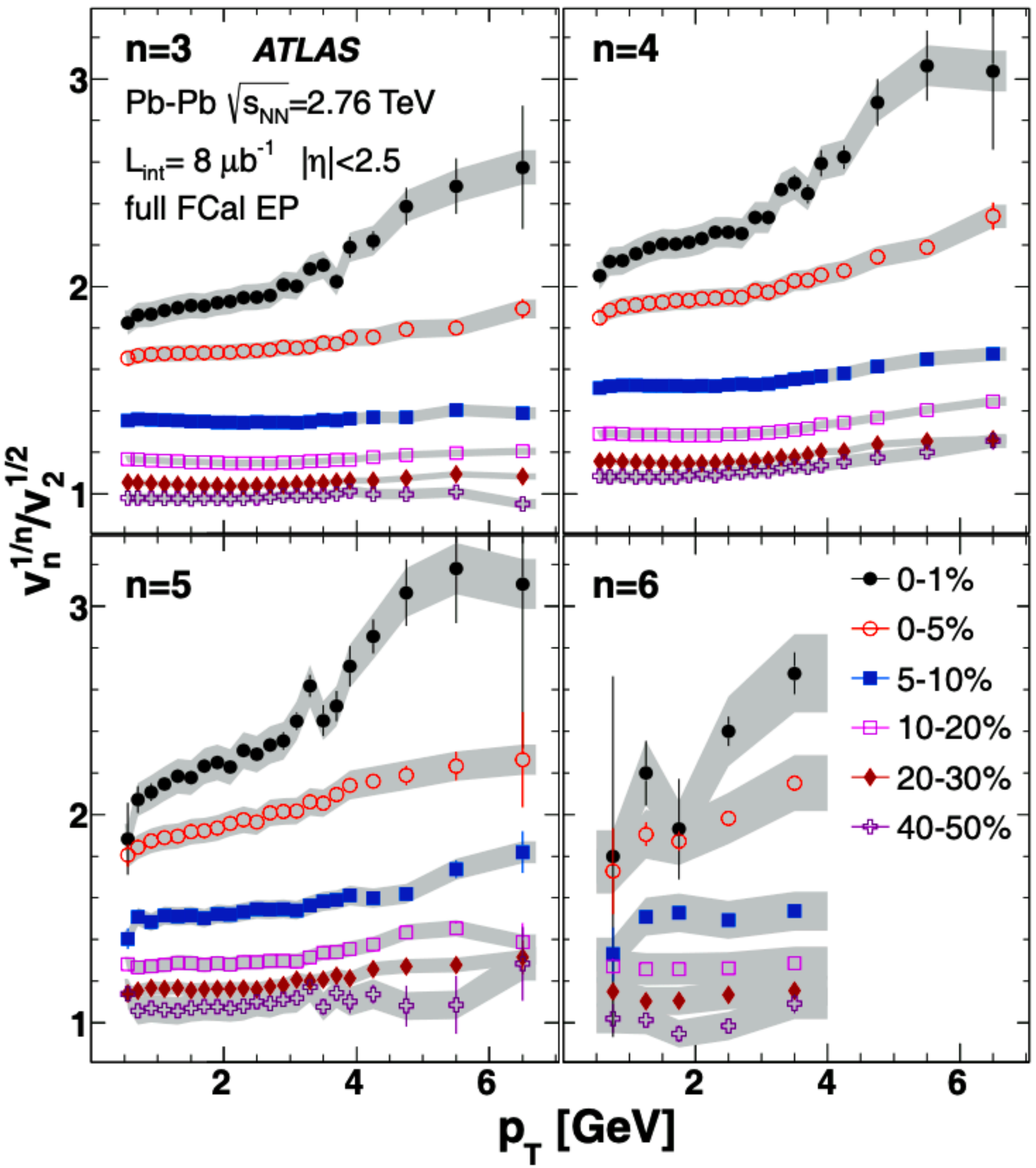

Correlations

Simple causal arguments: Correlations must have their origin in the initial stages of the collisions [39].

In AuAu collisions at RHIC [40-41]: A large correlation in the difference in rapidity and azimuthal angle for pairs of particles

Ridge: Correlation extended along several units of rapidity and collimated in azimuth at 0 and 180 degrees was observed for triggered and untriggered analysis, with a peak at (0, 0) in (Δη,Δϕ).

We observe similar structures in the heavy-ion collisions at LHC

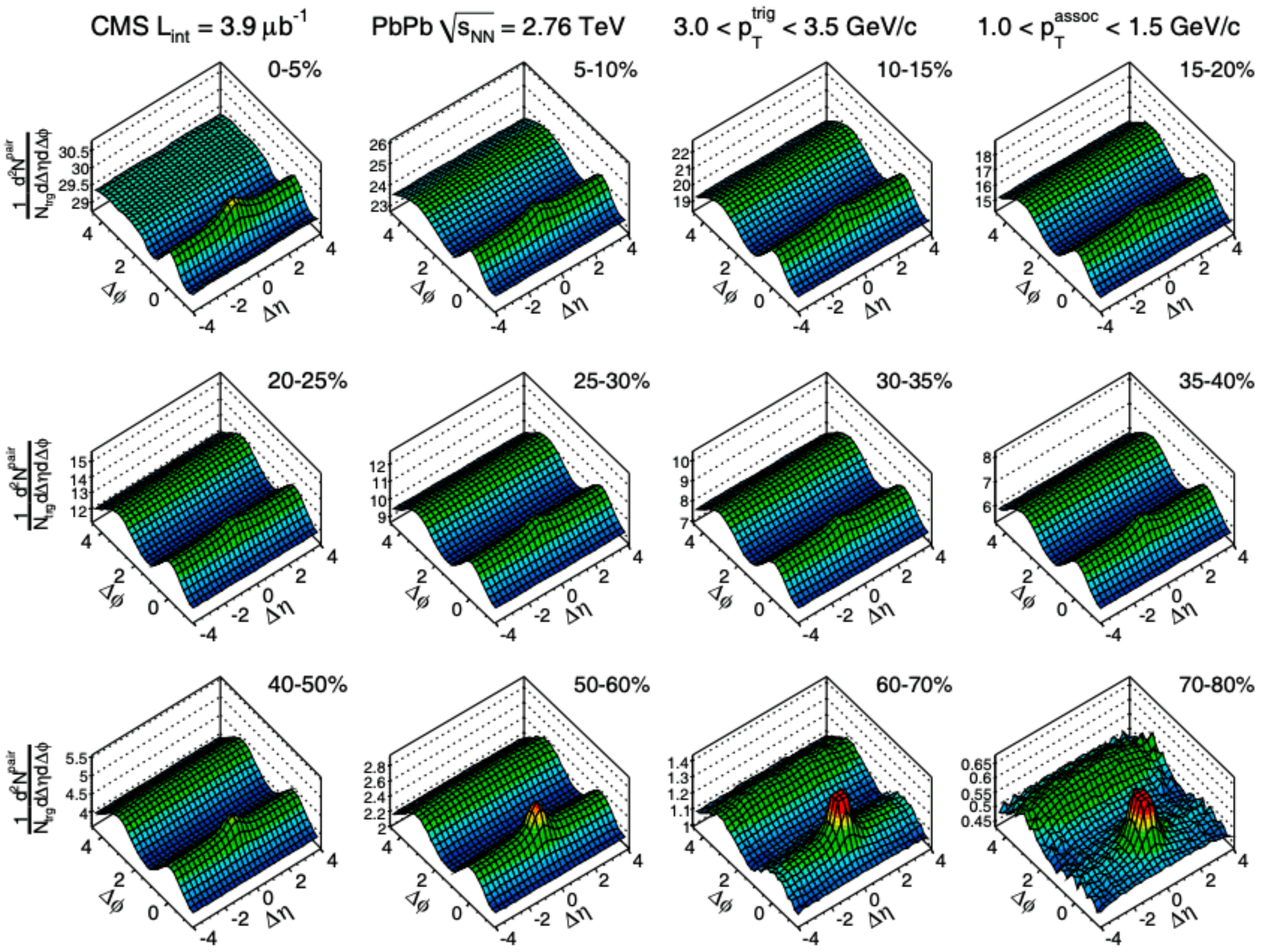

Correlations

ALICE showed that the structure in azimuth can be characterised by a Fourier decomposition even for pairs with large rapidity separations

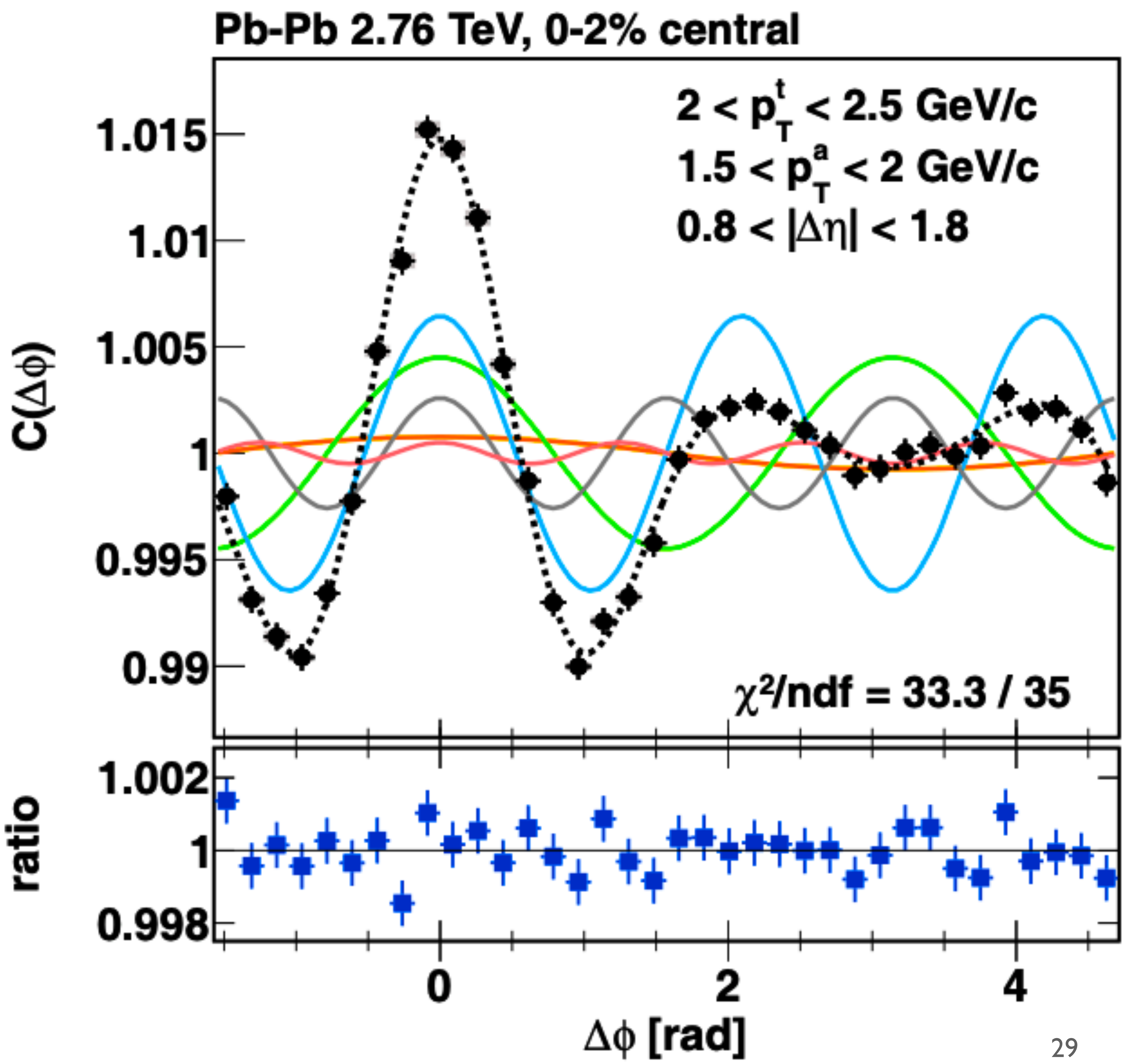

Correlations in small system

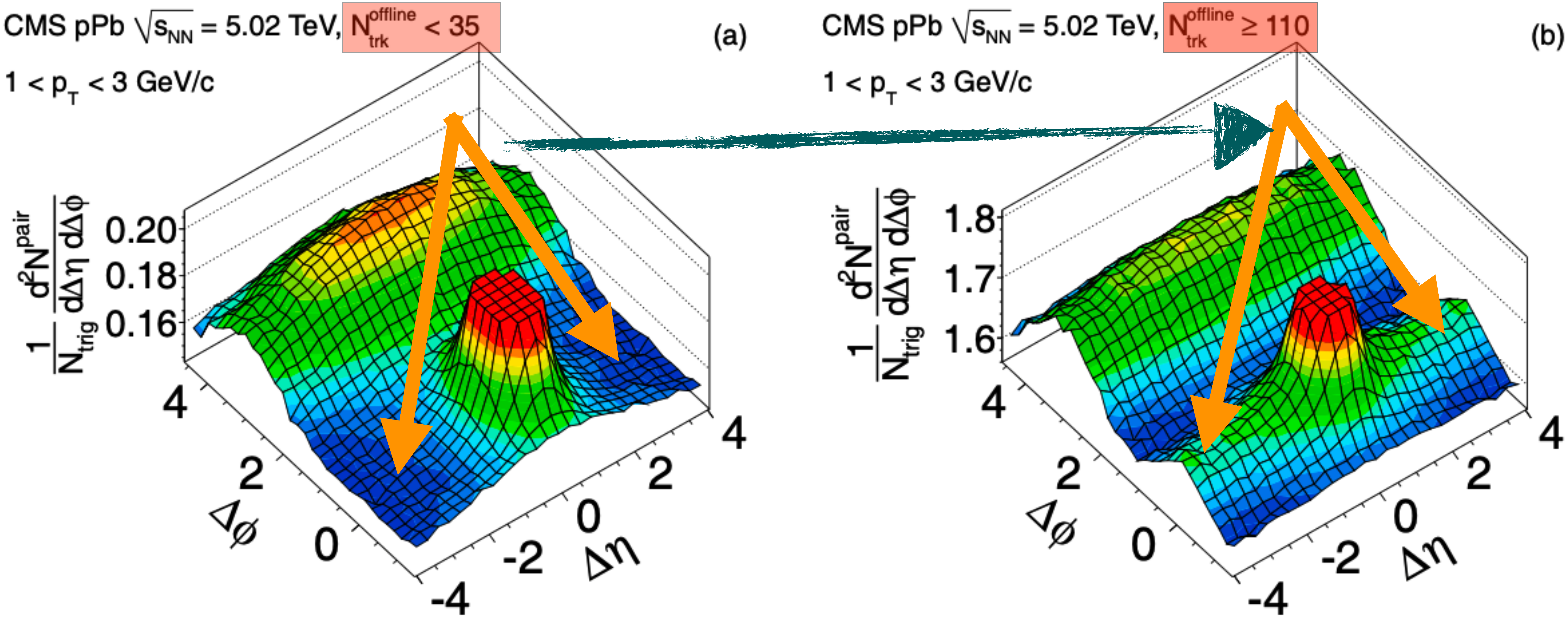

$\Delta\phi\Delta\eta$ structures have also been observed in pPb collisions [42-46]: A clear transition from the absence of a near-side ridge to a large signal with increasing centrality. The jet signal remains roughly constant with centrality [105].

Fourier azimuthal coefficients of identified particles extracted in pPb [47]: Shows the mass ordering expected if such azimuthal correlations would come from a collective flow driven by relativistic hydrodynamics.

Correlations

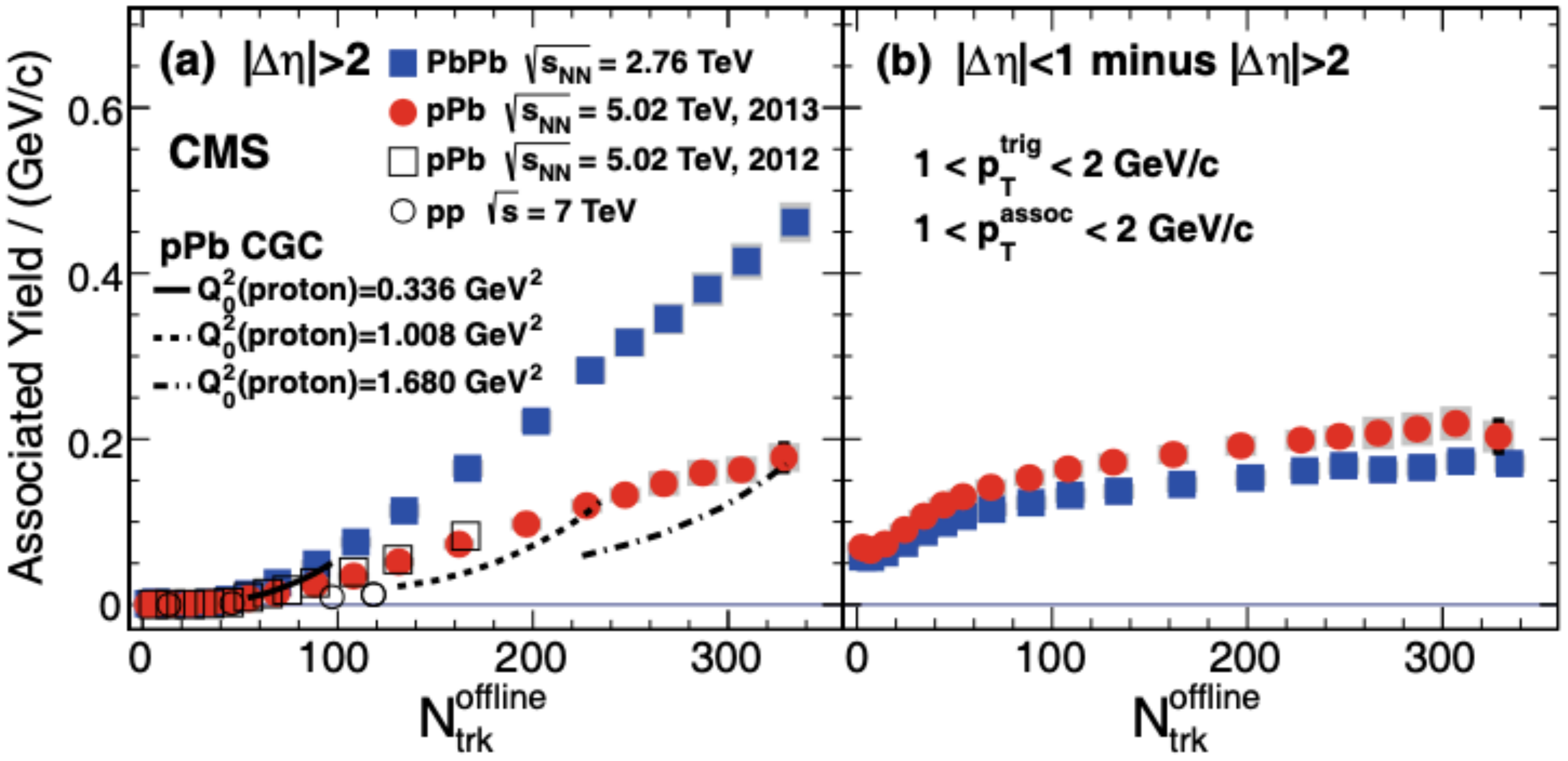

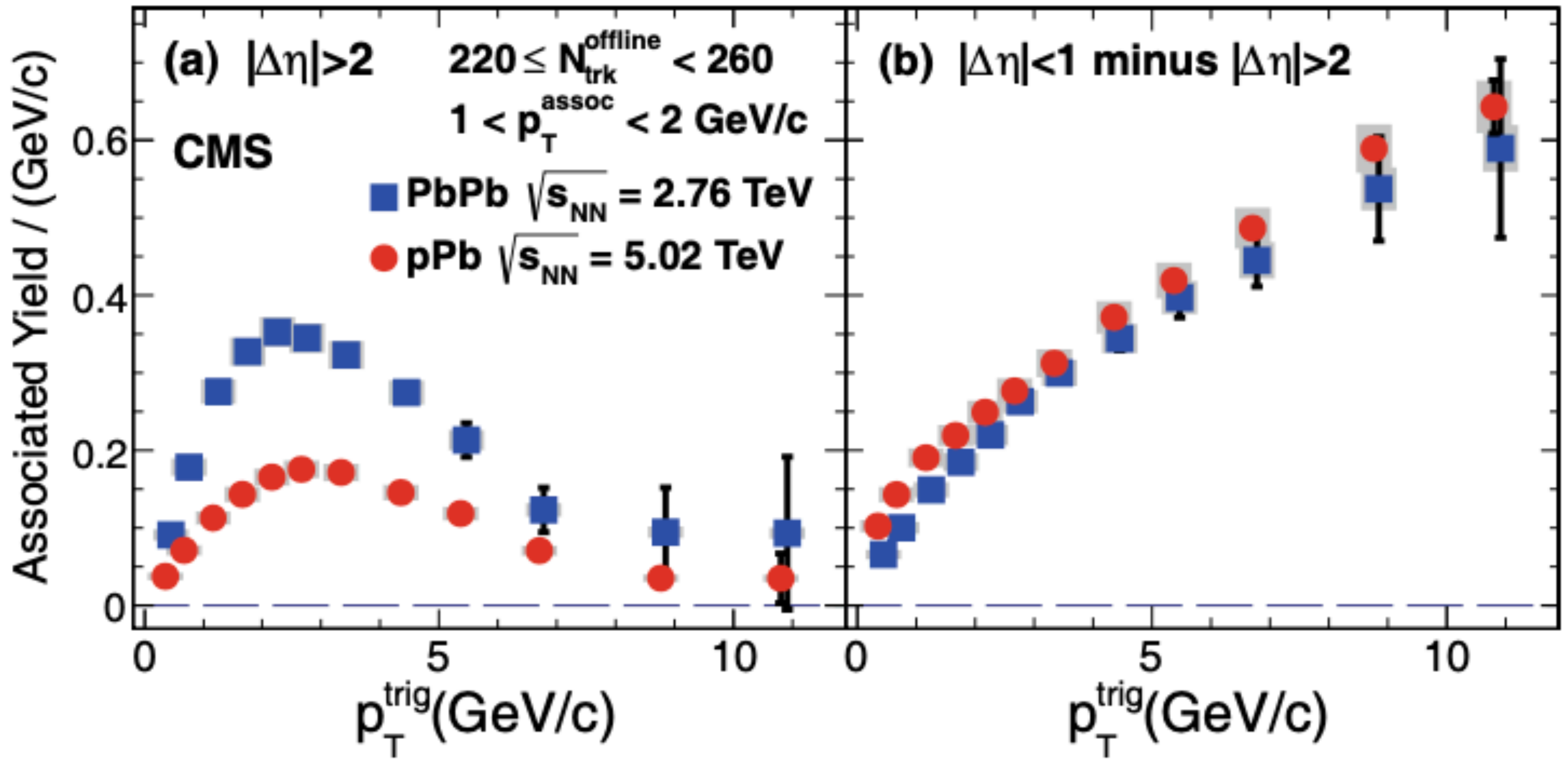

A comparison between the yields in pPb and PbPb at the same multiplicity [48] shows different features and magnitudes with increasing multiplicity and transverse momenta for correlations of short and long range in rapidity, but a very similar size for both colliding systems.

Ridge structure is an open puzzle!

The collectivity debate

The experimental observations resulted in an intense debate on the origin of collectivity and the possibility of collectivity in very high-multiplicity pp and pPb collisions at LHC energies.

Picture Courtesy: SAINA

Observations from the Femtoscopic analyses @ AGS, SPS and RHIC energies [49]

1. **A linear increase of the radius parameters** was measured as a function of $\langle dN_{ch}/d\eta \rangle$.

2. **A significant decrease of the radii with the momentum of the pair** : Characteristic feature of expanding particle sources since the HBT radii describe the *homogeneity length* (Size of the region that contributes to the pion spectrum at a particular three-momentum) rather than the overall size of the particle-emitting system [50].

3. **The decrease of the size with kT(** $K_T = |\vec{p}_{T_1} + \vec{p}_{T_2}|/2$): Observed in experimental data from heavy-ion collisions at all centralities, various collision energies and colliding system types. It is described quantitatively in hydrodynamic models

Femtoscopy @ ALICE

At the LHC: 0–5% Pb-Pb collisions at $\sqrt{s_{NN}} = 2.76$ TeV [51] are compared for $R_{long}, R_{out}, R_{side}$ to lower energy experiment results.

1. The LHC values are higher than the top RHIC energy values by 10–35%
2. The scaling with $\langle dN_{ch}/d\eta \rangle^{1/3}$ holds up to LHC energies.

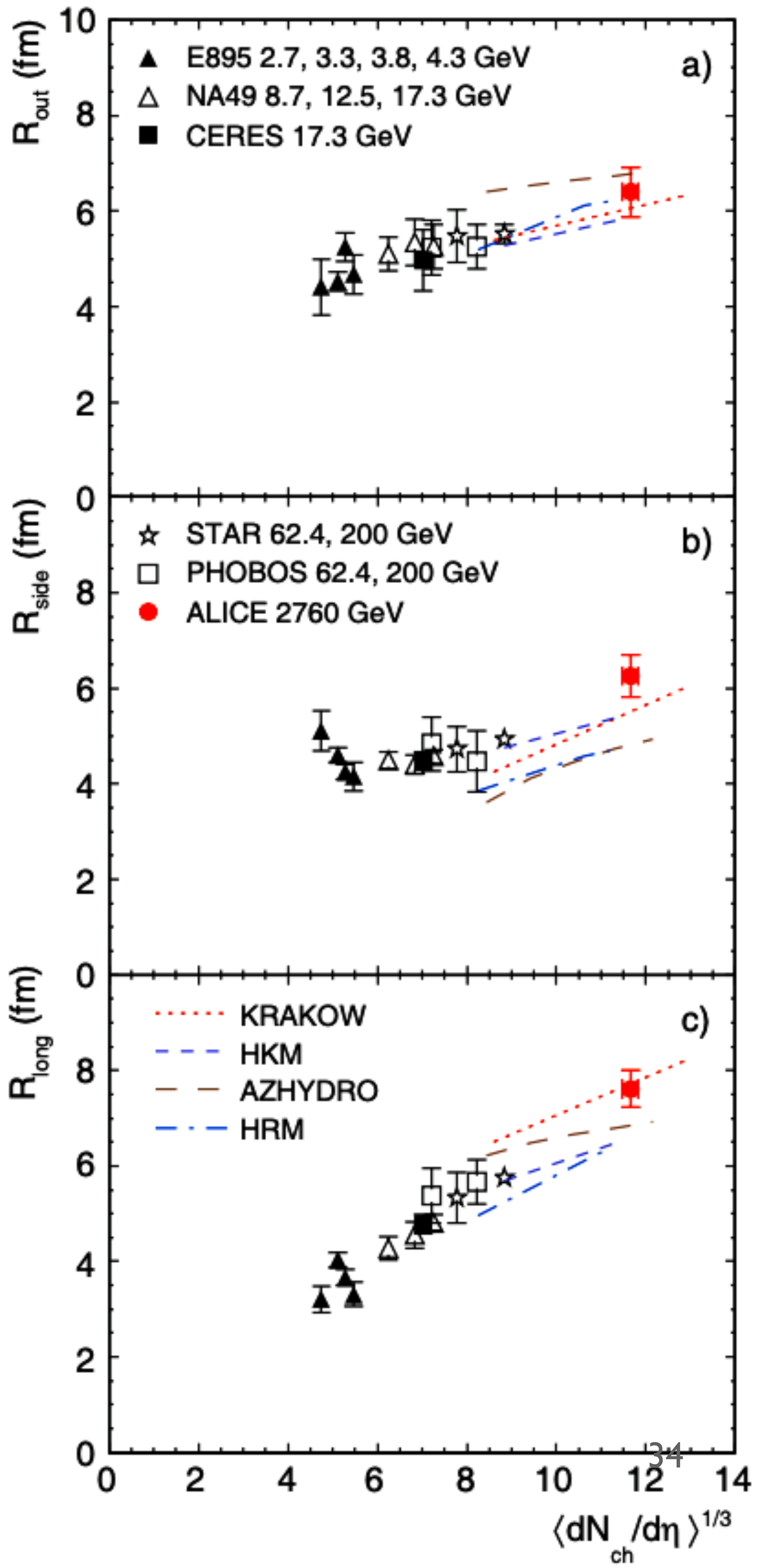

Femtoscopy

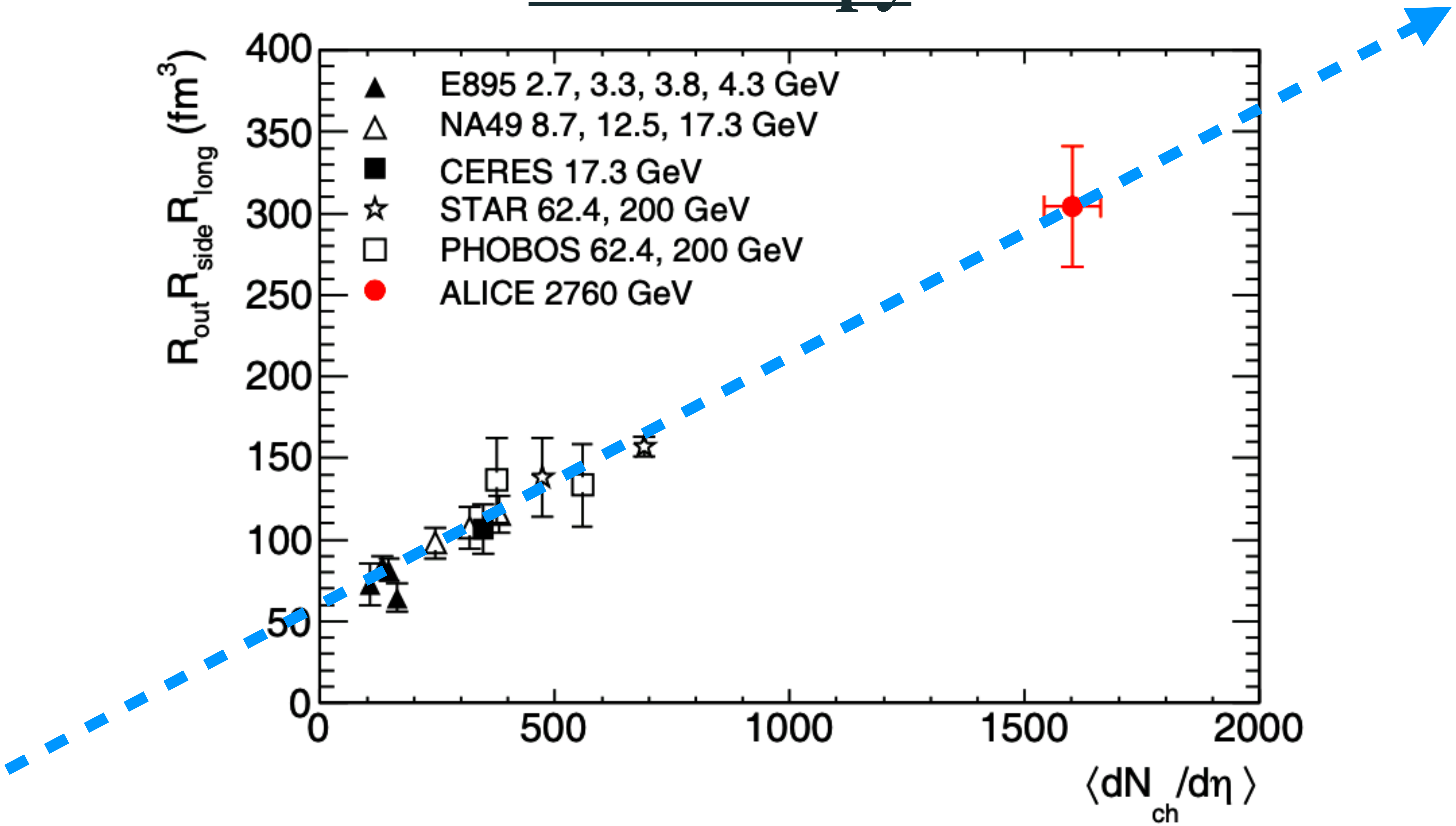

The product of the radii is connected to the volume of the homogeneity region [51].

1. **Linear dependence on the charged-particle pseudorapidity density;** Two times larger at the LHC than at RHIC.
2. **Decoupling time for pions > 10fm/c :** based on R_{long} measurements (40% larger than at RHIC)

Femtoscopy

The radius parameters show an increase with centrality: Expected from a simple geometric picture of the collisions.

Decreasing size with increasing m_T: Expected in the presence of collective radial flow which is in agreement with hydrodynamical models [52].

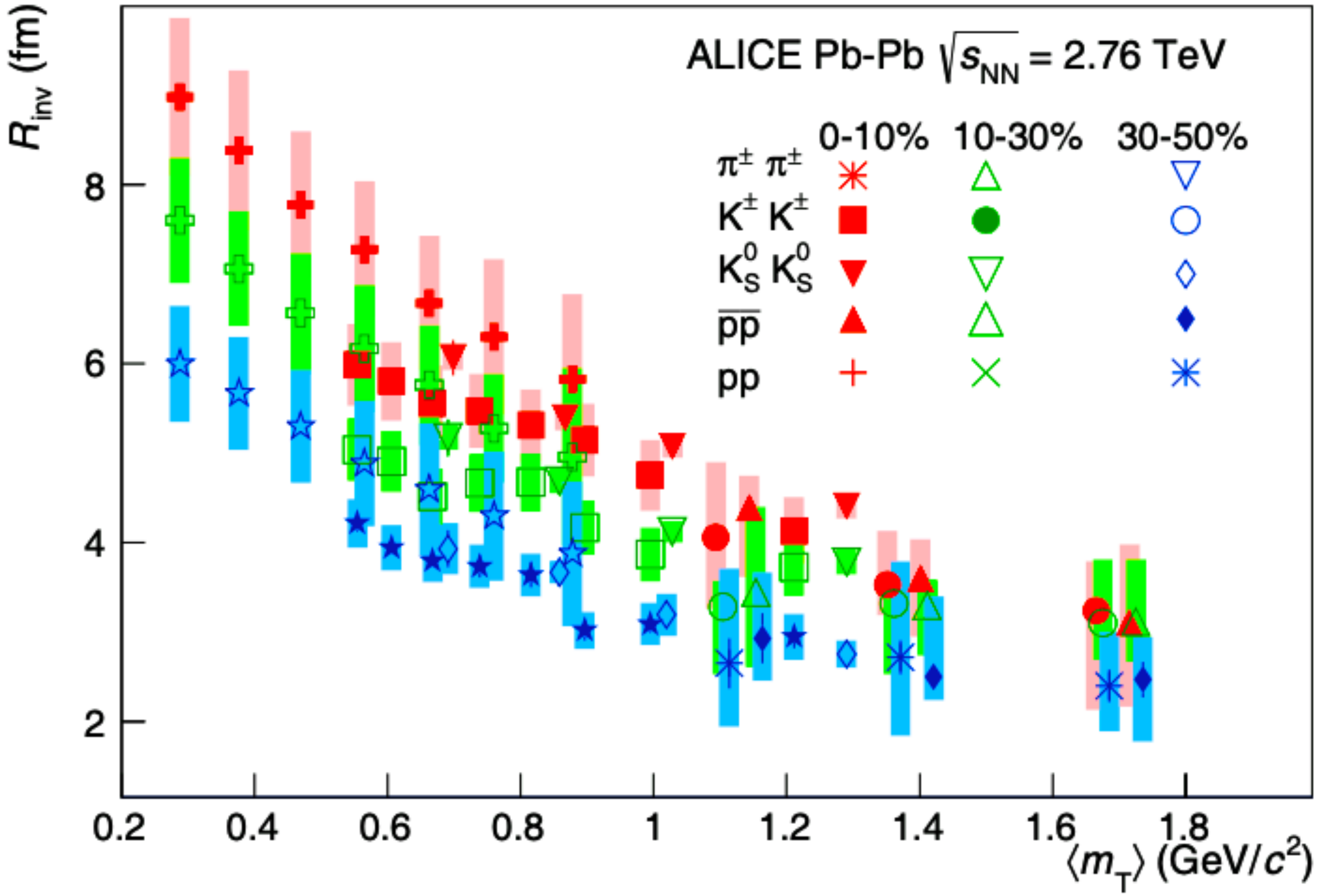

Hard and electromagnetic probes: Particle Production

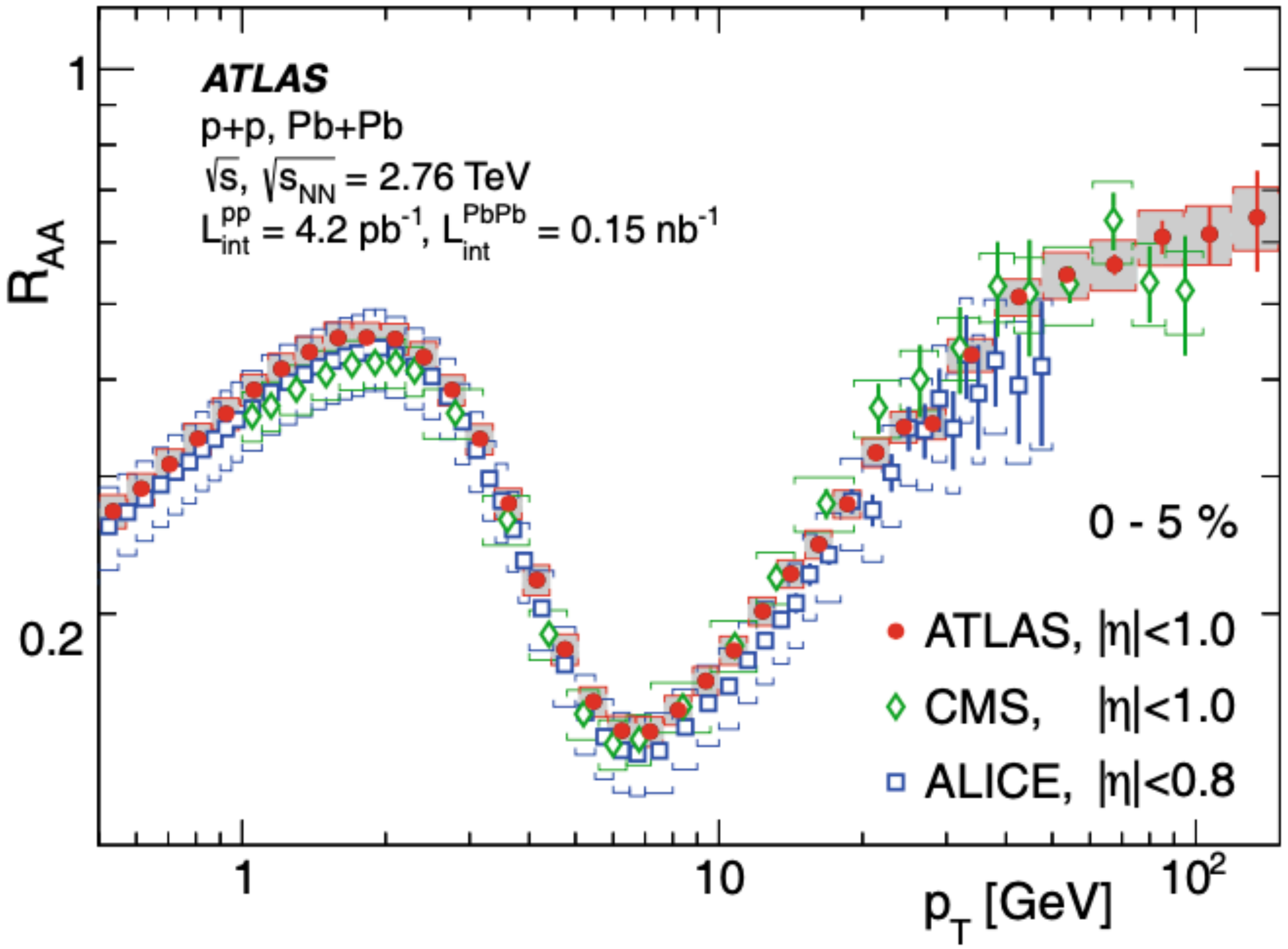

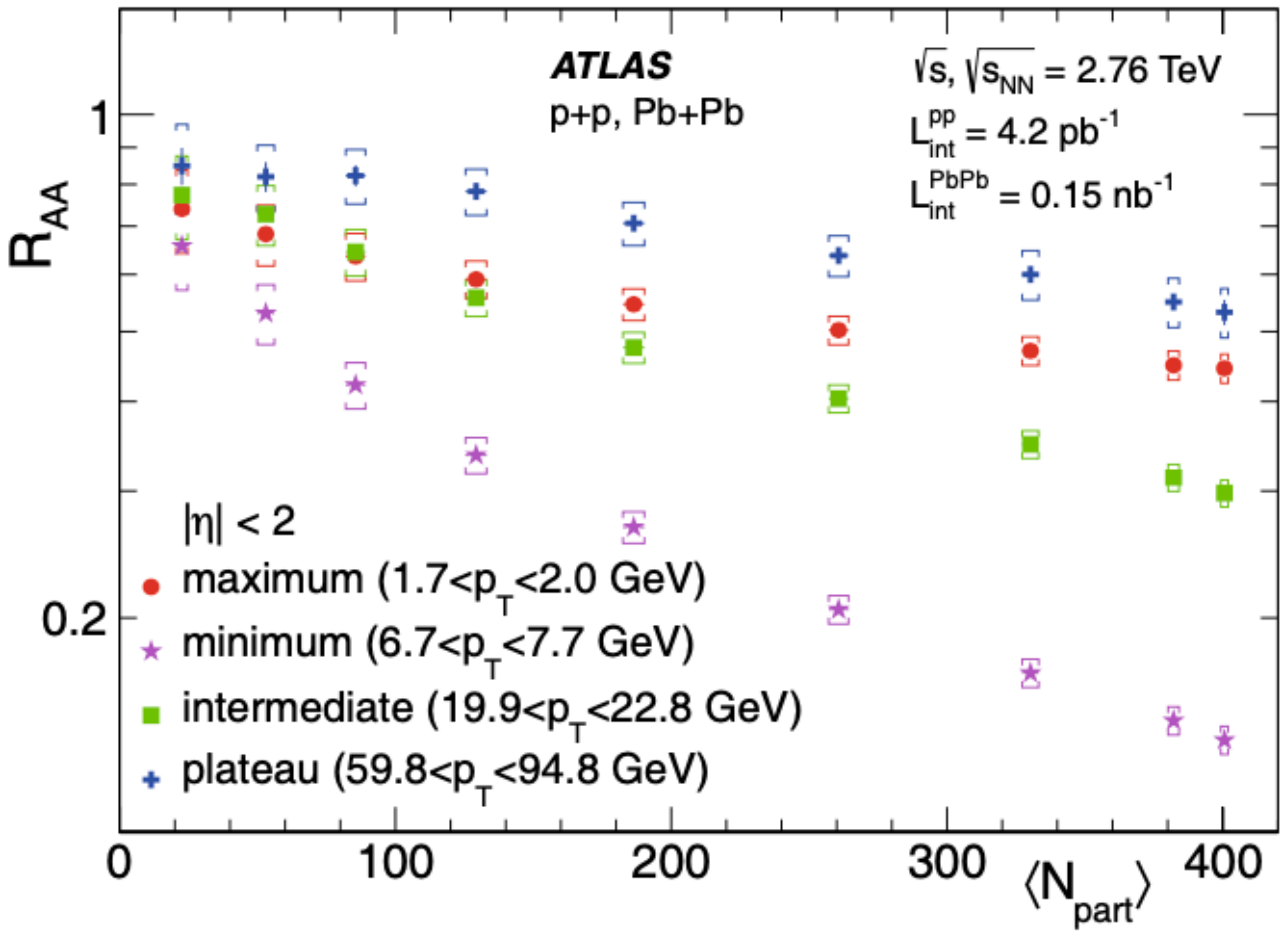

AT RHIC Energies [53-57]: The suppression of particles produced at large transverse momentum and the disappearance of back-to-back correlations at RHIC that established the dense partonic nature of the medium produced in nucleus-nucleus collisions.

AT LHC analogous results are found [58]: A steady decrease with increasing centrality is seen for all transverse momenta.

Hard and electromagnetic probes: Particle Production

CMS and ALICE [59,60] results for the nuclear modification factor of charged particles compared with different models

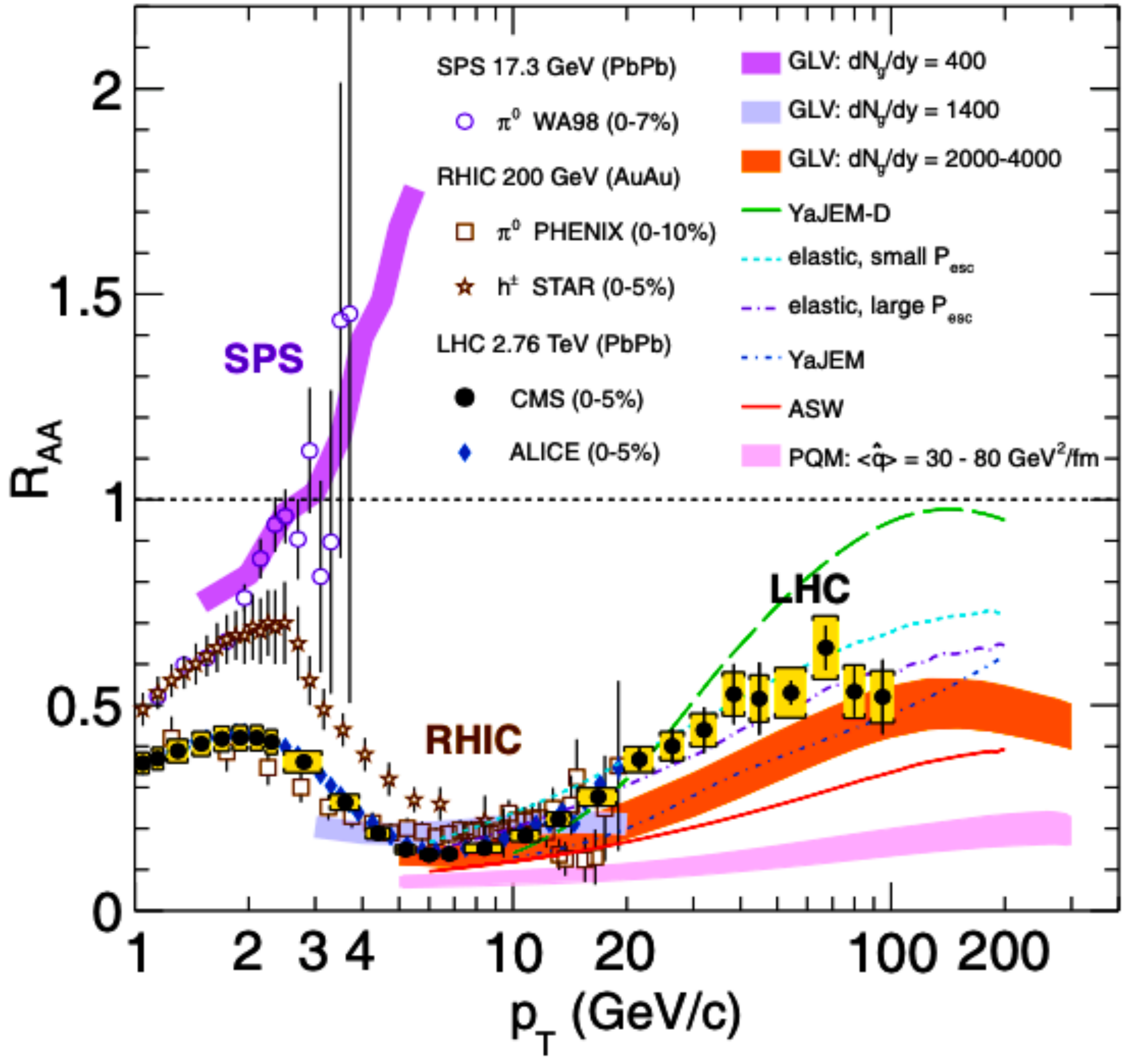

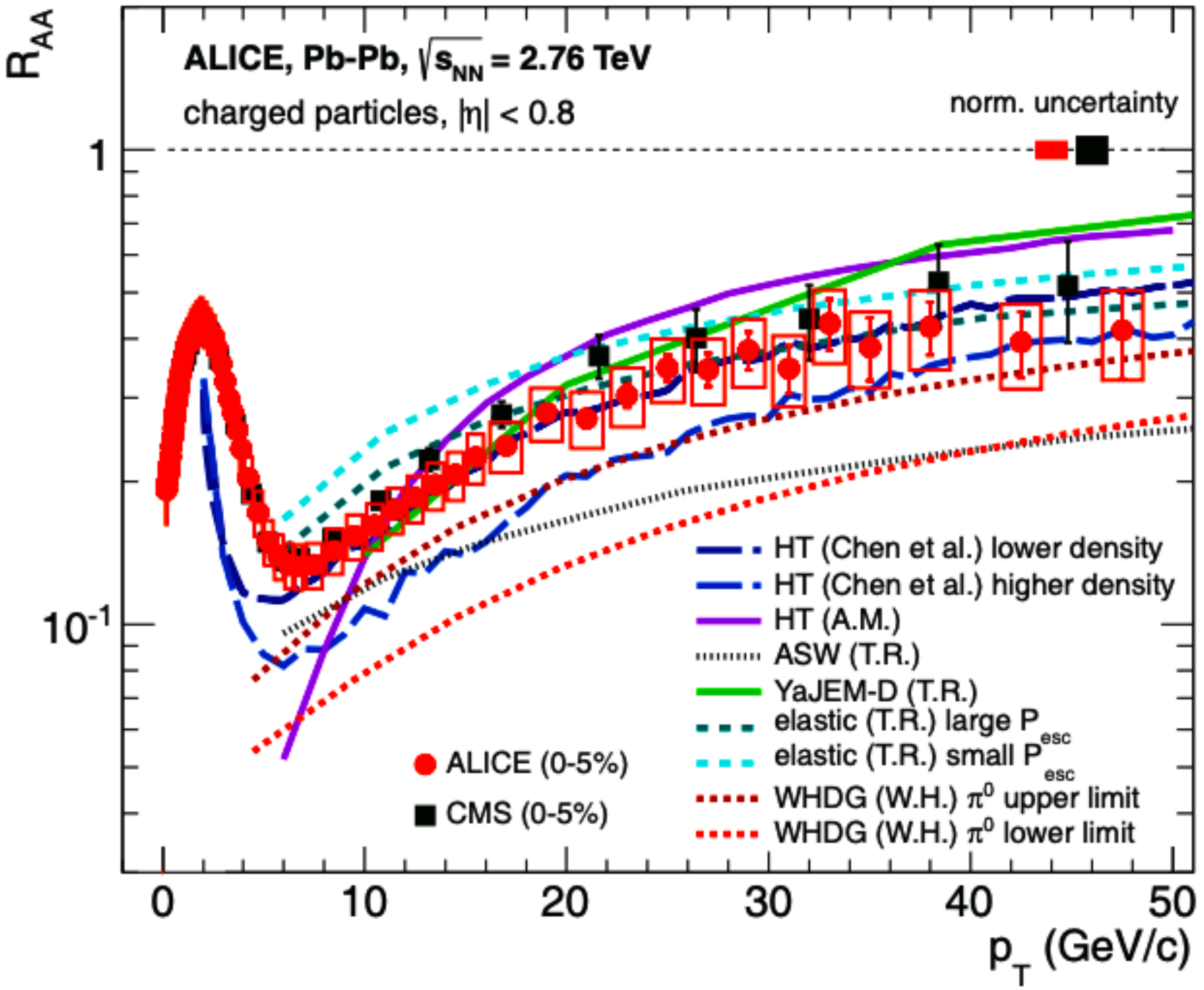

Good agreement by models that take into account energy loss of the parton traversing the medium : These models mainly differ in the inclusion elastic energy loss, and in the way in which energy and momentum conservation is imposed[61]

Hard and electromagnetic probes: jets

1. **The nuclear modification factor (for jets (both charged [62] and fully calorimetric [63] jets):** A suppression similar to that found for charged particles .

2. Significant dependence of suppression with the azimuthal angle (wrt the reaction plane) → **Expected from energy loss processes. [64,65]**

Hard and electromagnetic probes: jets

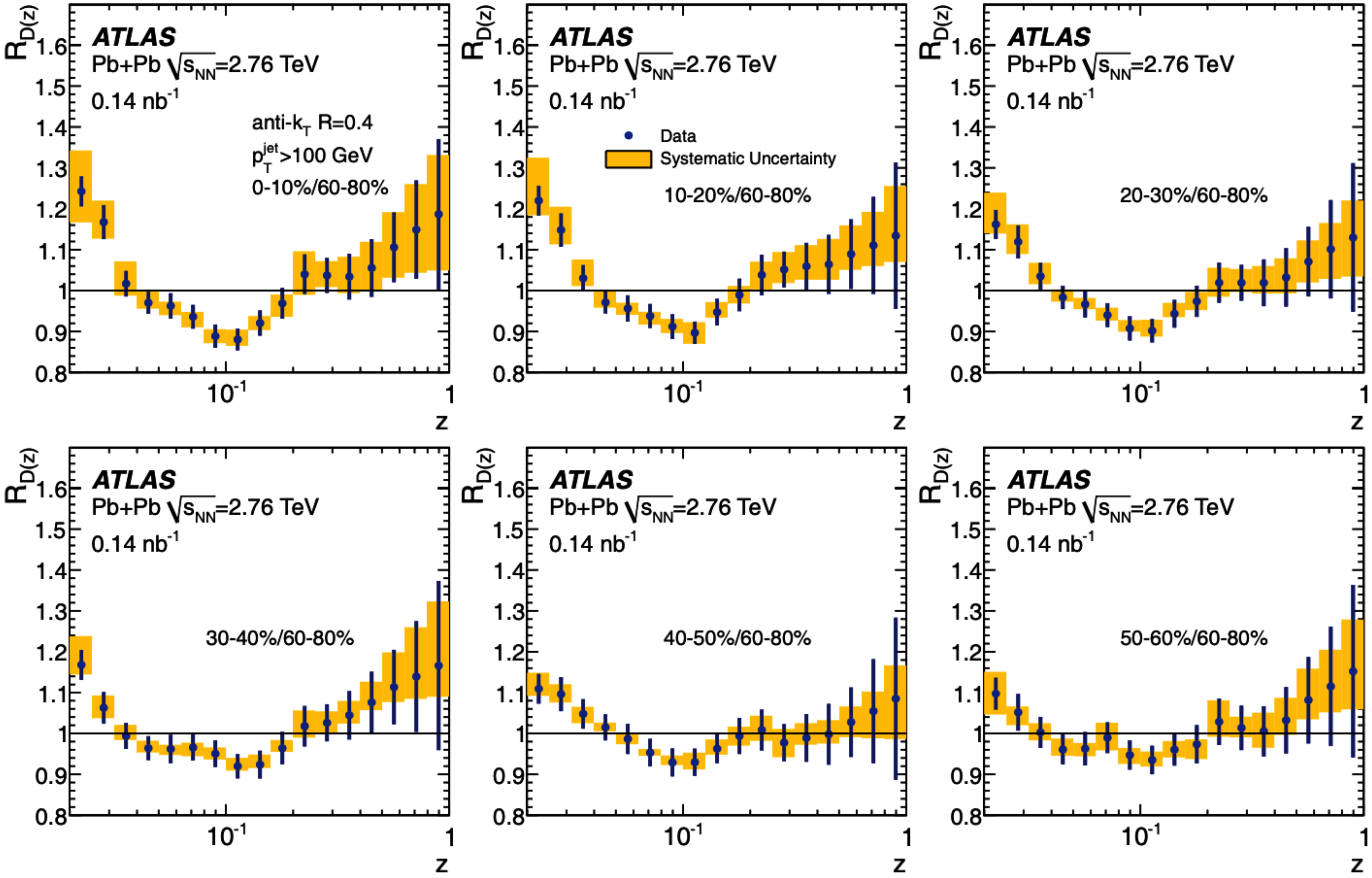

Ratio of jet fragmentation functions in PbPb and pp vs. the momentum fraction of the energy of the jet carried by the measured hadron(z).

The fragmentation function [66-69]: An enhancement of soft particles, a suppression of particles with intermediate momentum fractions, and little modification of hard ones .

The small enhancement: Understood in terms of the modification of the denominator

Hard and electromagnetic probes: jets

Serious challenges for the standard theoretical explanation of jet quenching due to:

1. A sizeable increase of the energy asymmetry in dijet systems without modification of their azimuthal correlation (w.r.t pp)

2. The recovery of missing energy at large angles away from the jet axis in the form of soft particles,

3. The lack of strong modification of the hard part of the jet fragmentation function

Phenomenological explanation[70-79] : None of the models provides a complete quantitative description of the data. It does lack the proper theoretical justification for some of the implemented assumptions.

Ratio of events with a second jet over the total number of leading jets, for pp and PbPb collisions

Ratio of events with a background jets over the total number of leading jets, for pp and PbPb collisions

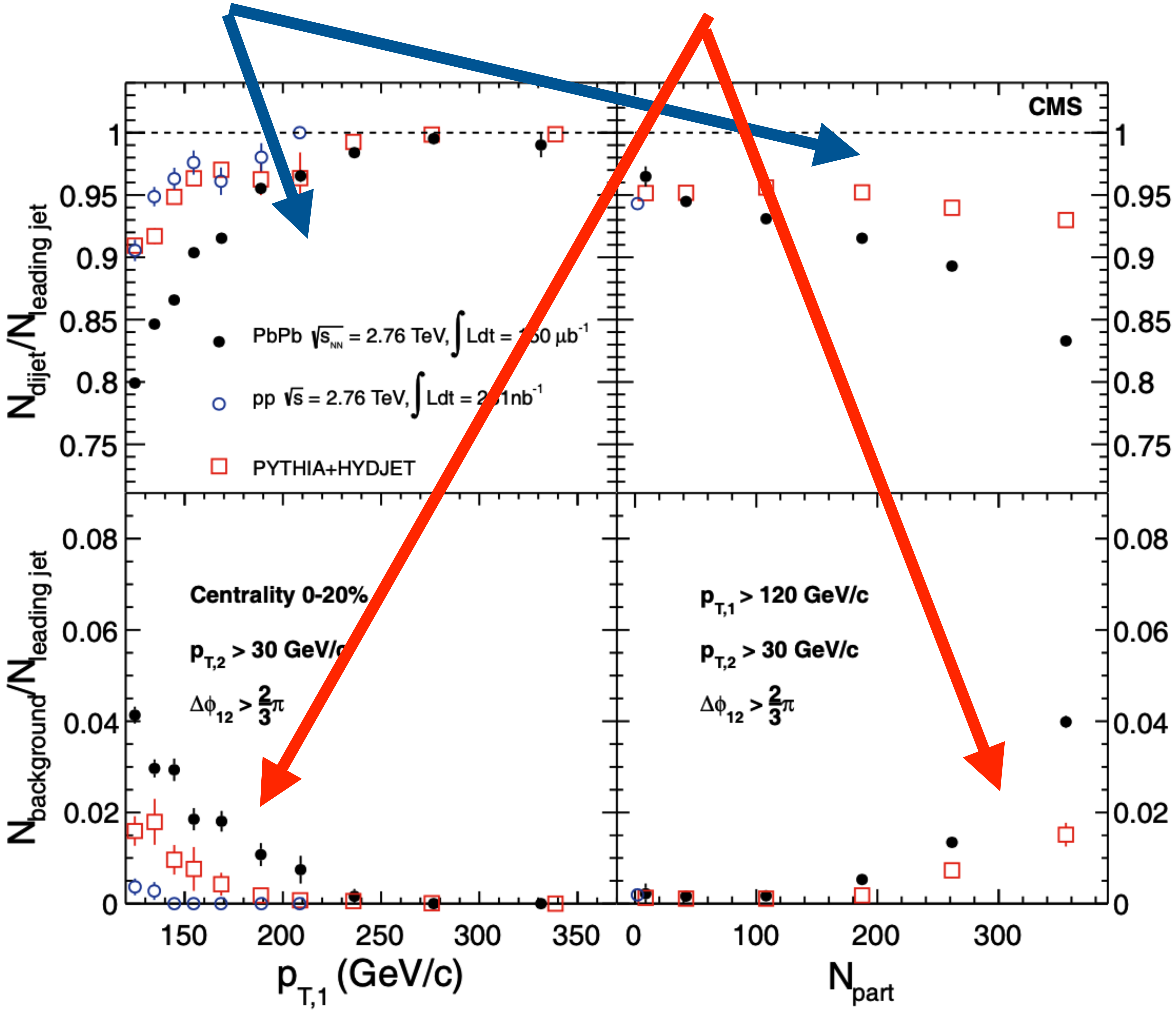

The transverse momentum of the leading jet

The number of participants.

Hard and electromagnetic probes: Heavy Flavour Physics

Average R_{AA} D mesons measured in PbPb collisions in $8 < pT < 16$ GeV/c, as a function of the centrality

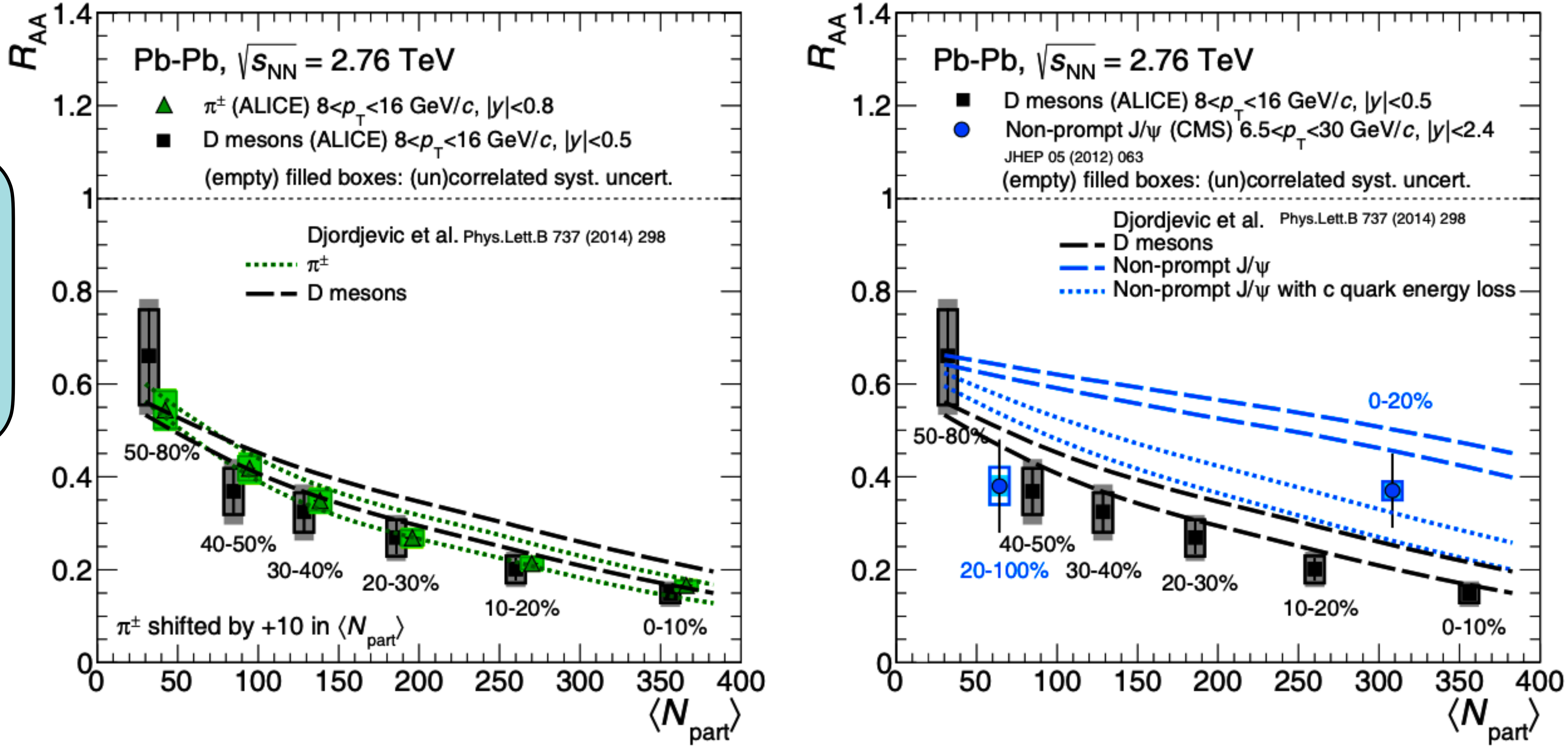

Comparison To:

1. Corresponding quantity for charged pions
2. Calculation implementing energy loss for partons (radiative and collisional processes) [80].
3. CMS data for J/ψ from b-decays [278], in the pT range $6.5 < pT < 30$ GeV/c

Hard and electromagnetic probes: Heavy Flavour Physics

A mass ordering is seen:

The heavier b quark are less suppressed than c quarks[83].

It is more evident when the ALICE results are compared results from CMS [284].

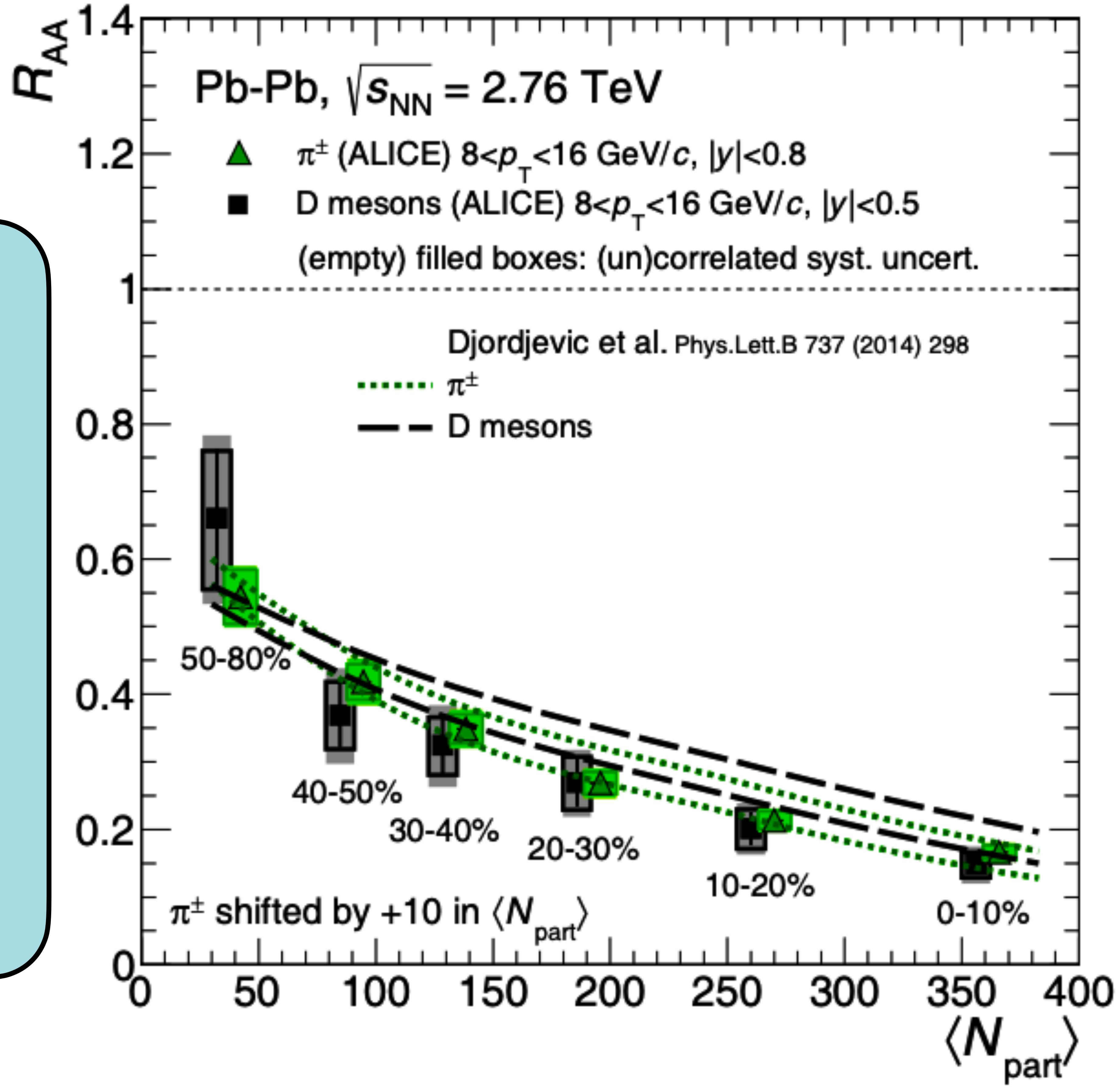

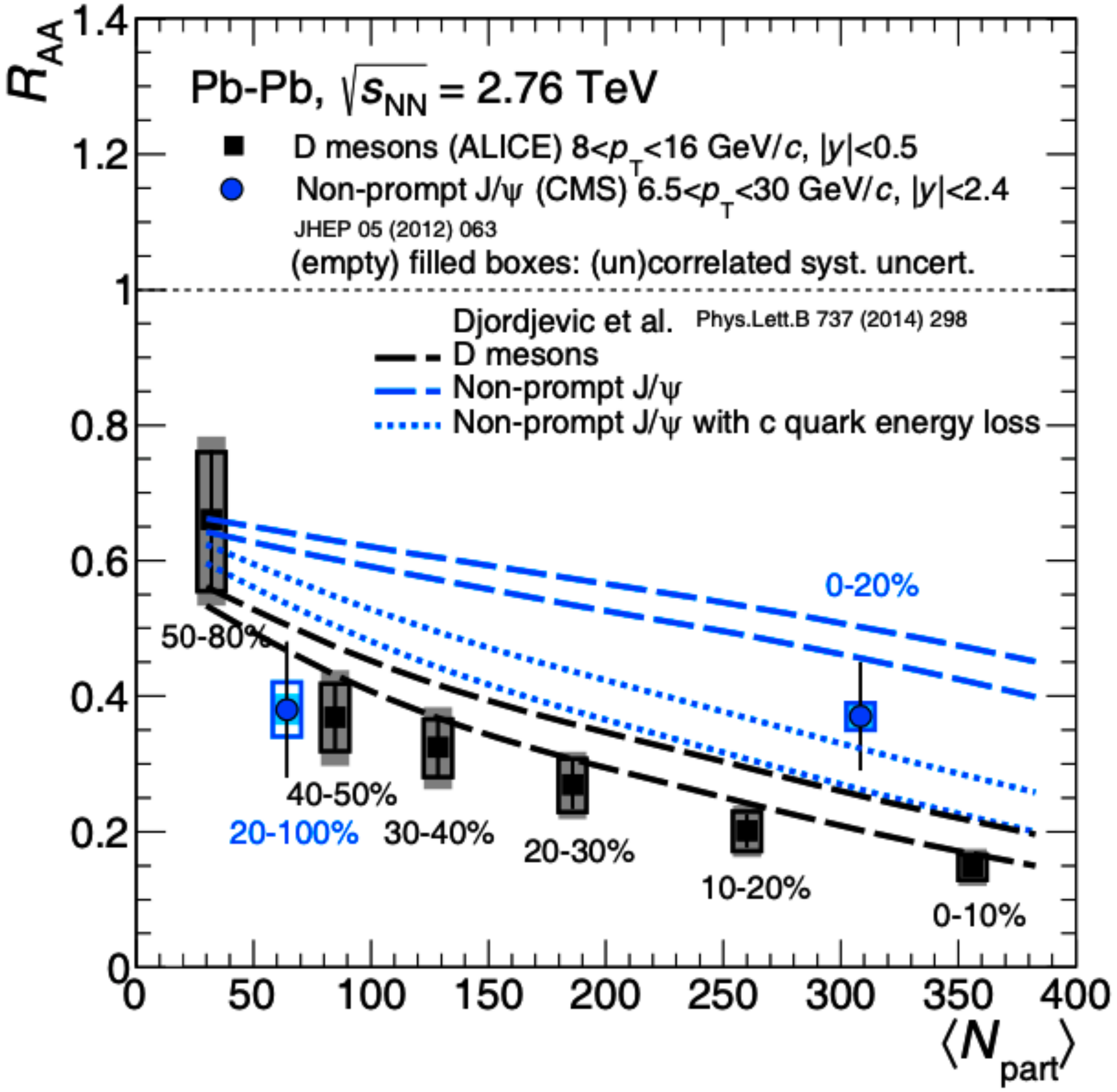

D meson suppression reaches a factor 5 for central (0–10%) PbPb events compatible with the corresponding result for $\pi^{\pm}$

Smaller suppression expected for particles resulting from the fragmentation of heavy quarks is not seen

(In data & models) as a consequence of the different fragmentation function and p_T spectrum of gluons, light and c quarks [81-82]

Hard and electromagnetic probes: Heavy Flavour Physics

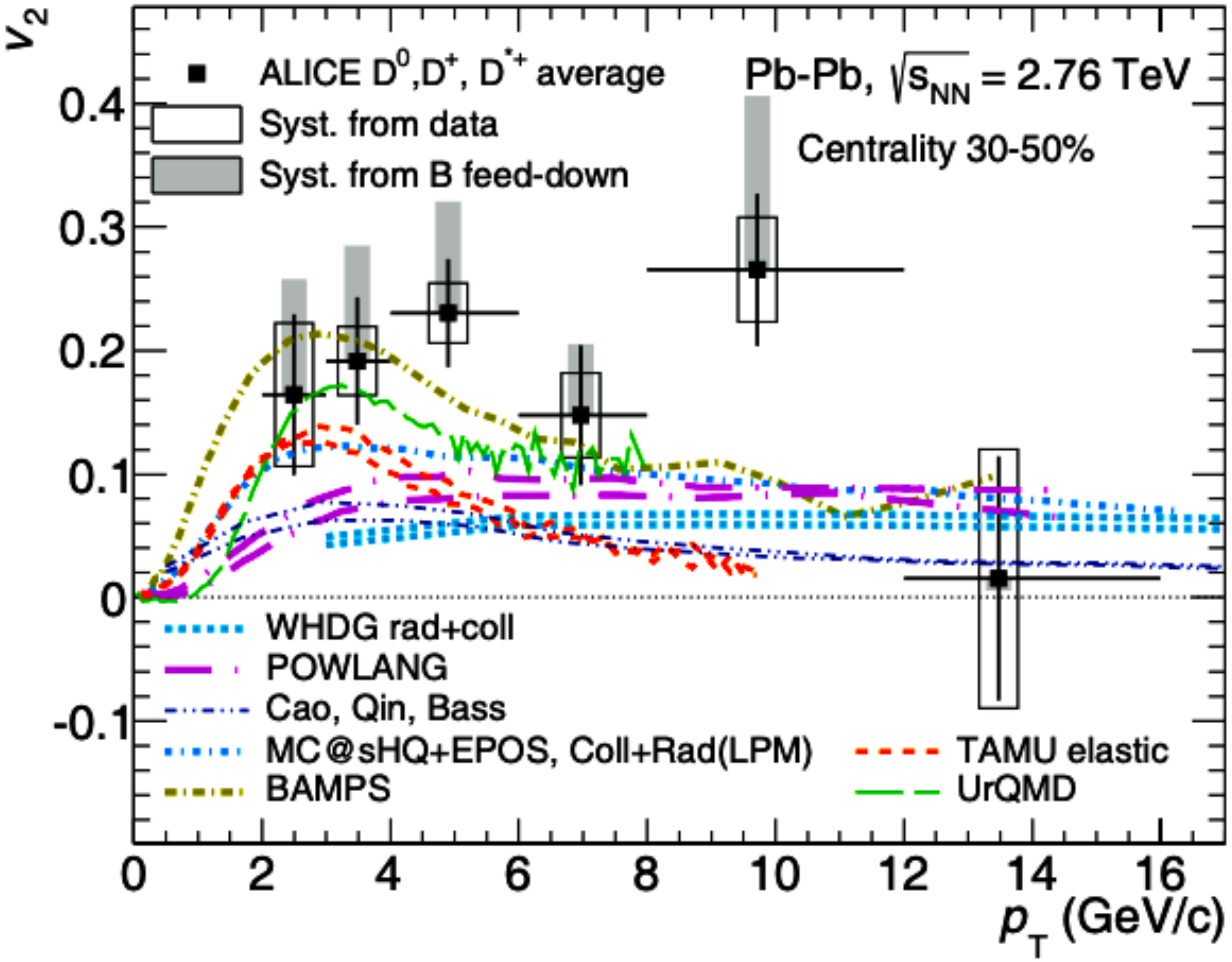

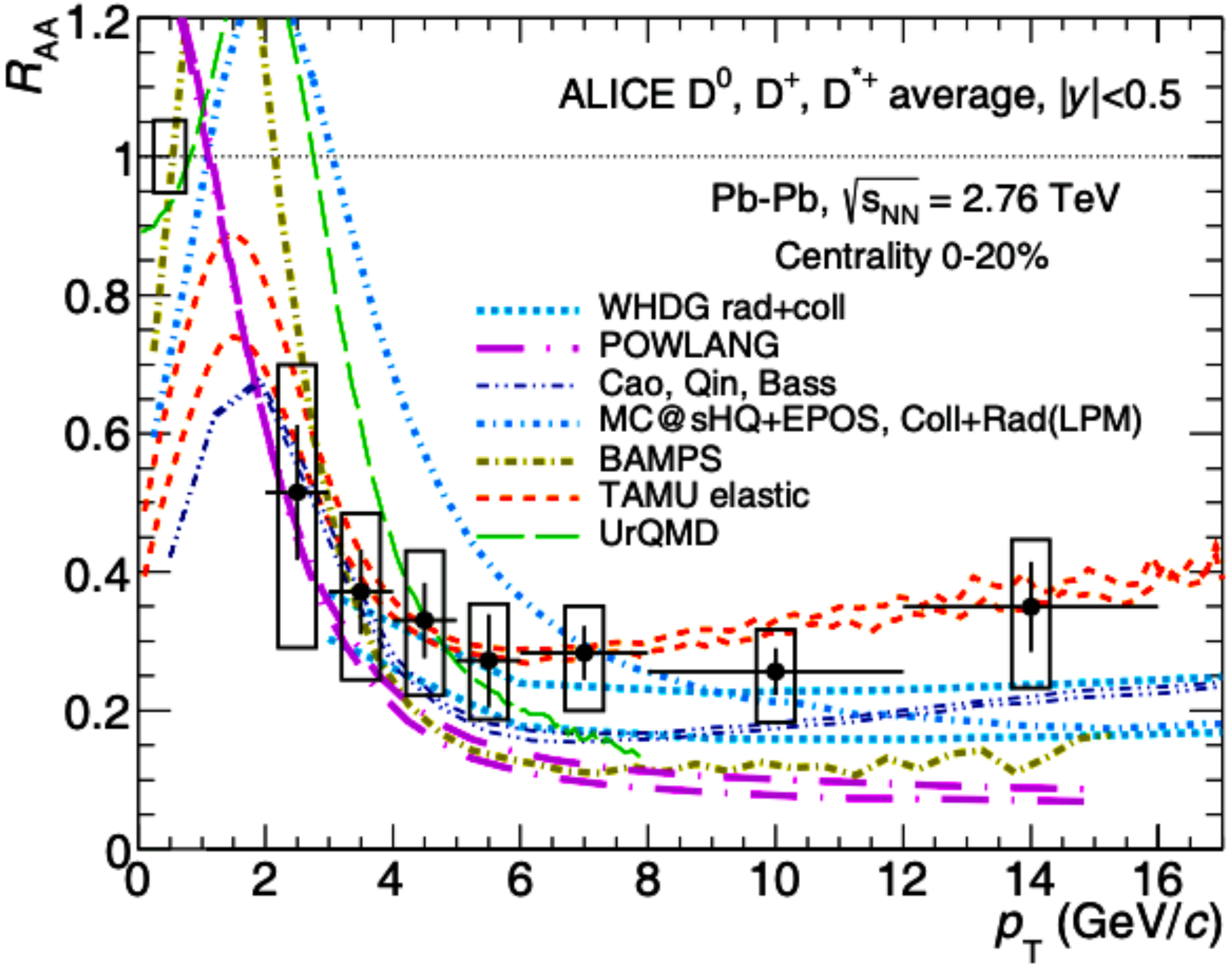

RAA for the 0–20% centrality [106]: A strong suppression, reaching a factor 3–4, is seen for pT > 5 GeV/c, with a tendency towards a smaller suppression for decreasing pT.

Challenging to describe quantitatively both observables over the full pT range.

Hard and electromagnetic probes: Heavy Flavour Physics

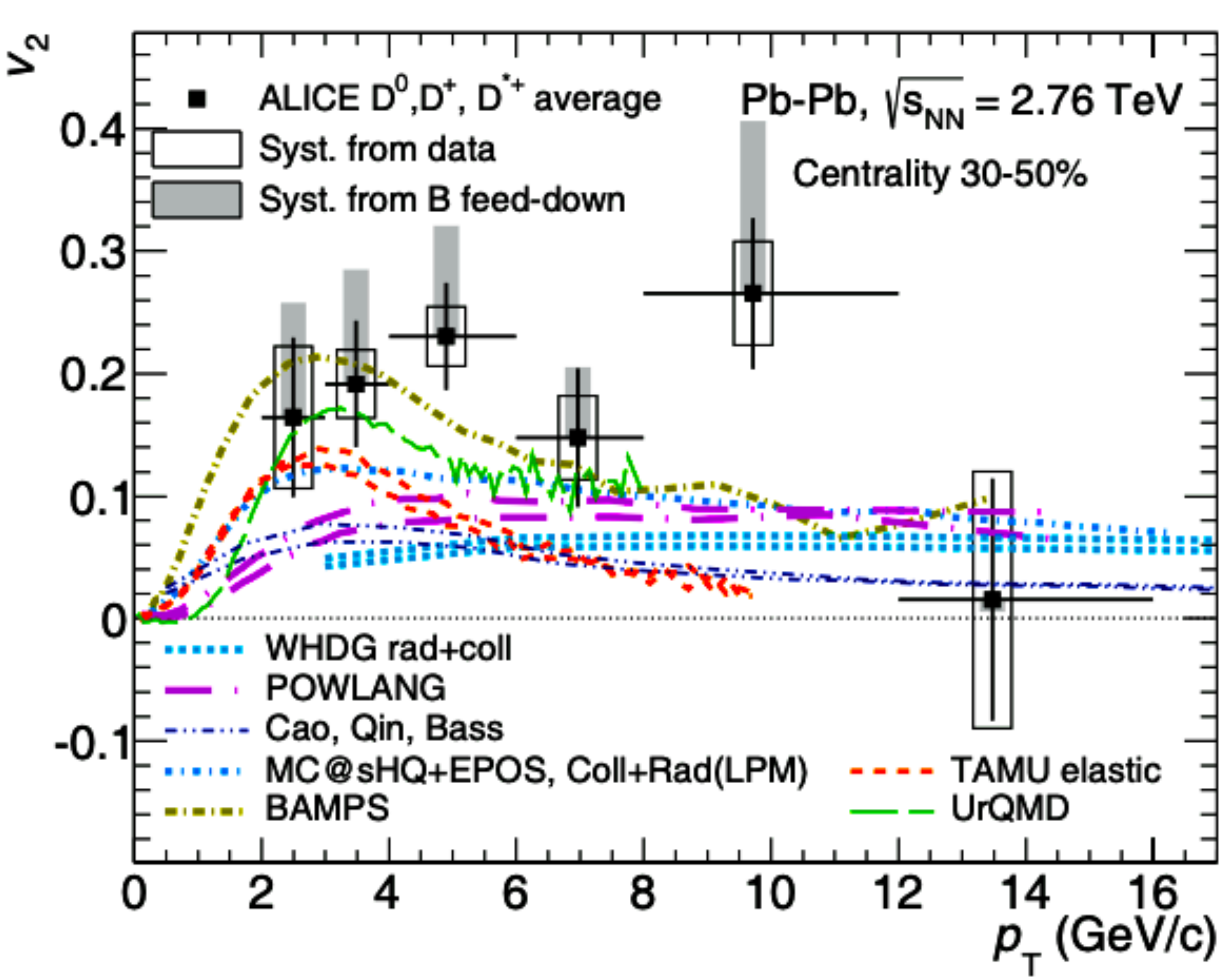

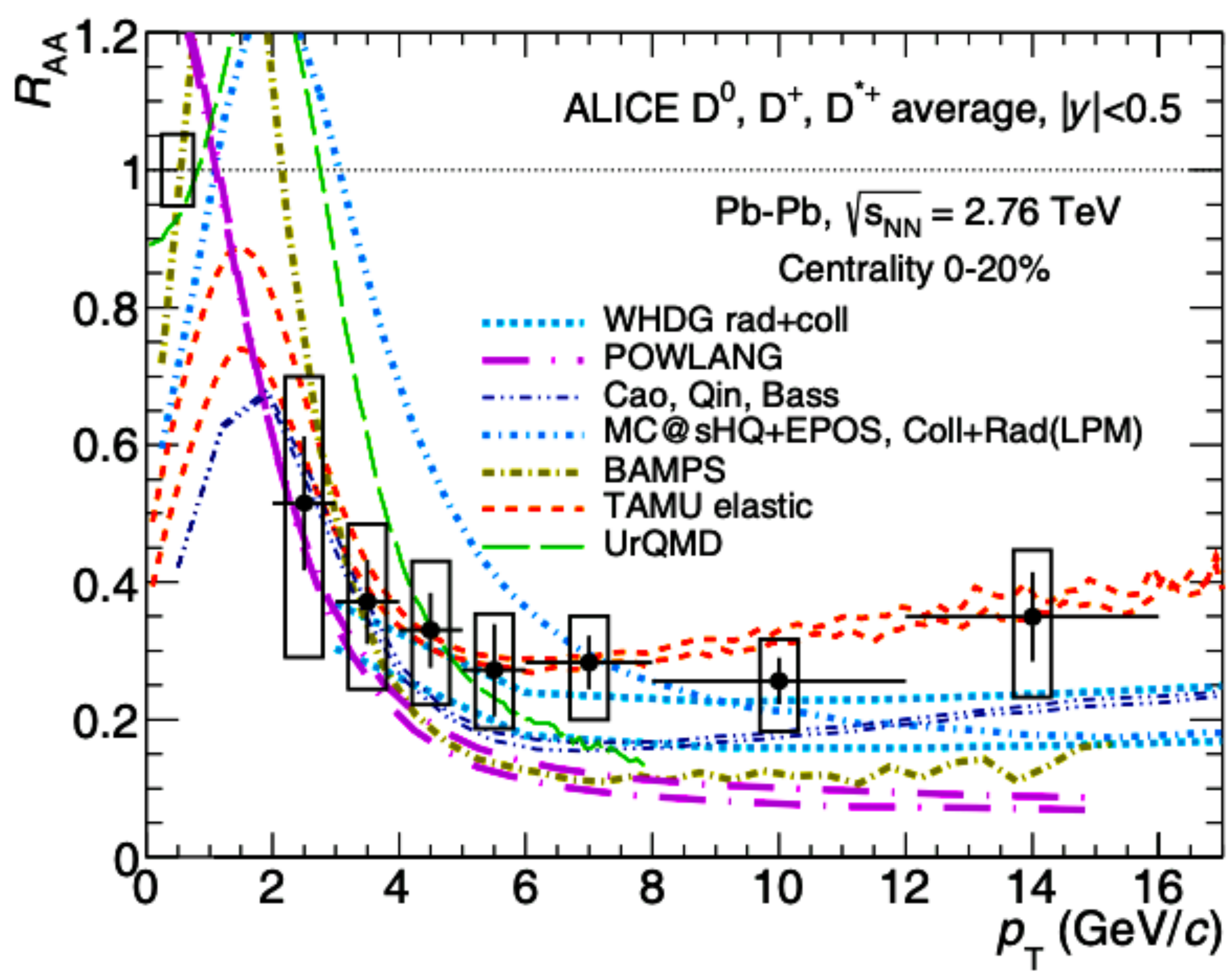

ALICE results on the average D-meson v2 measured in PbPb collisions in the 30–50% centrality

A significant non-zero v2 is observed: @large pT→ Difference in the in-medium path length between D mesons emitted in-plane or out-of- plane.

@low pT → In medium interactions of the produced heavy-quarks leading to momentum anisotropy.

Charmonium Suppression: PHENIX v/s ALICE

$< N_{part} >$ dependence of the inclusive J/Ψ R_{AA} on : ALICE at forward rapidity [84] v/s PHENIX (Au-Au, 1.2 < |y| < 2.2) [107]

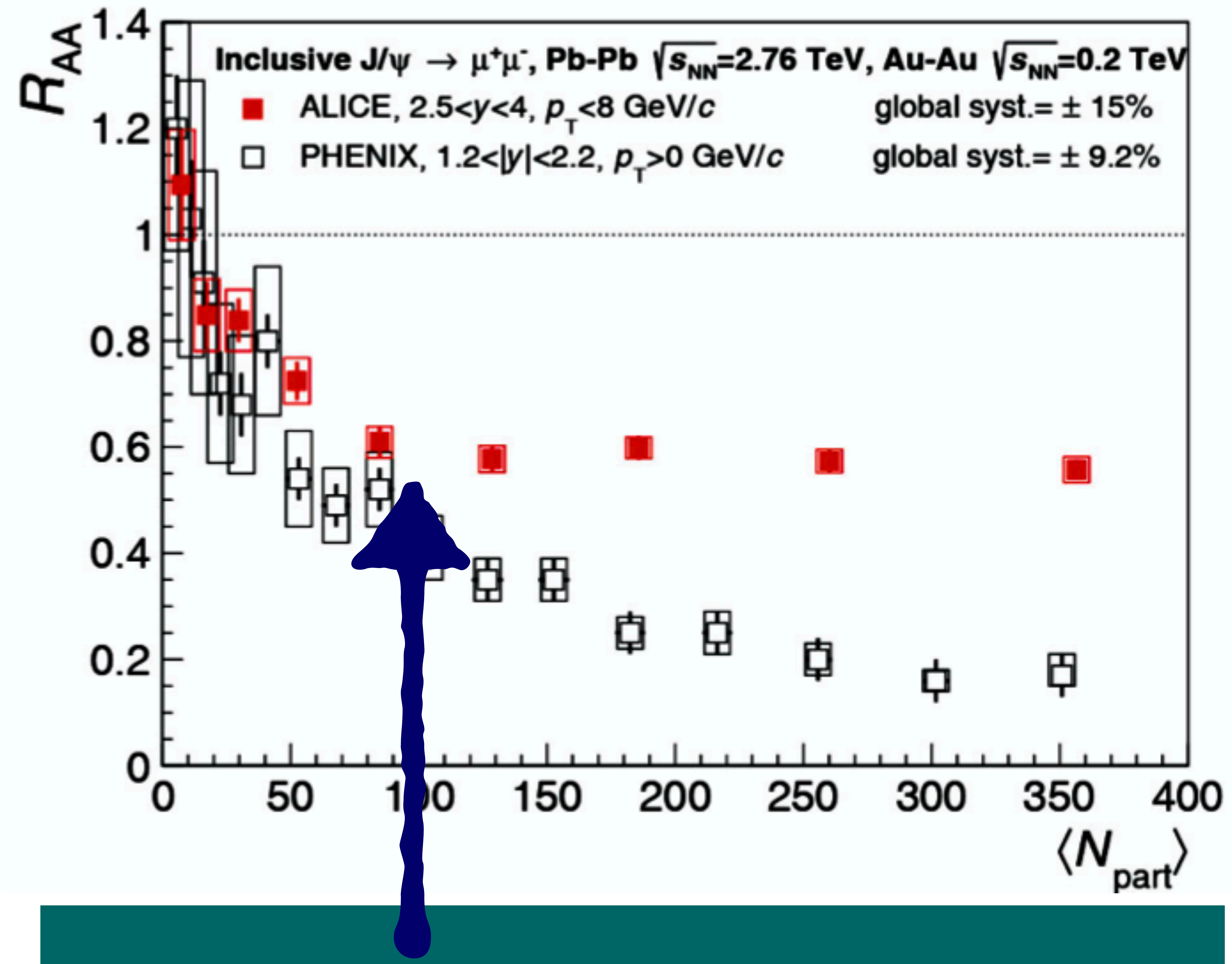

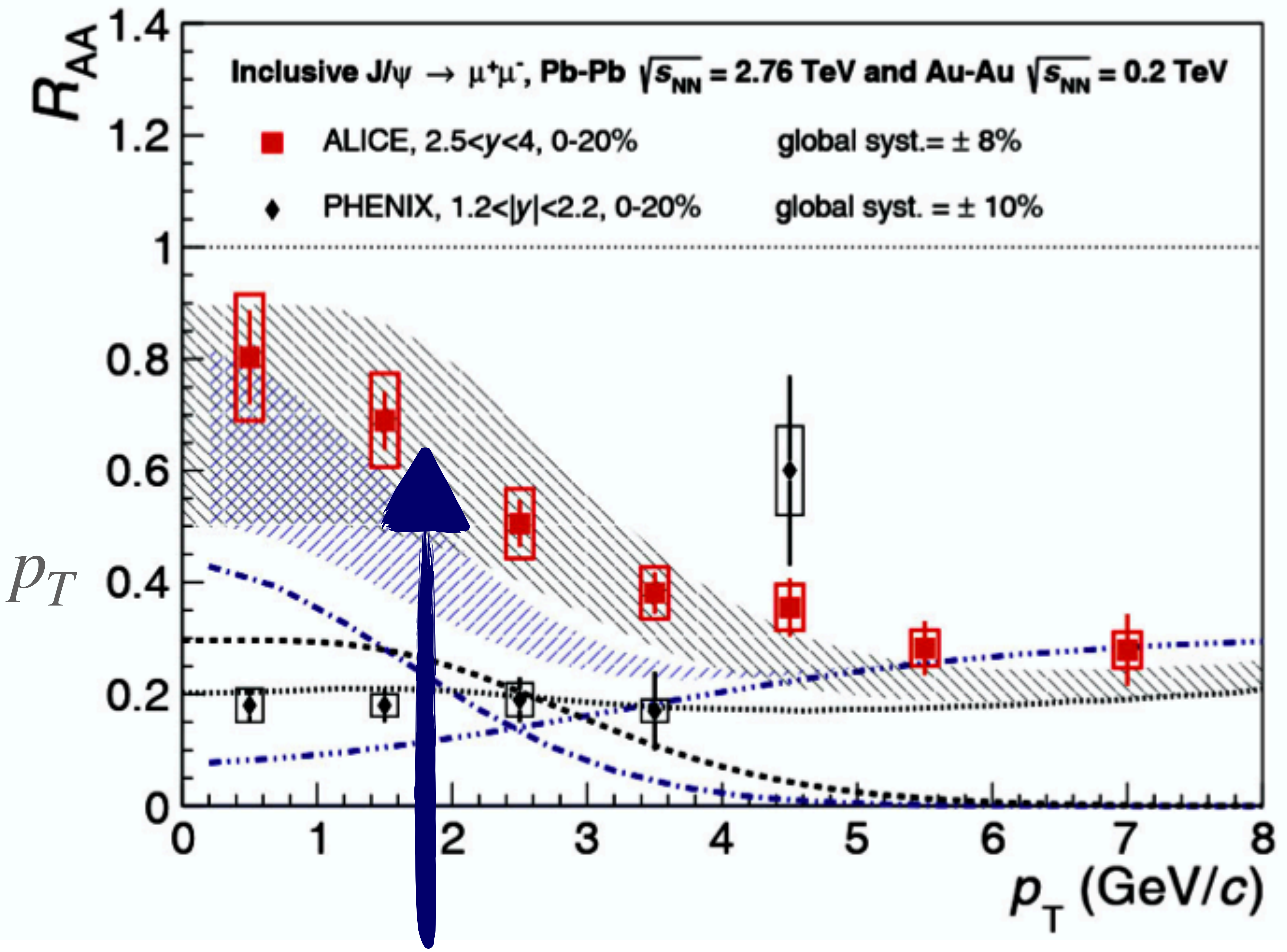

Pb-Pb Collsions : Suppression & regeneration of J/Ψ for $N_{part} > 100$ (prominent for low p_T)

Transport models: Implement charmonium dissociation and regeneration in a thermally expanding fireball [more than 50% of the measured J/ψ is produced via regeneration[86-89]].

Hard and electromagnetic probes: Direct Photons

- **Direct photon studies** have been carried out by ALICE by using photon conversions to e^+e^- or calorimetric measurement [90]. (See Talk-2 in this series)
- **NLO pQCD calculations** [91-94] well describe the spectrum above pT ~ 5 GeV/c.
- **In the region 0.9 < pT < 2.1 GeV/c:** a 2.6σ excess is found for the 0–20% centrality class. **It is compatible with a thermal slope with T = 297 ± 12(stat) ± 41(syst) MeV.**

→ **Reported as the temperature of QGP in ALICE**

- **Non Zero v2 for direct photons [95]:** Reflecting the development of collective expansion at early stages.

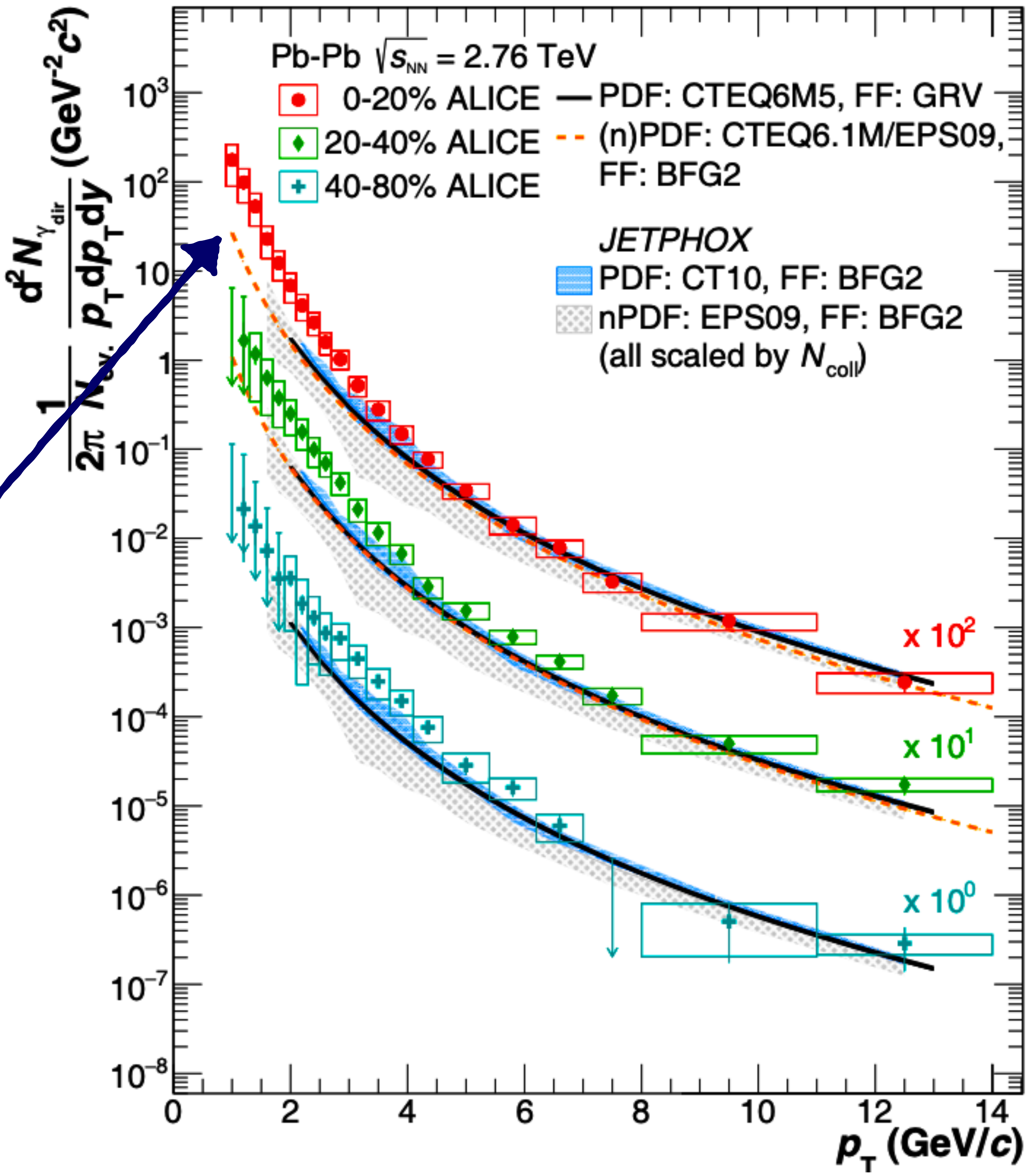

Hard and electromagnetic probes: Ultraperipheral collisions

In ultraperipheral collisions one or both nuclei act as quasi-real photon source that collide with the other nucleus or photon [96]: Nucleus remains intact (coherent production) or gets excited and dissolves but without filling the rapidity gap between the nucleus and the produced particle (incoherent production).

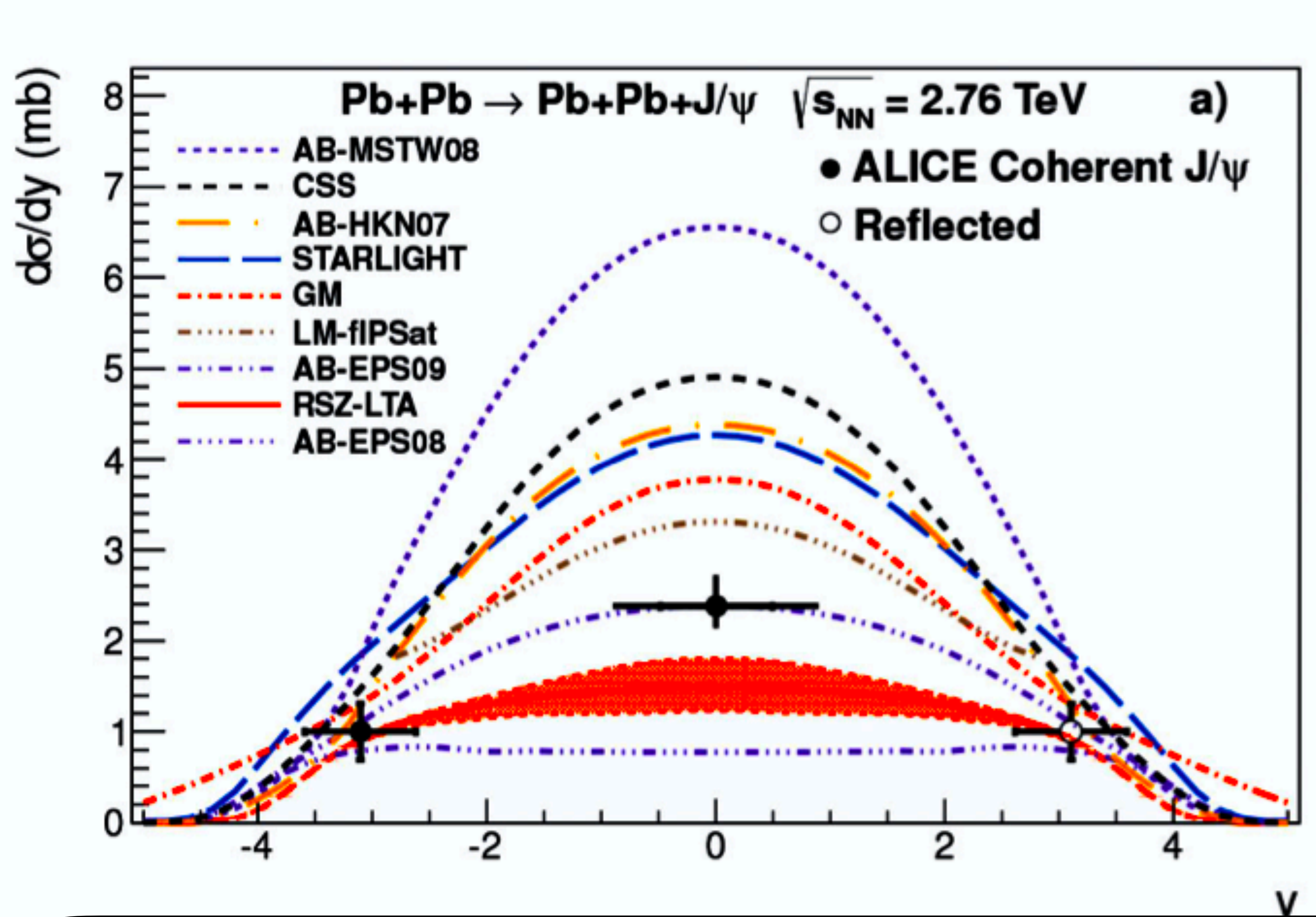

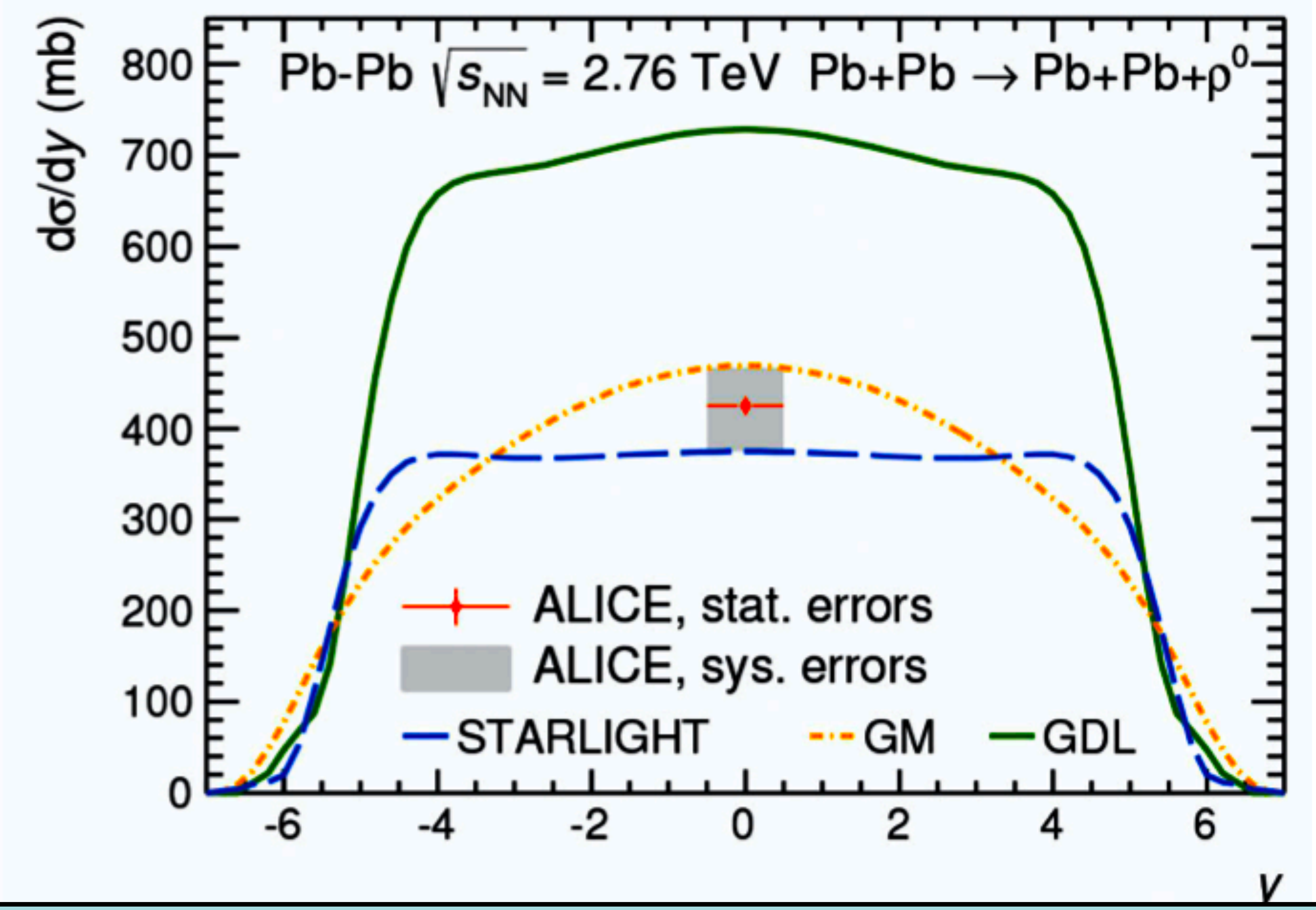

ALICE has measured exclusive coherent and incoherent charmonium production [97-99] and exclusive coherent ρ^0 production [108]: Data show a large discriminatory power on models and gave **first direct evidence of gluon shadowing in nuclei** [100]. They have also been used to test dipole models that describe data in lepton-hadron collisions [101-102].

Some of the recent results from ALICE with LHC Run 2 data

Strangeness enhancement in proton-proton collisions

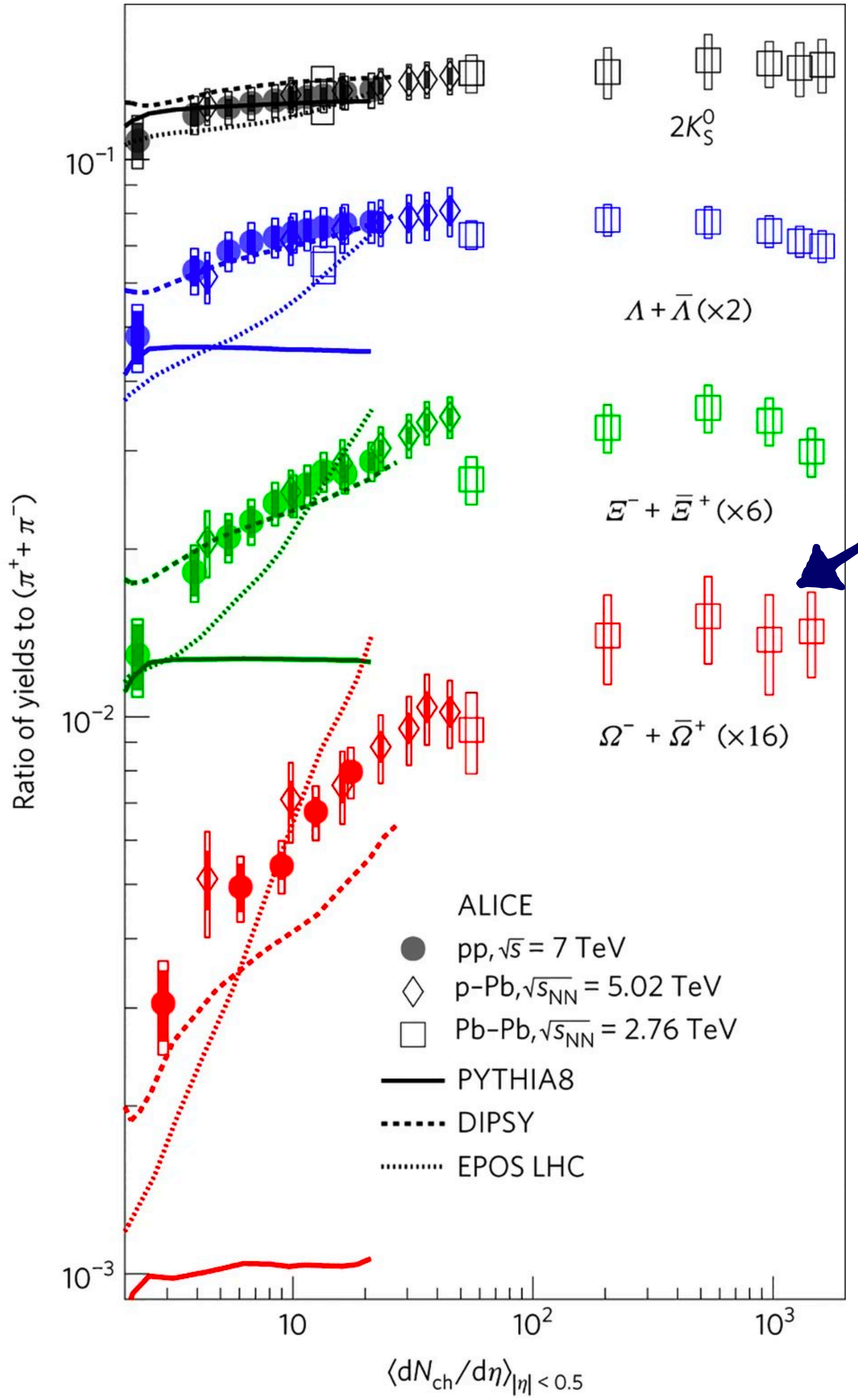

Strangeness enhancement in proton-proton collisions at ALICE increases with the system size and strangeness content of the hadron.

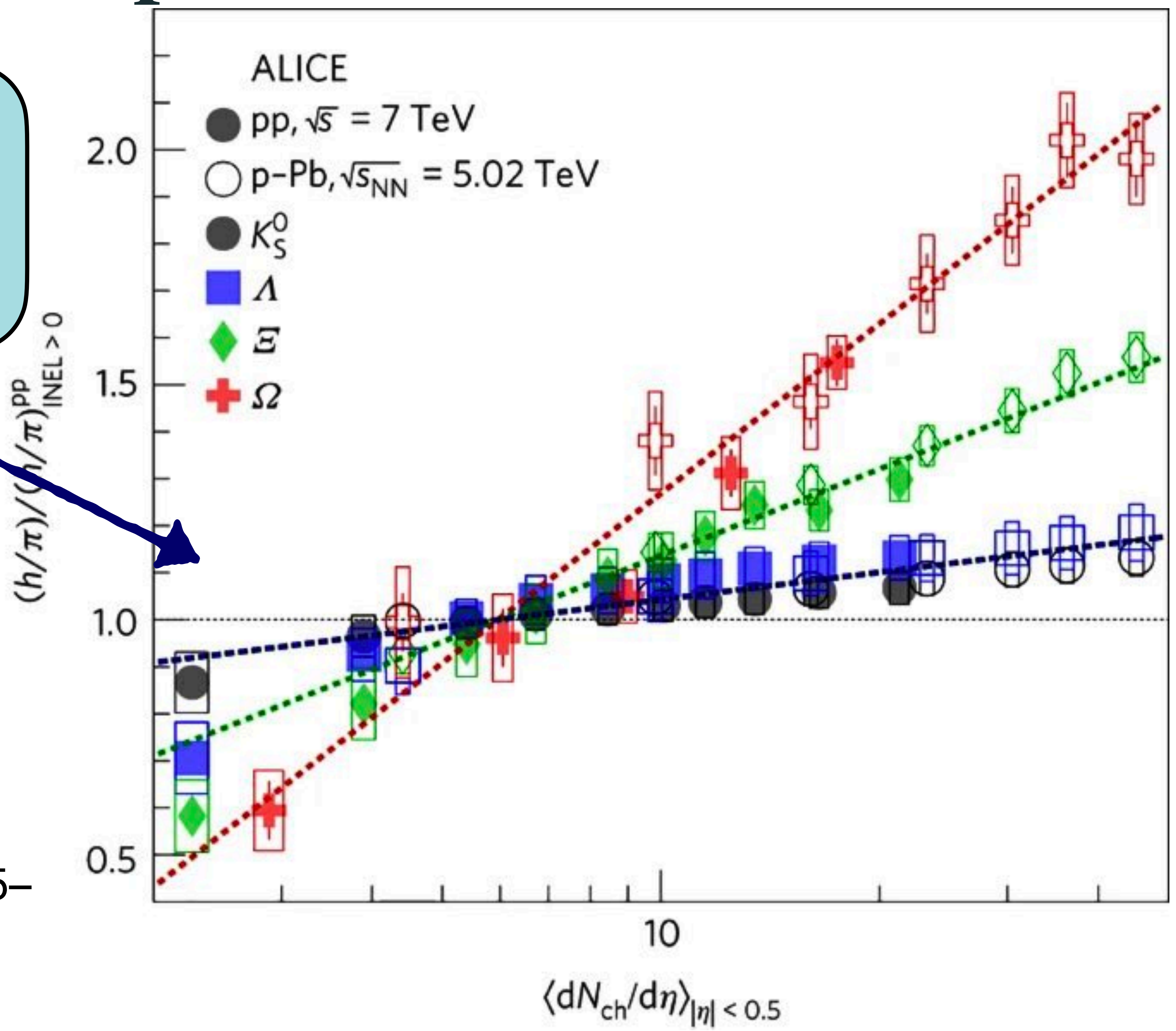

ALICE Collaboration. Nature Physics volume13, pages 535–539 (2017)

Empirical Fit: The observed the observed strangeness hierarchy can be described reasonably well with the empirical formula of the following form:

$$\frac{(h/\pi)}{(h/\pi)^{pp}_{INEL>0}} = 1 + a\, S^b \log\left[\frac{\langle dN_{ch}/d\eta\rangle}{\langle dN_{ch}/d\eta\rangle^{pp}_{INEL>0}}\right] \quad (1)$$

S = Strange Quark content in the hadron

Flow measurements in Run 2 at ALICE

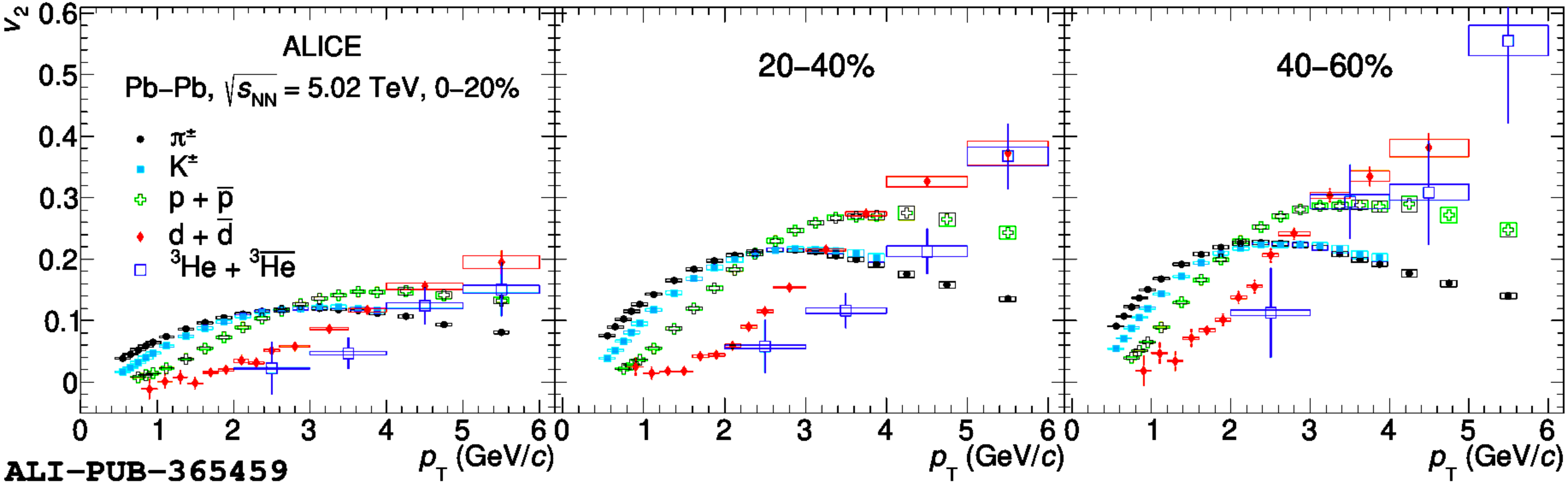

Measured v_2 exhibit mass ordering at low momenta: It is expected from hydro models. The v_2 has been found to be non-zero for D mesons, J/ψ and $\bar{e}$ from b-decay.

Heavier states Υ(1S): v_2 consistent with zero within uncertainties in the measured momentum range → They do not participate in the collective motion in those momentum region.

ALICE Collaboration. Phys. Lett. B **805** (2020) 135414; Phys. Rev. C **102**, 055203 (2020)

Hard and electromagnetic probes: Jet

Measurements of inclusive jet cross-sections in pp collisions for $R = 0.1 - 0.6$ and comparison to NNLO calculations

Large range of R down to low $p_{T,jet}$: Measurements span a range regimes including small- R resummation, and a wide range of non-perturbative effects

(Hadronization-domination at small R and Underlaying Event domination at large R)

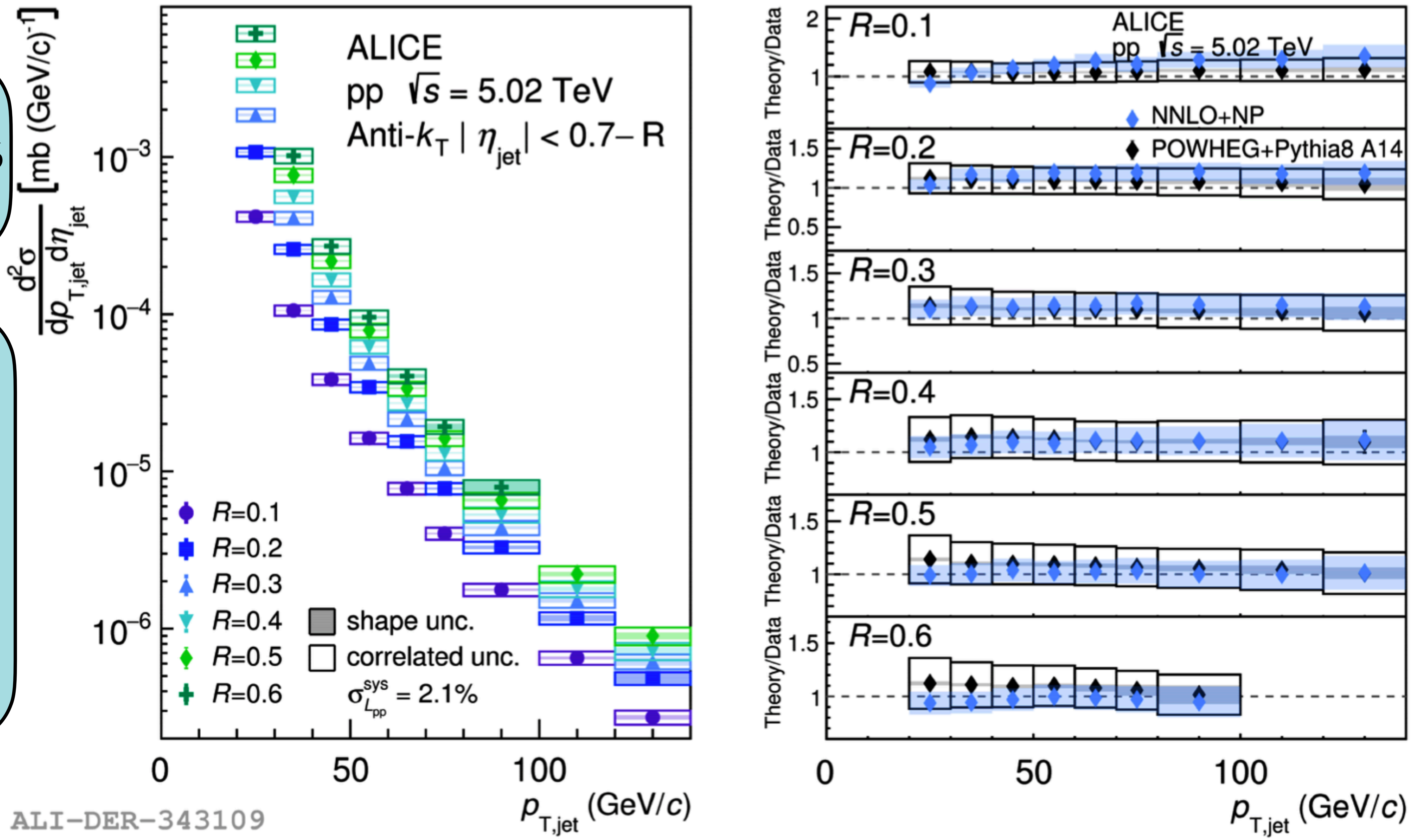

NNLO calculations and POWHEG+PYTHIA8 predictions are consistent with the data for all R and $p_{T,jet}$

It demonstrates the importance of NNLO effects and NLL resummations.

ALICE Collaboration, PRC **101** (2020), 034911.; PRL **118** (2017), 072002.

Jet quenching in a QGP medium

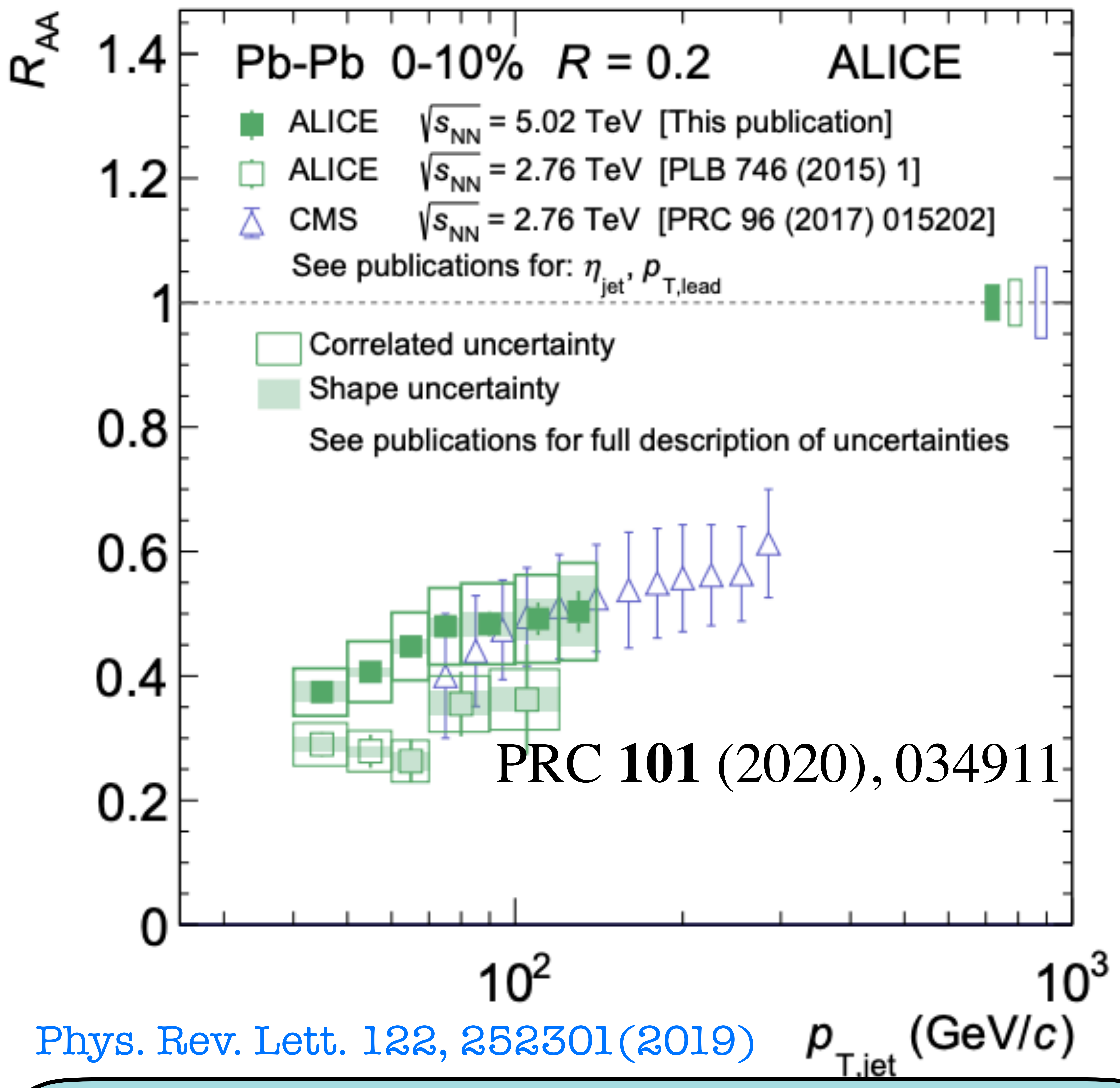

Phys. Rev. Lett. 122, 252301(2019)

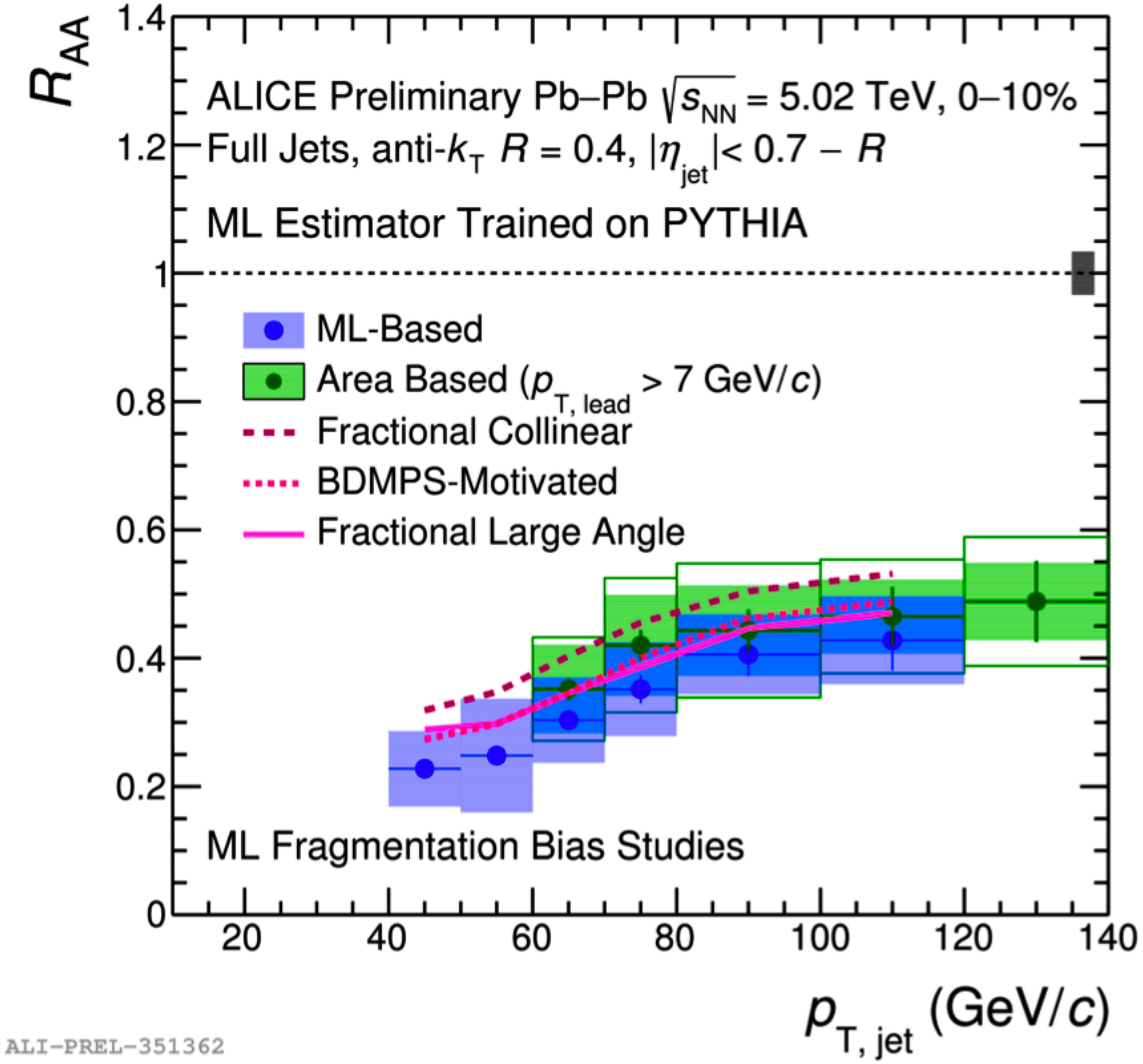

PoS(HardProbes2020)135

Extending measurements to low *p*T and large *R* :
Constrains competing effects between the recovery of out-of-cone radiation and changes in the jet population.

Machine Learning based background correction for Jets:
Inclusive jet suppression measurements down to 40 GeV/c.

Jet quenching in a QGP medium

The R_{AA} was measured for prompt and non-prompt(coming from the decay of beauty hadrons) D0 mesons : **A strong suppression is observed in the R_{AA}.**

The non-prompt D^0 nuclear modification factor is slightly higher than the prompt D^0 value between a transverse momentum of 5 and 10 GeV/c → **Beauty quarks undergo less quenching in the QGP than charm quarks.**

Dead Cone Effect ?

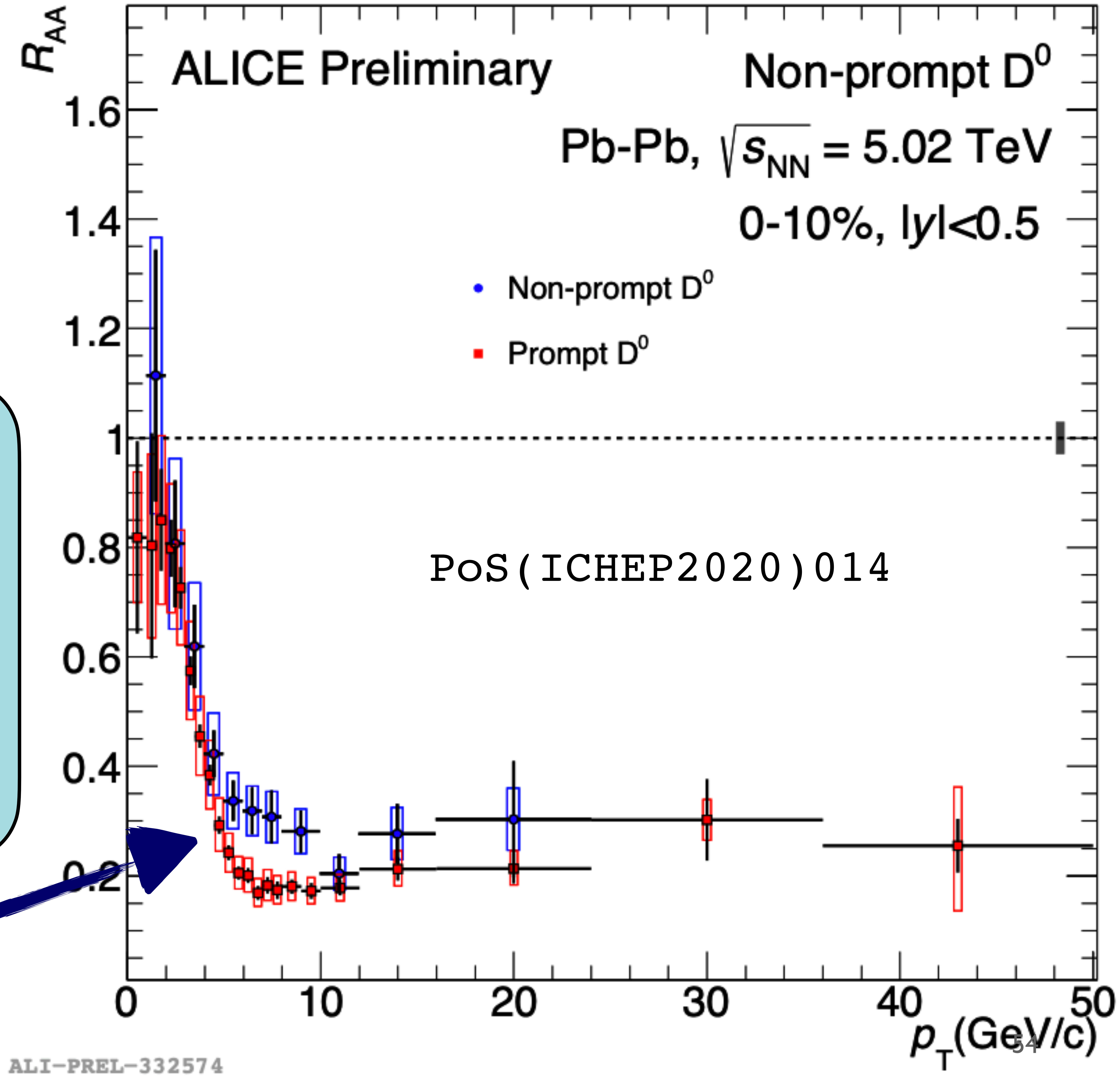

Direct observation of the dead cone effect

Dead cone effect: Collinear gluon emissions are suppressed in $\theta < mq/Eq$, where θ is the emission angle and mq and Eq are the mass and energy of the emitting quark, respectively.

The observable consequence: Charged-particle yield at small angles with respect to the jet axis are expected to be suppressed if the jet originated from a heavy-flavour quark.

Observable and Measurement: The ratio of jet-associated particle yields is plotted as a function of the logarithm of the inverse of the opening angle for inclusive and for D^0–tagged jets.

Observation: At small opening angle θ, D^0–tagged jets only exhibit half of the charged-particle yields than an inclusive jet sample

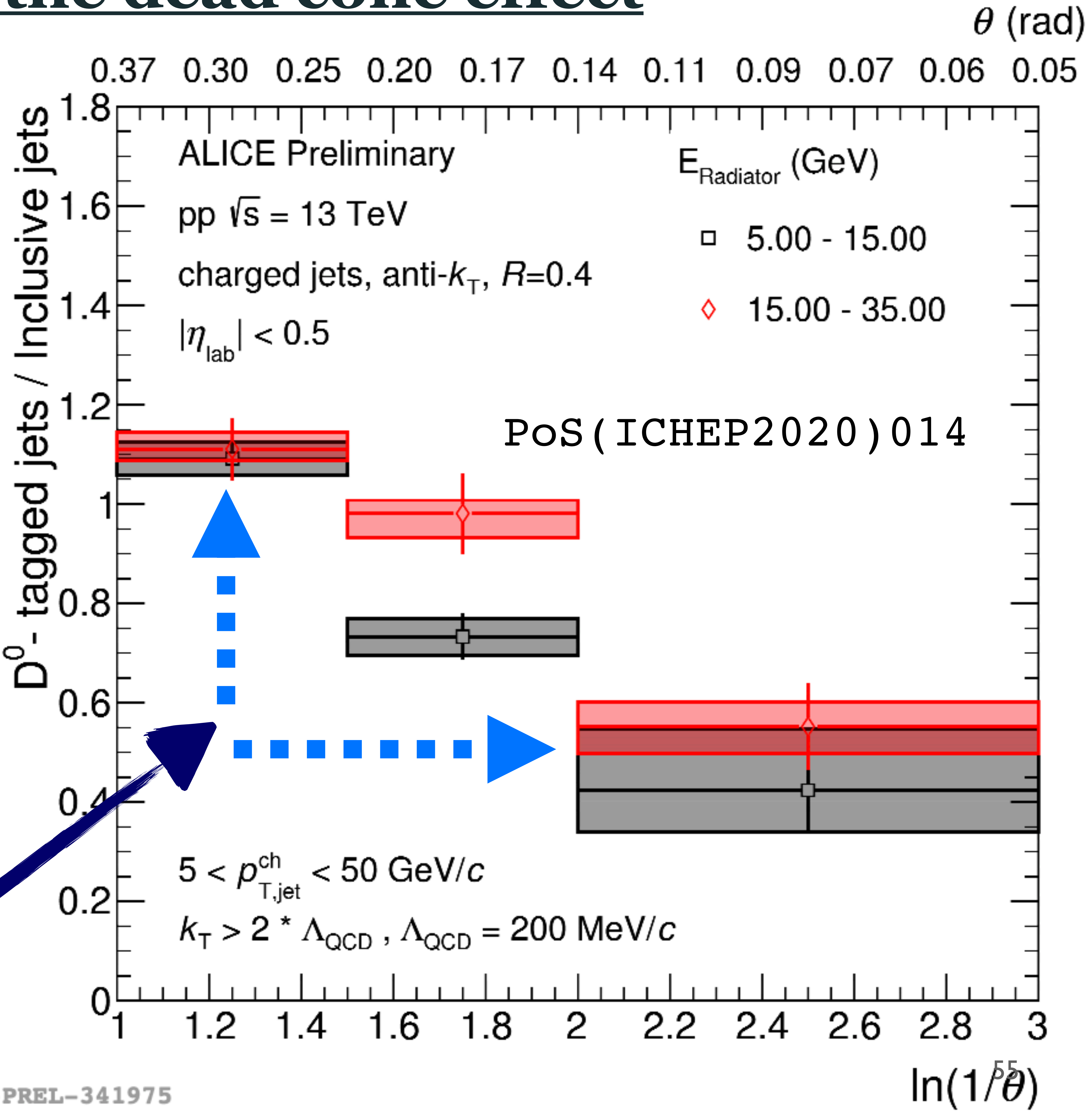

Evidence of Spin-Orbital Angular Momentum Interactions

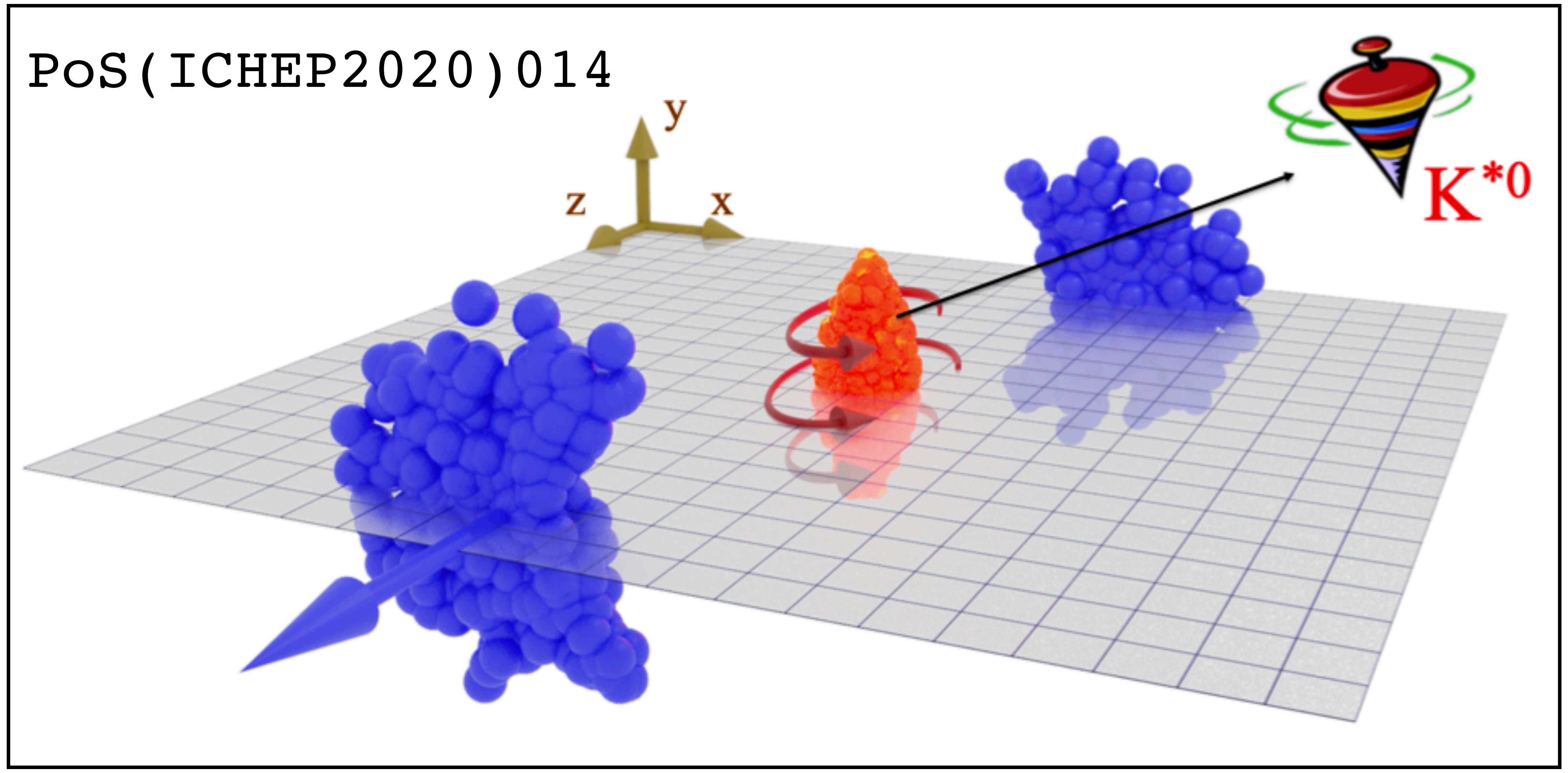

In a semi-central collision, the system, as a whole rotates. : The spin of vector mesons such as K^{*0} is expected to be aligned with that motion. **This is observed in measurements of the spin density matrix element ρ_{00} in Pb-Pb collisions.**

The magnitude of the effect is significantly more pronounced than the Λ polarisation measurements by ALICE and STAR→ **Unresolved problem.**

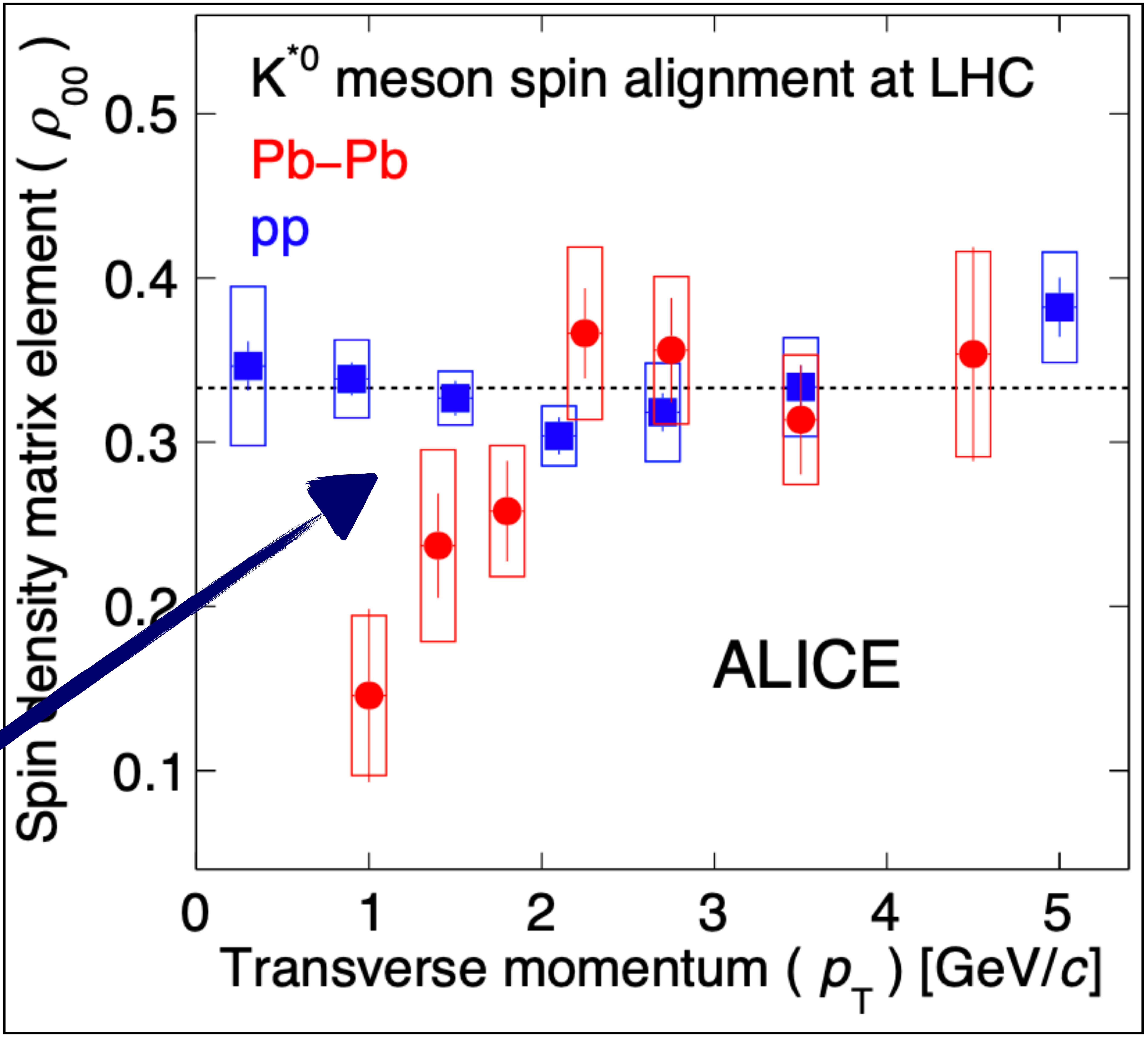

ALICE Collaboration. PRL **125** 012301 (2020)

Proton-hyperon interactions

Proton - hyperon interaction: Can be studied by measuring proton-hyperon pair momentum correlations, which, combined with a determination of the particle-emitting source size, allows for a precise comparison of the interaction characteristics to predictions from lattice QCD.

These measurements are relevant for constraining the E.O.S of neutron stars. This is the first measurement of an attractive strong interaction between protons and Ω baryons.

Experimental $p-\Xi^{-}$ and $p-\Omega^{-}$ CF:

Measured in high-multiplicity pp collisions $\sqrt{s}$ = 13 TeV against predictions from lattice QCD using various combinations of interaction terms.

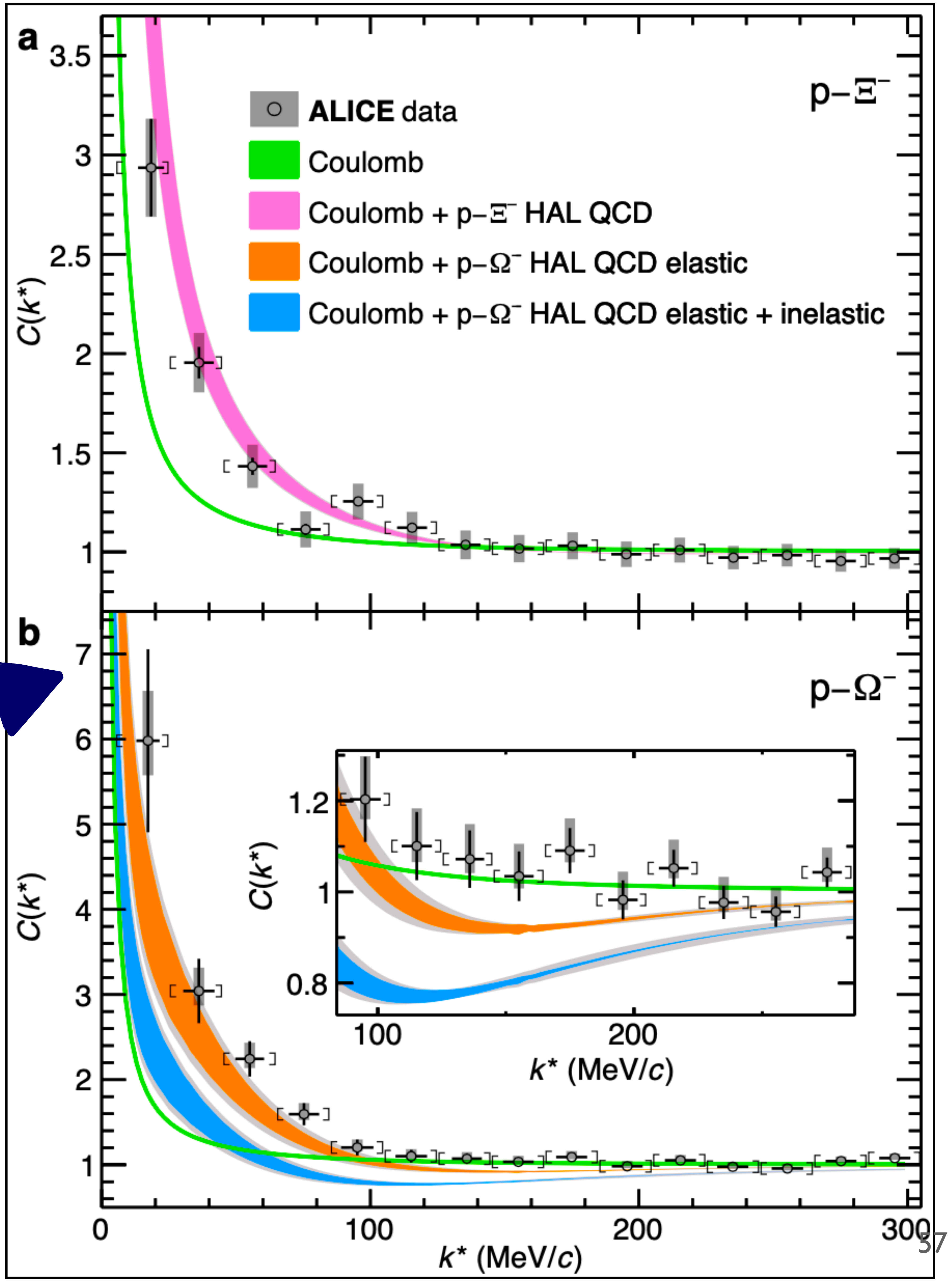

ALICE Collaboration. Nature 588 (2020) 232–238.

Attractive p-φ Interaction

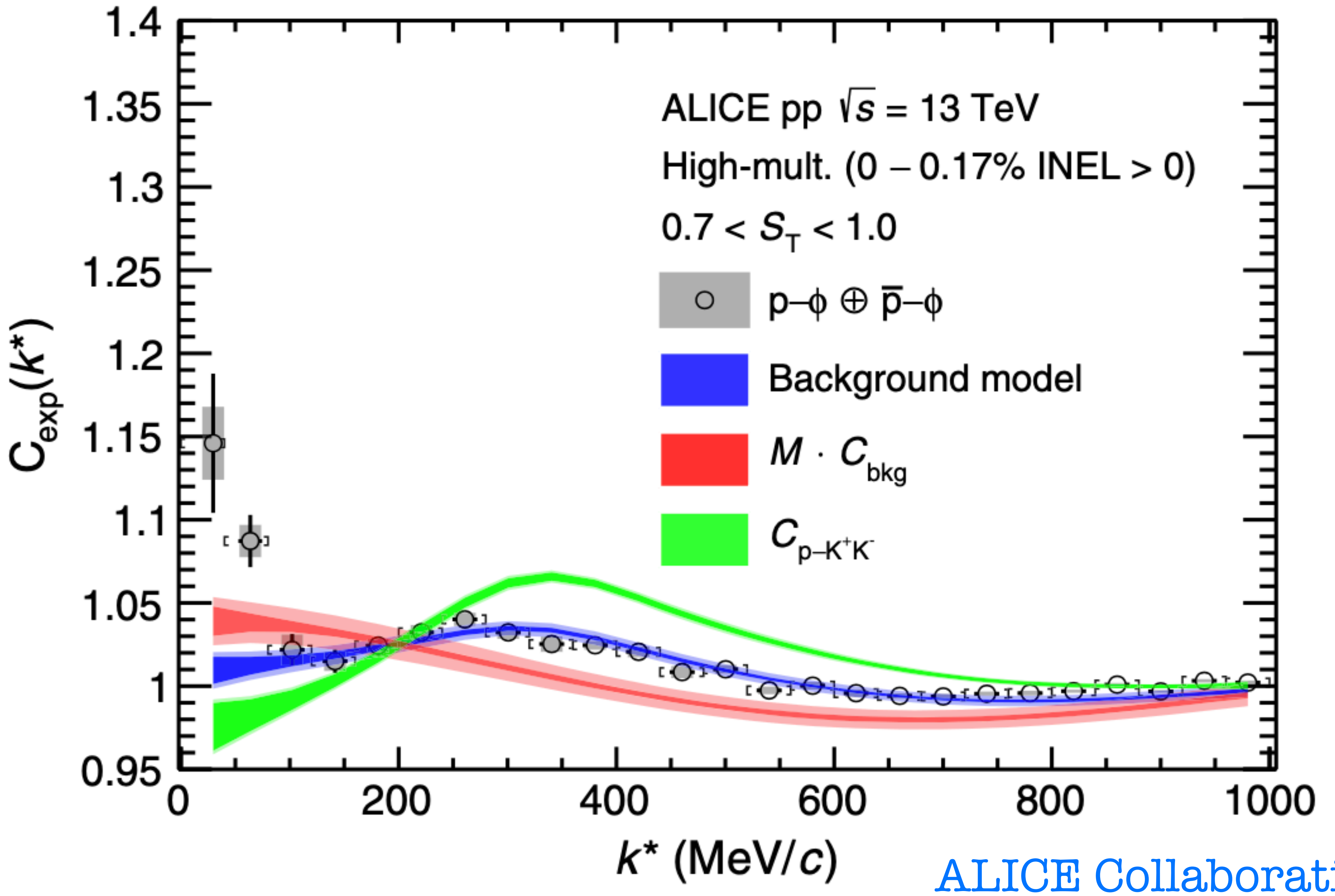

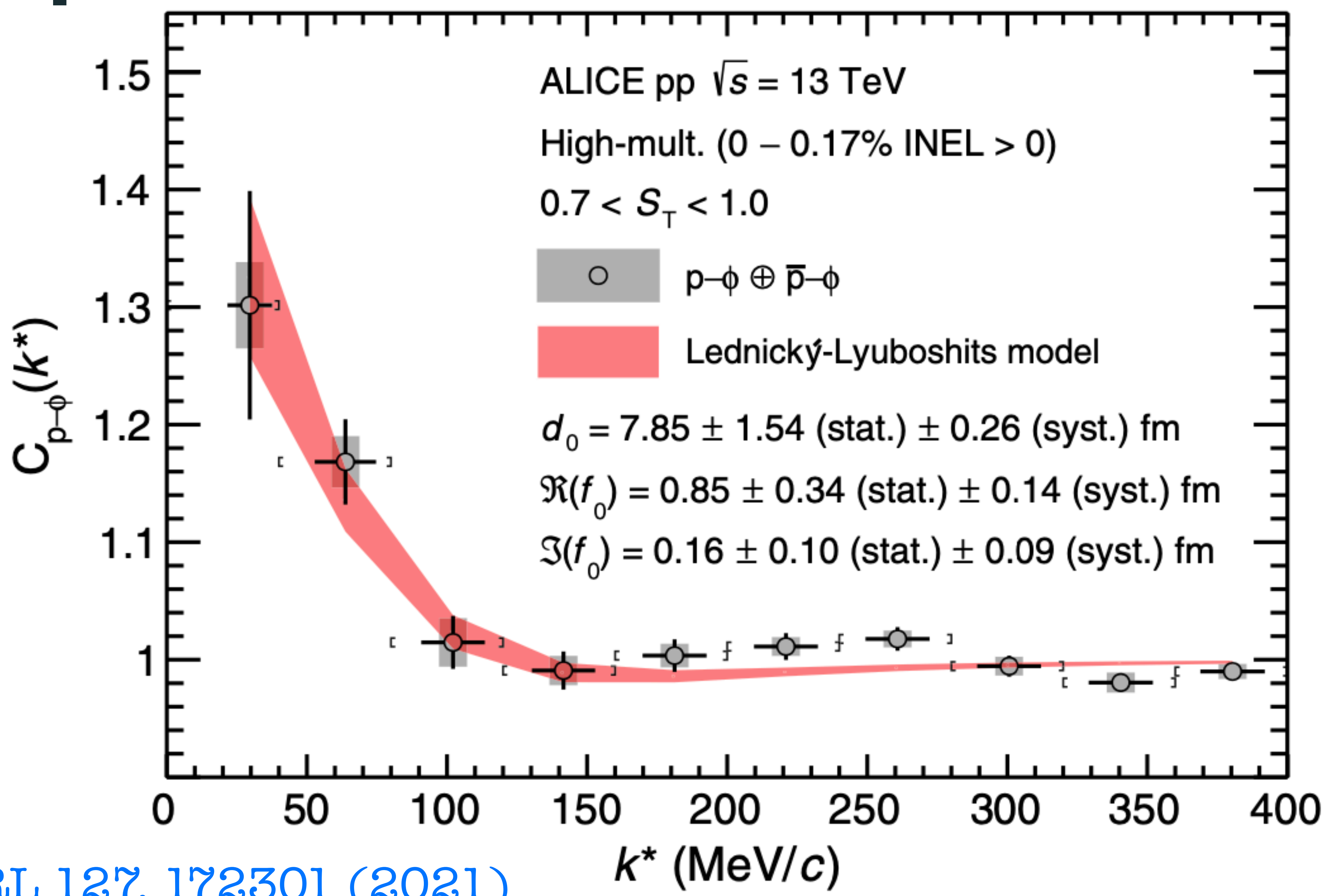

ALICE Collaboration. PRL 127, 172301 (2021)

Demonstrates for the first time that the p-ϕ interaction in vacuum is attractive and dominated by elastic scattering.

- **Lednický-Lyuboshits approach:** The spin- averaged scattering length and effective range of the p-ϕ interaction are extracted from the fully corrected correlation function.
- **Gaussian- and Yukawa-type potential analysis:** N-ϕ coupling constant is found to be $g_{N-\phi} = 0.14 \pm 0.03(stat) \pm 0.02(sys)$
- **Input to accomplish a self-consistent description of the N-ϕ interaction:** Relevant for the studies on partial restoration of chiral symmetry in nuclear medium.

References

1. PHYS.LETT.B 523227 (2001)
2. PHYS.REV.LETT. 88202301 (2002)
3. PHYS.REV.C 65061901 (2002)
4. PHYS.REV.C 70054907 (2004)
5. PHYS.REV.C 71034908 (2005)
6. PHYS. LETT. B 710, 363 (2012)
7. JHEP 08, 141 (2011)
8. PHYS. REV. LETT. 106, 032301 (2011)
9. J. PHYS. G 35 , 5 (2008) 054001.20
10. PHYS. LETT. B 701, 133 (2011)
11. PHYS. REV. LETT. 94, 022002 (2005)
12. NUCL. PHYS. A 747, 609 (2005)
13. ARXIV:1011.5161 [HEP-PH].
14. PHYS. LETT. B 726, 610 (2013)
15. ARXIV:1509.07299 [NUCL-EX].
16. PHYS. LETT. B 736, 196 (2014)
17. ARXIV:1506.07287 [NUCL-EX].
18. PHYS. REV. LETT. 101, 232301 (2008)
19. PHYS. REV. C 82, 011902 (2010)
20. PHYS. REV. LETT. 108, 072302 (2012)
21. EUR. PHYS. J. C 55, 293 (2008)
22. PHYS. REV. LETT. 86, 402 (2001)
23. NUCL. PHYS. A 757, 1 (2005)
24. NUCL. PHYS. A 757, 28 (2005)
25. NUCL. PHYS. A 757, 102 (2005)
26. NUCL. PHYS. A 757, 184 (2005)
27. PHYS. REV. LETT. 87, 182301 (2001)
28. NUCL. PHYS. A 761, 296 (2005)
29. PHYS. REV. LETT. 105, 252302 (2010)
30. PHYS. LETT. B 707, 330 (2012)
31. PHYS. REV. LETT. 109, 022301 (2012)
32. PHYS. REV. C 86, 054908 (2012)
33. JHEP 06, 190 (2015)
34. PHYS. REV. LETT. 106, 192301 (2011)
35. PHYS. REV. C 90, 054901 (2014)
36. PHYS. REV. C 86, 014907 (2012)
37. PHYS. REV. LETT. 107, 032301 (2011)
38. PHYS. REV. C 89, 044906 (2014)
39. NUCL. PHYS. A 810, 91 (2008)
40. PHYS. REV. LETT. 104, 062301 (2010)

References

41. PHYS. REV. C 80, 064912 (2009)
42. PHYS. REV. C 90, 044906 (2014)
43. PHYS. LETT. B 718, 795 (2013)
44. PHYS. LETT. B 719, 29 (2013)
45. PHYS. REV. LETT. 110, 182302 (2013)
46. ARXIV:1506.08032
47. PHYS. LETT. B 726, 164 (2013)
48. PHYS. LETT. B 724, 213 (2013)
49. ANNU. REV. NUCL. PART. SCI. 55, 357 (2005)
50. PHYS. LETT. B 356, 525 (1995)
51. PHYS. LETT. B 696, 328 (2011)
52. NUCL. PHYS. A 929, 1 (2014)
53. PHYS. REV. C 69, 034910 (2004)
54. PHYS. REV. LETT. 91, 172302 (2003)
55. PHYS. REV. LETT. 91, 072304 (2003)
56. PHYS. REV. LETT. 97, 052301 (2006)
57. PHYS. REV. LETT. 95, 152301 (2005)
58. ARXIV:1504.04337 [HEP-EX].
59. EUR. PHYS. J. C 72, 1945 (2012)
60. PHYS. LETT. B 720, 52 (2013)
61. PHYS. REV. C 86, 064904 (2012)
62. JHEP 03, 013 (2014)
63. PHYS. LETT. B 719, 220 (2013)
64. PHYS. REV. LETT. 111, 152301 (2013)
65. ARXIV:1509.07334 [NUCL-EX].
66. JHEP 10, 087 (2012)
67. PHYS. LETT. B 730, 243 (2014)
68. PHYS. REV. C 90, 024908 (2014)
69. PHYS. LETT. B 739, 320 (2014)
70. J. PHYS. G 38, 035006 (2011)
71. PHYS. REV. LETT. 106, 162302 (2011) 108, 189904(E) (2012)
72. PHYS. LETT. B 713, 224 (2012)
73. PHYS. REV. C 84, 024907 (2011)
74. EUR. PHYS. J. C 71, 1650 (2011)
75. PHYS. REV. C 85, 064908 (2012)
76. JHEP 02, 022 (2013)
77. JHEP 03, 080 (2013)
78. PHYS. LETT. B 725, 357 (2013)
79. PHYS. LETT. B 744, 284 (2015)
80. PHYS. LETT. B 737, 298 (2014)

References

81. PHYS. REV. D 71, 054027 (2005)
82. PHYS. REV. LETT. 112, 042302 (2014)
83. ARXIV:1506.06604 [NUCL-EX]
84. ARXIV:1506.08804 [NUCL-EX].
84. PHYS. LETT. B 734, 314 (2014)
86. NUCL. PHYS. A 859, 114 (2011)
87. PHYS. REV. C 89, 054911 (2014)
88. J. PHYS. G 38, 124081 (2011)
89. PHYS. LETT. B 731, 57 (2014)
90. ARXIV:1509.07324 [NUCL-EX]
91. JHEP 10, 119 (2013)
92. PHYS. REV. D 48, 3136 (1993)
93. J. PHYS. G 23, A1 (1997)
94. ARXIV:1509.06738 [HEP-PH]
95. ARXIV:1409.4456 [NUCL-EX]
96. PHYS. REP. 458, 1 (2008)
97. PHYS. LETT. B 718, 1273 (2013)
98. EUR. PHYS. J. C 73, 2617 (2013)
99. ARXIV:1508.05076 [NUCL-EX]
100. PHYS. LETT. B 726, 290 (2013)
101. AIP CONF. PROC. 1654, 100002 (2015).
102. PHYS. REV. C 87, 032201 (2013)
103. PHYS. REV. C 83, 024913 (2011)
104. PHYS. REV. C 68, 044902 (2003)
105. PHYS. LETT. B 741, 38 (2015)
106. PHYS. REV. C 90, 034904 (2014)
107. PHYS. REV. C 84, 054912 (2011)
108. ARXIV:1503.09177

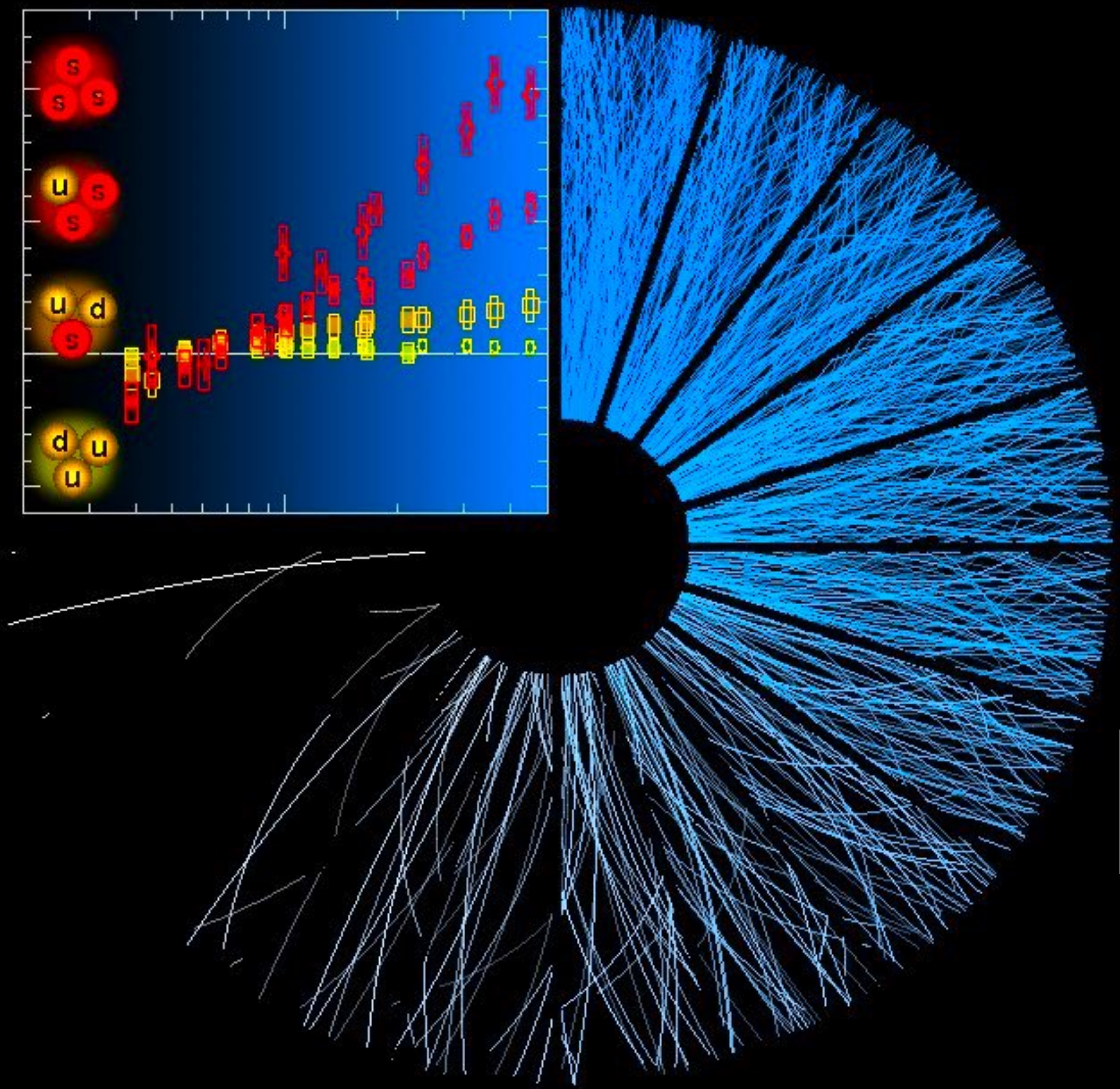

THANK YOU!

Picture Courtesy: CERN

Backup Slides

TOPIC: 1

Strangeness enhancement in high-multiplicity proton–proton collisions at the ALICE experiment

Why strangeness enhancement is expected in quark gluon plasma?

Müller and Rafelski found that $s\bar{s}$ production in QGP is dominated by $gg \to s\bar{s}$ channel, leading to equilibration times comparable to the QGP lifetime.

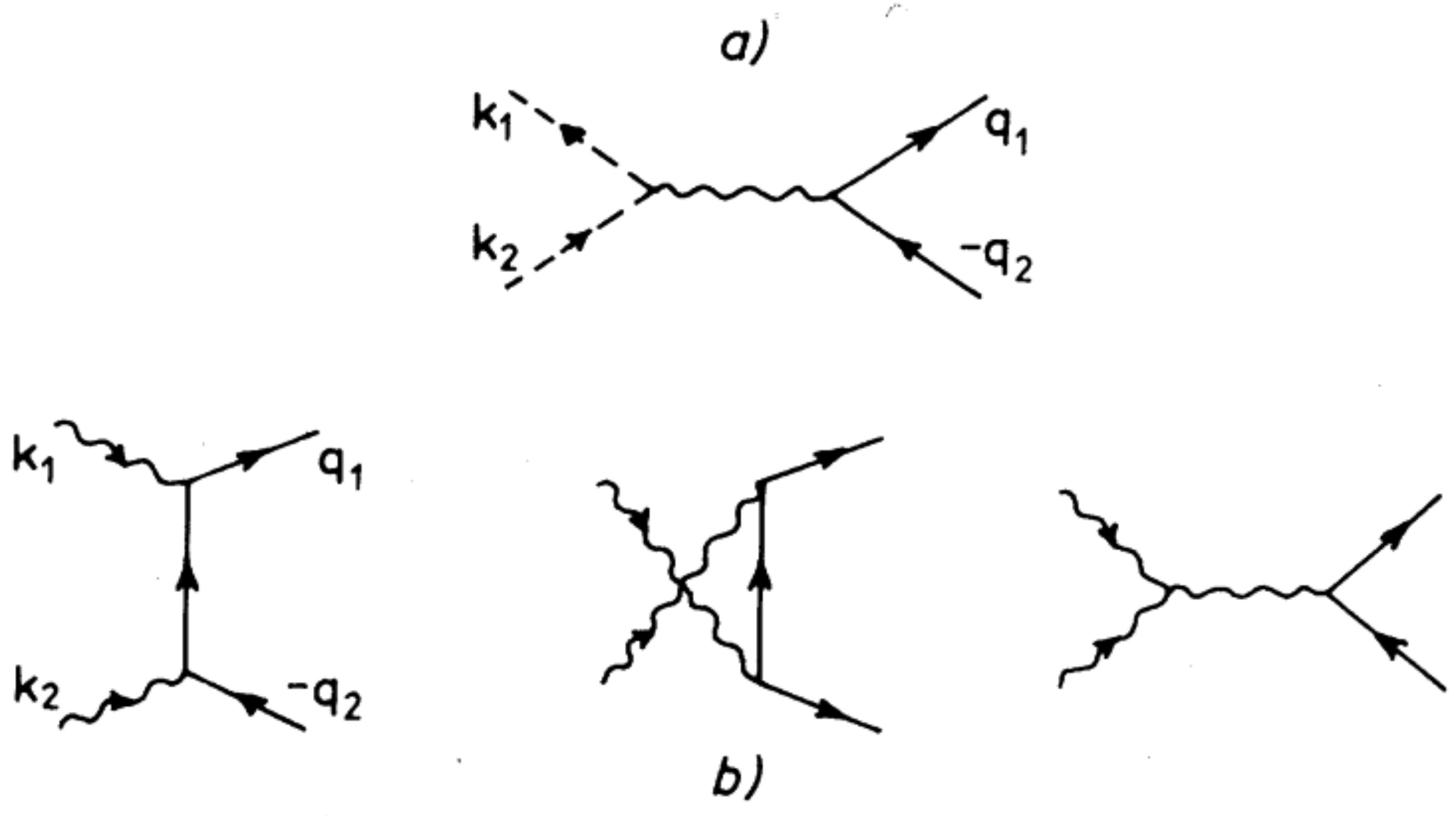

FIG. 1. Lowest-order QCD diagrams for $s\bar{s}$ production: (a) $q\bar{q} \to s\bar{s}$, (b) $gg \to s\bar{s}$.

Strangeness enhancement is expected due to:

1. The dominance of the gluonic production channel for strangeness in the QGP
2. High gluon density in the QGP
3. m_S being similar to the critical temperature for the QCD phase transition

Reference: Strangeness Production in the Quark-Gluon Plasma. Johann Rafelski and Berndt Müller. Phys. Rev. Lett. 48, 1066 (1982)

Why strangeness enhancement is expected in quark gluon plasma?

1. Koch-Müller-Rafelski found that with $m_S = 0.5 - 1.0 \times T_C$ the strangeness formation time is similar to the expected lifetime of the QGP.

2. If one assumes $T_C \approx 200$ **MeV,** the mass range for this to happen is m_s **=100-200 MeV**

3. From PDG: The physical mass of strange quark is 95^{+9}_{-3} **MeV.**

4. This means that the strangeness chemical equilibration in QGP is possible, leading to abundant strange quark density in QGP

5. We therefore we expect to have a Quark Gluon Plasma made of u,d,s quarks and gluons.

6. **Strangeness as a part of the QGP itself:** Hence an enhanced production of hadrons with strange quarks is considered as a signature for the existence of QGP.

Reference: Koch, P., Müller, B. & Rafelski, J.
Strangeness in relativistic heavy ion collisions. Phys. Rep. 142, 167–262 (1986).

Strangeness enhancement in heavy-ion collisions at SPS

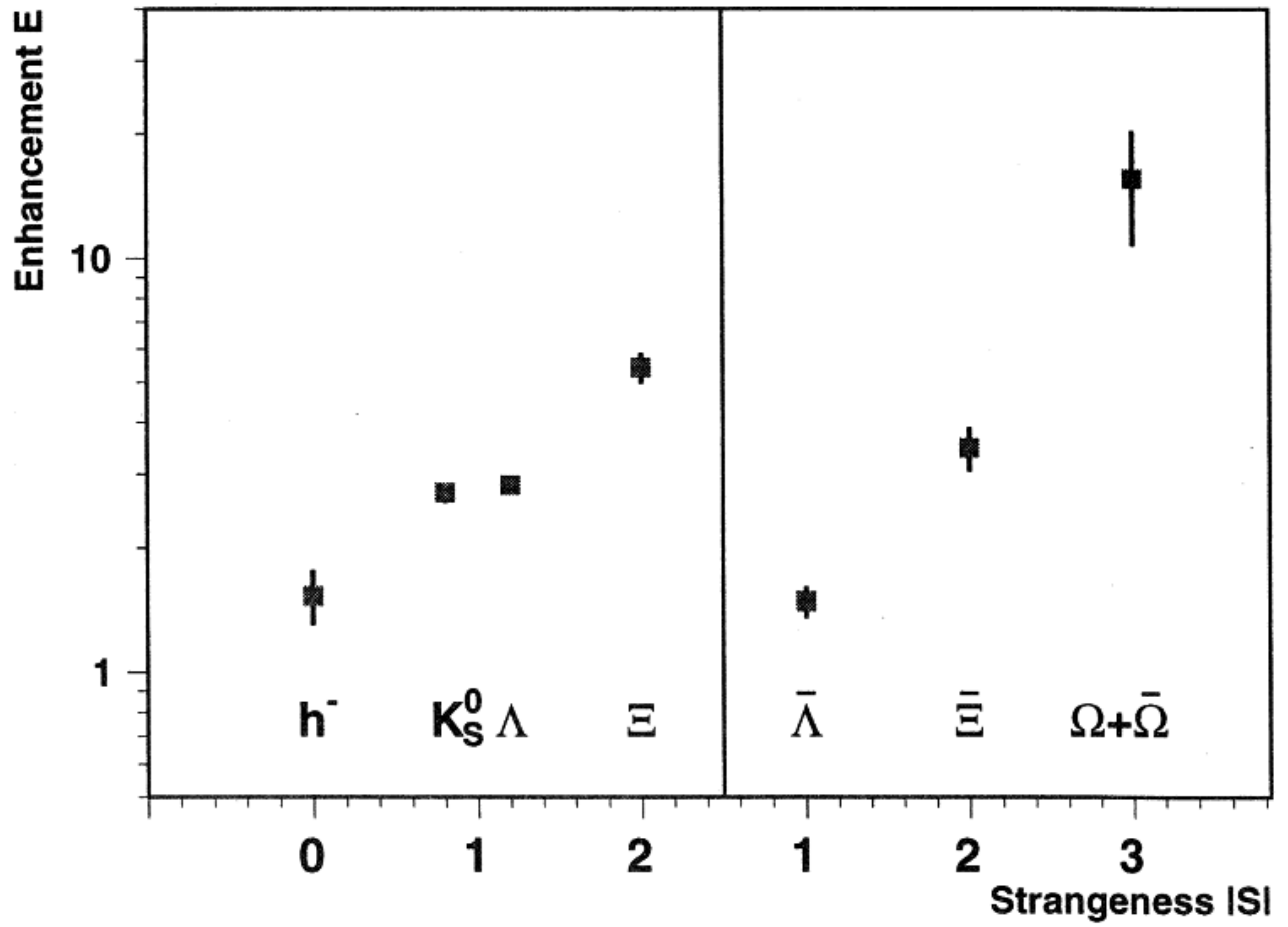

Fig. 4. Strange particle enhancement versus strangeness content.

Yield per Event

$$Y = \int_0^\infty dp_T \int_{y_{cm}-0.5}^{y_{cm}+0.5} dy \frac{d^2N}{dy\,dp_T}$$

Enhancement

$$E = \left(\frac{\langle Y \rangle}{\langle N_{part} \rangle} \right)_{Pb-Pb} \Bigg/ \left(\frac{\langle Y \rangle}{\langle N_{part} \rangle} \right)_{p-Pb}$$

$$E(\Omega^- + \overline{\Omega}^+) > E(\overline{\Xi}^+) > E(\overline{\Lambda})$$

and

$$E(\Xi^-) > E(\Lambda) \approx E(\mathrm{K}^0_\mathrm{S}).$$

Strangeness enhancement at WA97

- All yields appear to increase with centrality from p–Pb to Pb–Pb faster than linearly with the number of participants

- The enhancement is more pronounced for multi-strange particles, and exceeds one order of magnitude in the case of Ω

Reference: Andersen, E. et al. (WA97 Collaboration)
Strangeness enhancement at mid-rapidity in Pb–Pb collisions at 158 AGeV/c. Phys. Lett. B 449, 401–406 (1999).

Strangeness enhancement in heavy-ion collisions at RHIC

Yield per Event

$$Y = \int_0^\infty dp_T \int_{y_{cm}-0.5}^{y_{cm}+0.5} dy \frac{d^2N}{dy dp_T}$$

Enhancement

$$E = \left(\frac{\langle Y \rangle}{\langle N_{part} \rangle} \right)_{Pb-Pb} \Bigg/ \left(\frac{\langle Y \rangle}{\langle N_{part} \rangle} \right)_{p-p}$$

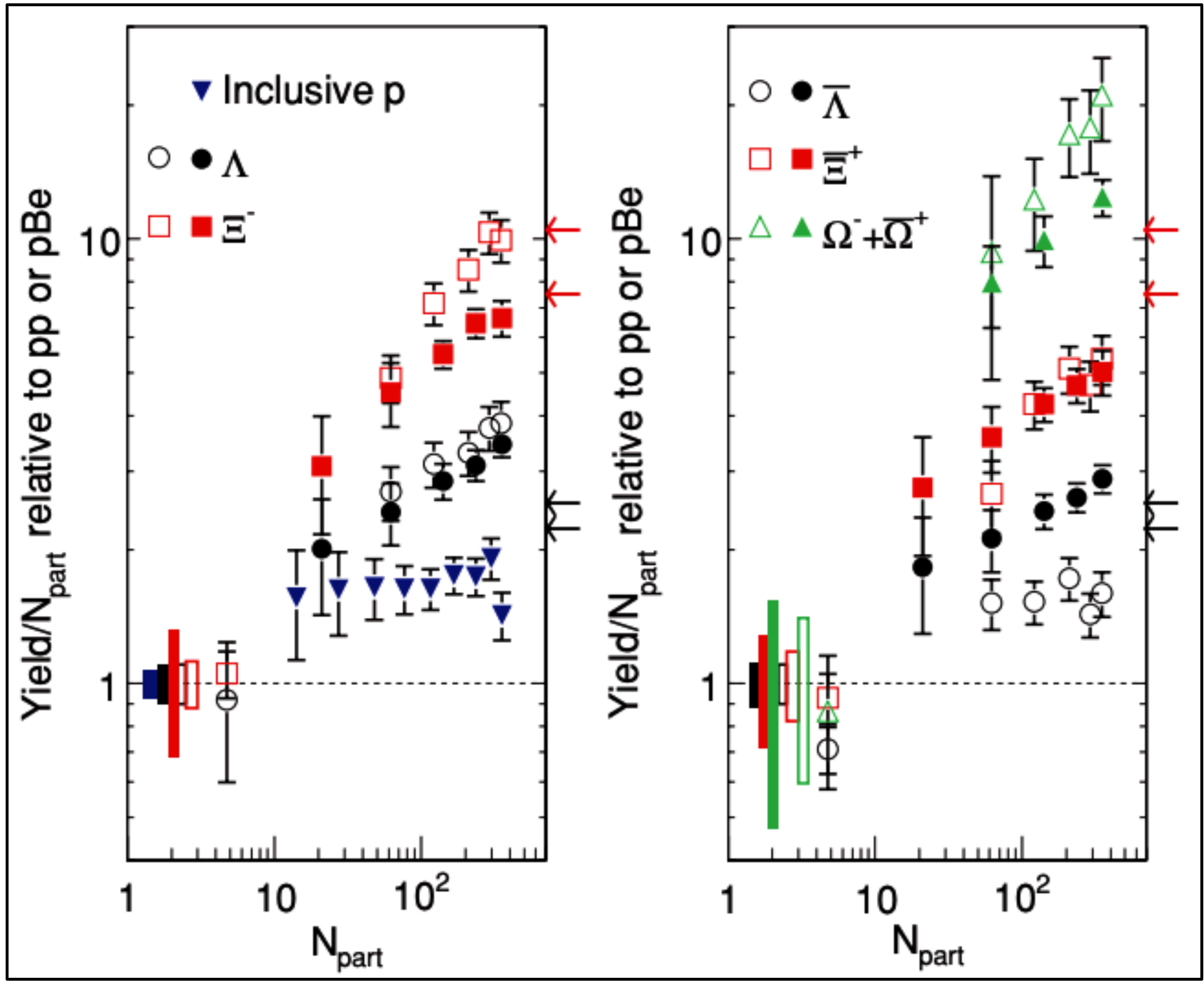

Strangeness enhancement at STAR

- An enhanced strange baryon midrapidity production is observed in Au+Au collisions at $\sqrt{s} = 200$ GeV
- The enhancement is pronounced for more central events, when compared to the N_{part} scaled p-p data from the same energy.

Enhancement hierarchy

$$E(\Omega) > E(\Xi) > E(\Lambda)$$

Reference: Abelev, B. I. et al. (STAR Collaboration)
Enhanced strange baryon production in Au+Au collisions compared to p+p at . Phys. Rev. C 77, 044908 (2008).

Strangeness enhancement in heavy-ion collisions at LHC

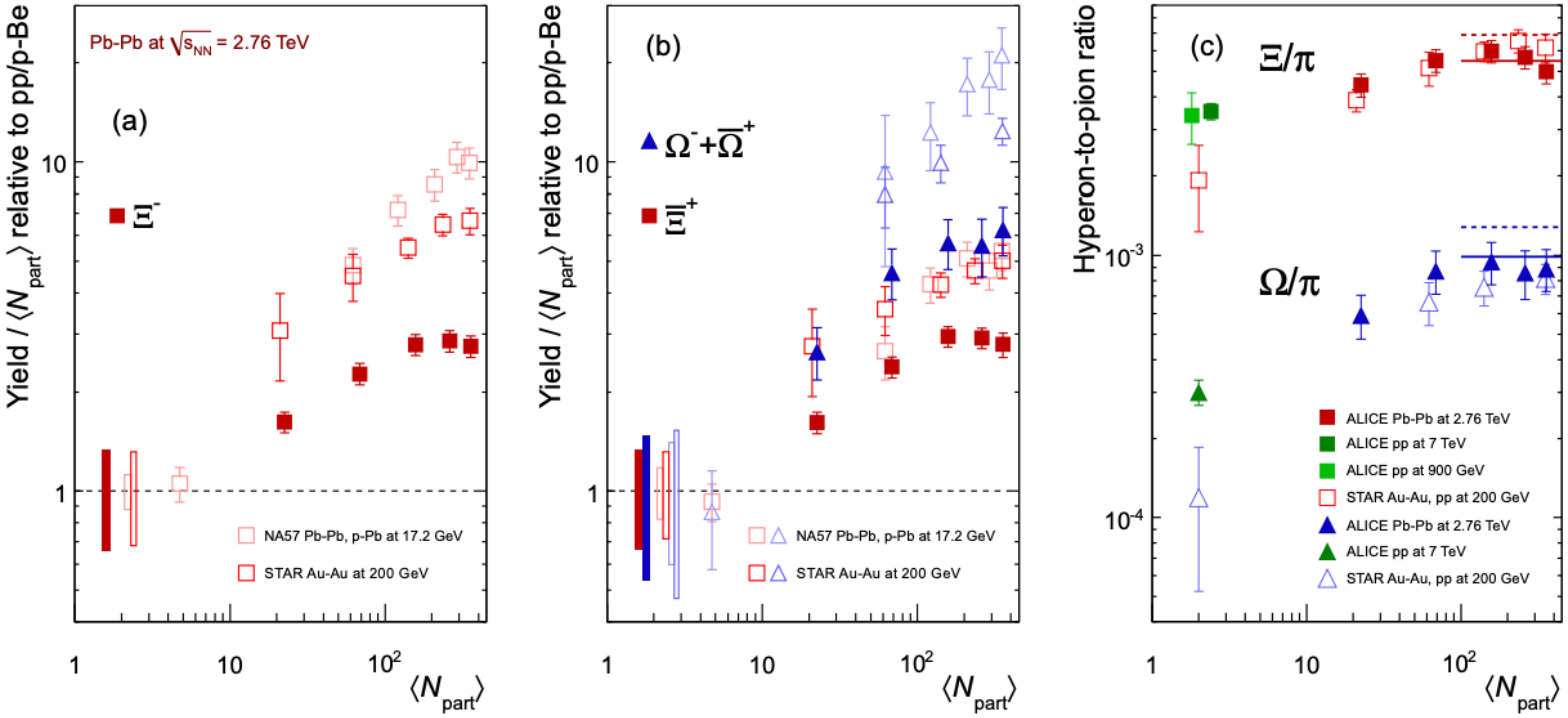

Strangeness enhancement at ALICE

- An enhanced strange baryon mid-rapidity production is observed in Pb-Pb collisions at $\sqrt{s} = 2.76$ TeV
- The enhancements relative to pp increase both with the strangeness content of the baryon and with centrality, but are less pronounced than at lower energies.

Phys. Lett. B 728, 216–227; erratum 734, 409 (2014).

Motivation to study strangeness enhancement in pp collisions

General Expectation

Proton-Proton Collisions :

Relativistic Heavy-Ion Collisions :

Nuclear Modification factor.

$$R_{AA} = \frac{1}{N}\frac{(dN/dp_T)_{AA}}{(dN/dp_T)_{pp}}$$

Extensively used to study QGP formation and QGP induced effects in Heavy-Ion collisions.

It is very crucial to be sure that there is no significant QGP effects formed during a proton proton collision for relying on such observables where they are taken as a bench mark to interpret heavy-ion collision results

ALICE Experiment and Particle Identification(PID)

Charged hadrons are unambiguously identified if their mass and charge are determined

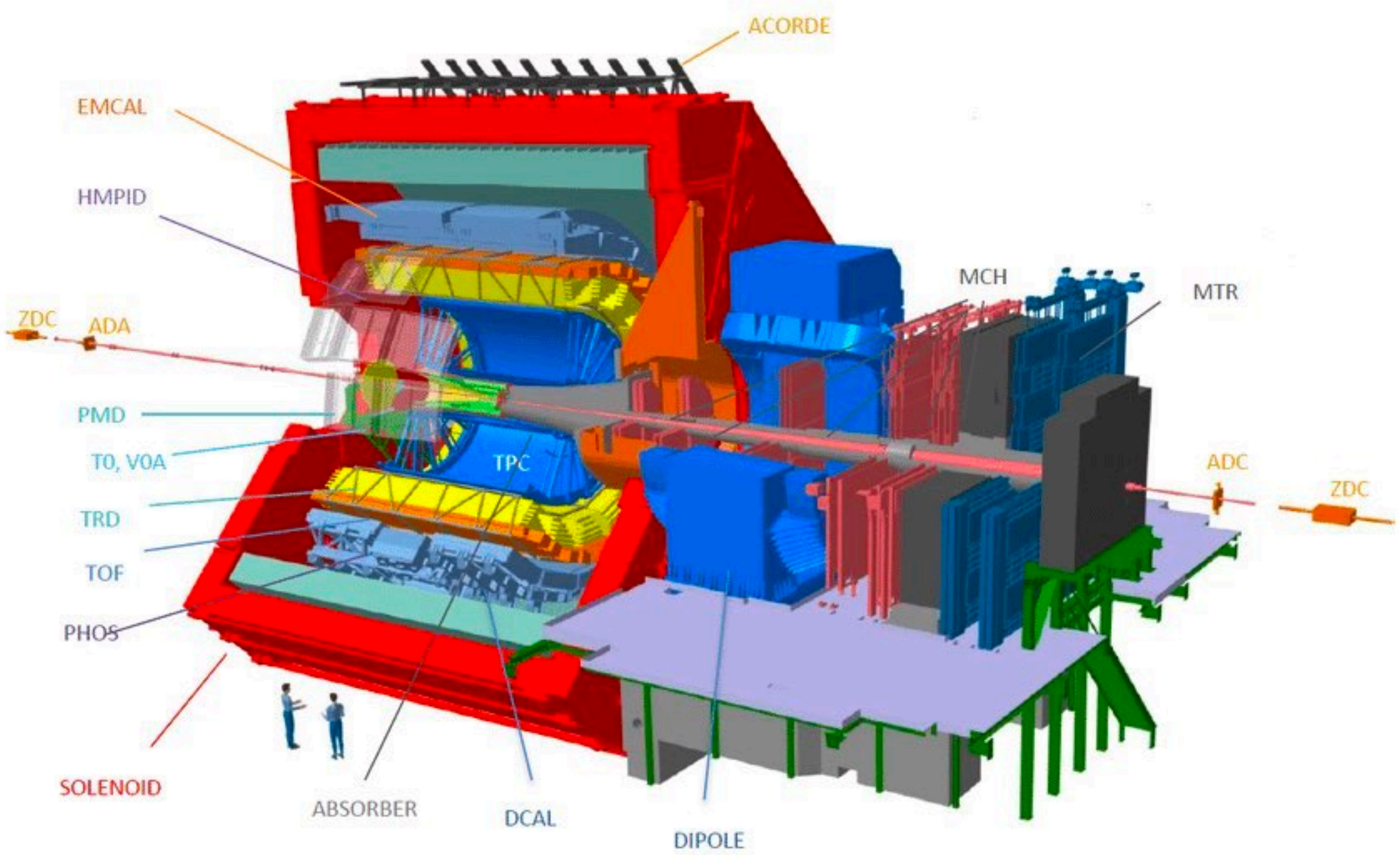

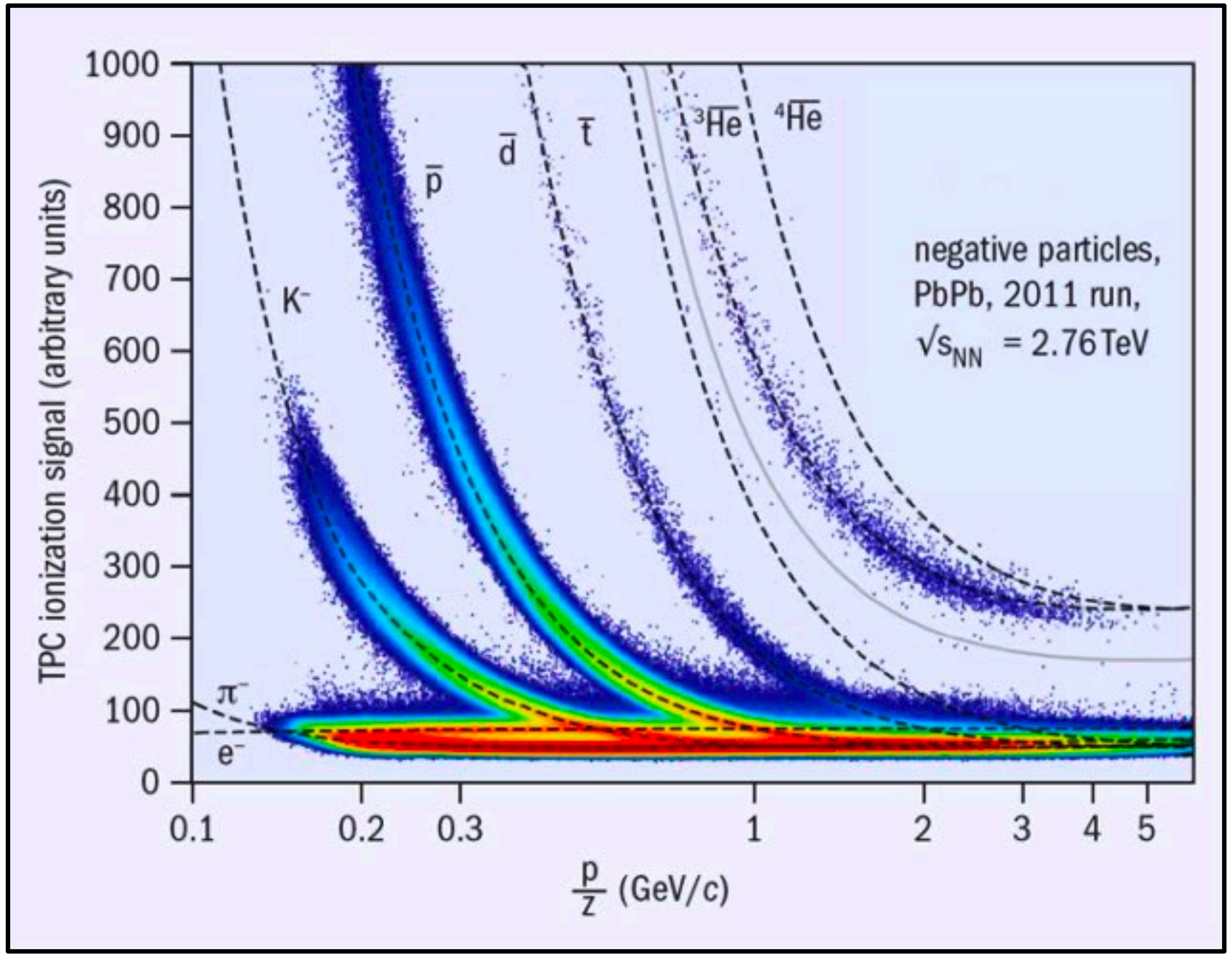

The characteristics of the ionization process caused by fast, charged particles passing through a medium can be used for PID. The velocity dependence of the ionization strength is connected to the Bethe-Bloch formula, which describes the average energy loss of charged particles through inelastic Coulomb collisions with the atomic electrons of the medium.

Strangeness enhancement in pp collisions in ALICE at $\sqrt{s} = 7$ TeV

- Multi-strange baryons are measured through the reconstruction of the cascade topology of the following weak decays
  1. $\Xi^- \rightarrow \Lambda + \pi^-$ (Branching Ratio 99.9%)
  2. $\Omega^- \rightarrow \Lambda + K^-$(67.8%)
     A. Subsequent decay $\Lambda \rightarrow p + \pi^-$ (63.9%) and their charge conjugates for the anti-particle decays.
     B. B.R = 63.9% and 43.3% for the Ξ and the Ω respectively.
- Candidates are found by combining charged tracks reconstructed in the ITS and TPC volume

The figure shows the transverse momentum distribution of hyperons originated from the proton proton collisions at $\sqrt{s} = 7$ TeV measured in the ALICE experiment.

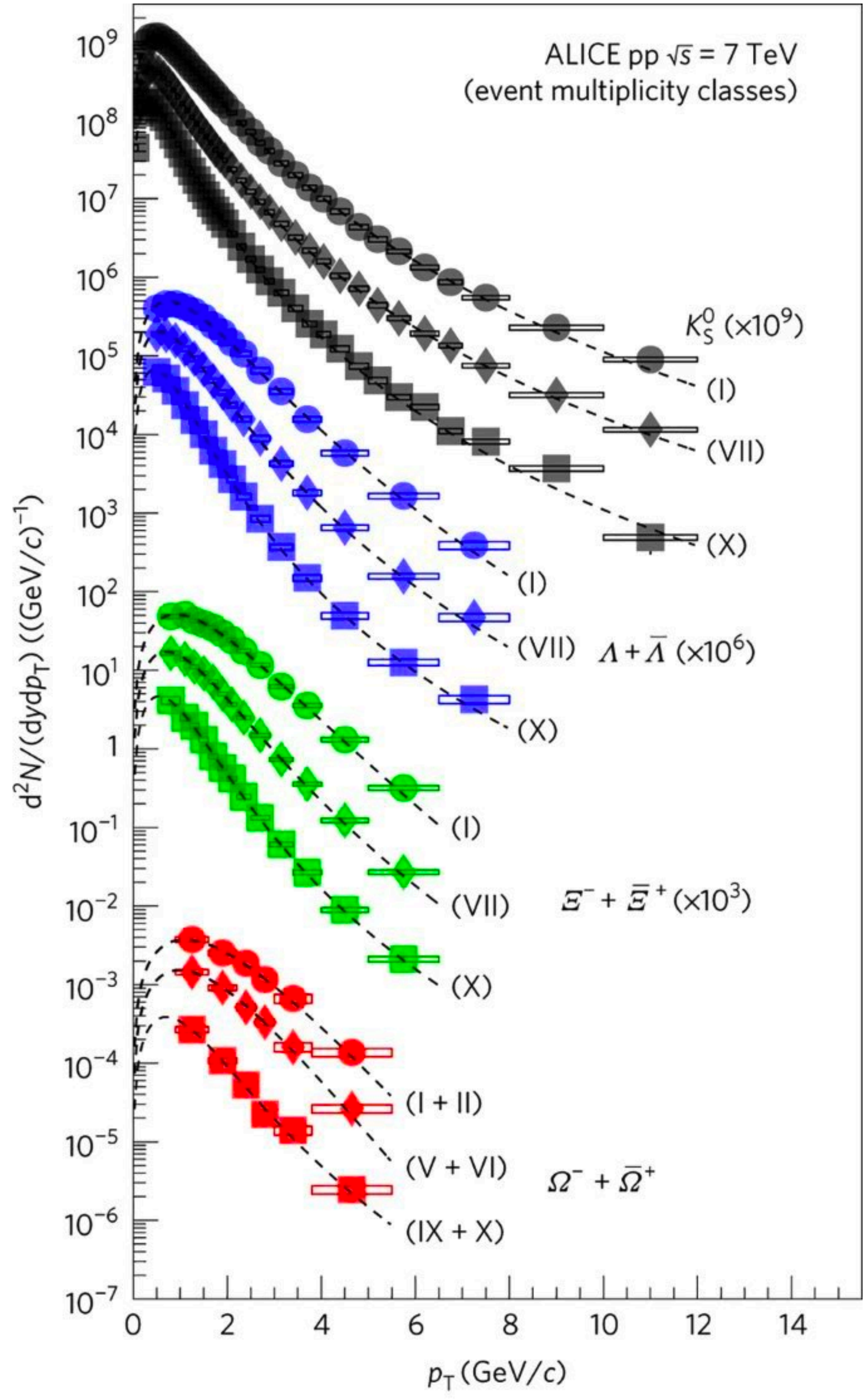

Strangeness enhancement in pp collisions in ALICE at $\sqrt{s} = 7$ TeV

Taking the ratio of the production of hyperons with respect to pions will give us idea about strangeness production mechanism in proton-proton collisions.

In the figure: The ratios of the yields of K_s^0, Λ, Ξ and Ω to the pion $(\pi^+ + \pi^-)$ yield as a function of pseudorapidity density are compared to p–Pb and Pb–Pb results at the LHC.

Observation: A significant enhancement of strange to non-strange hadron production is observed with increasing particle multiplicity in pp collisions similar to the observation in p–Pb collisions at a slightly lower centre-of-mass energy.

As no significant dependence on the centre-of-mass energy is observed at the LHC for inclusive inelastic collisions, the origin of strangeness production in hadronic collisions is apparently driven by the characteristics of the final state rather than by the collision system or energy

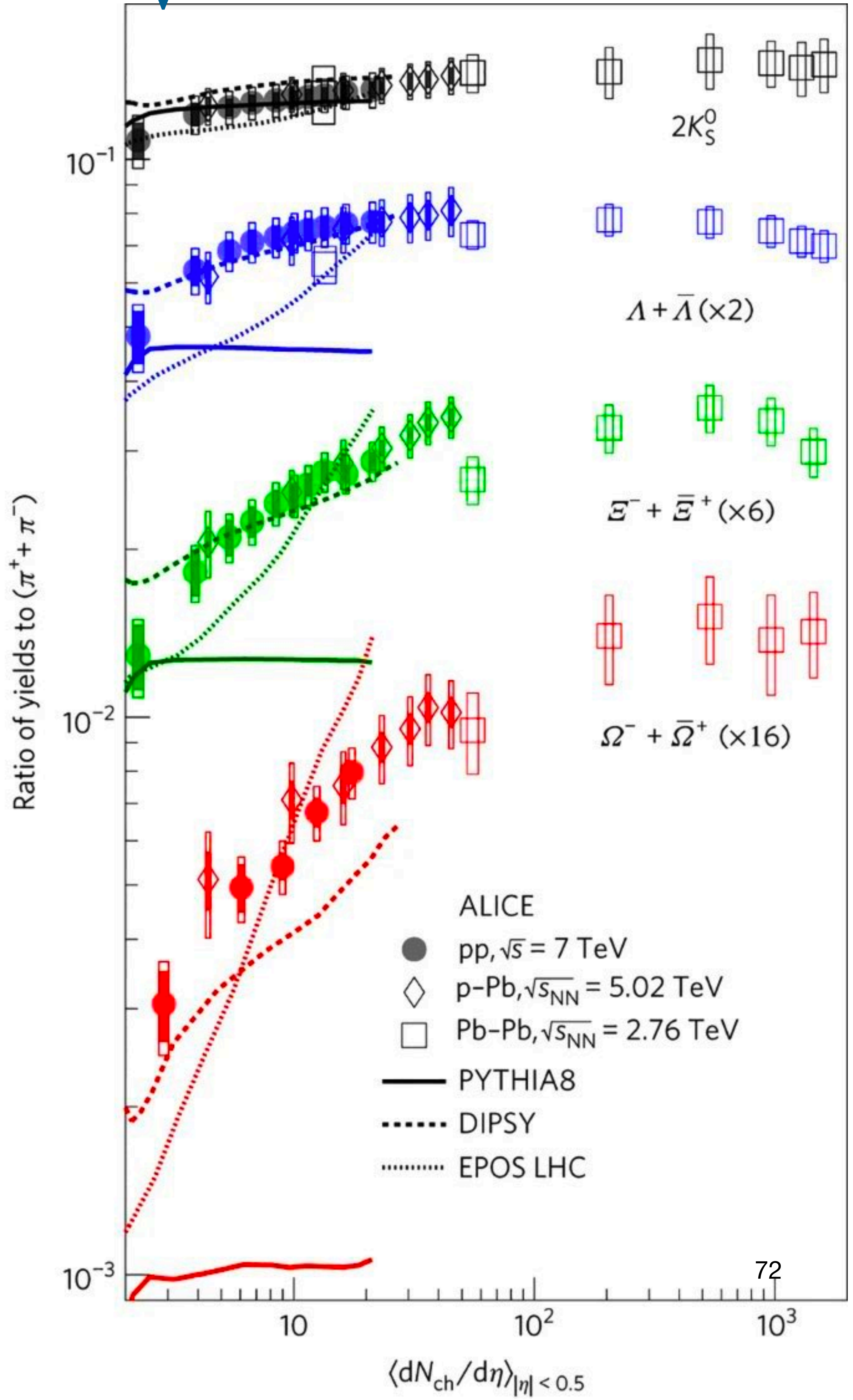

Strangeness enhancement in pp collisions in ALICE at $\sqrt{s} = 7$ TeV

In the figure: The ratios of the yields of Λ/K_s^0 and p/π.

Observation: The ratio do not change significantly with multiplicity, demonstrating that the observed enhanced production rates of strange hadrons with respect to pions is not due to the difference in the hadron masses.

Monte Carlo Model Comparisons: The results in are compared to calculations from MC models commonly used for pp collisions at the LHC: PYTHIA8, EPOS LHC and DIPSY.

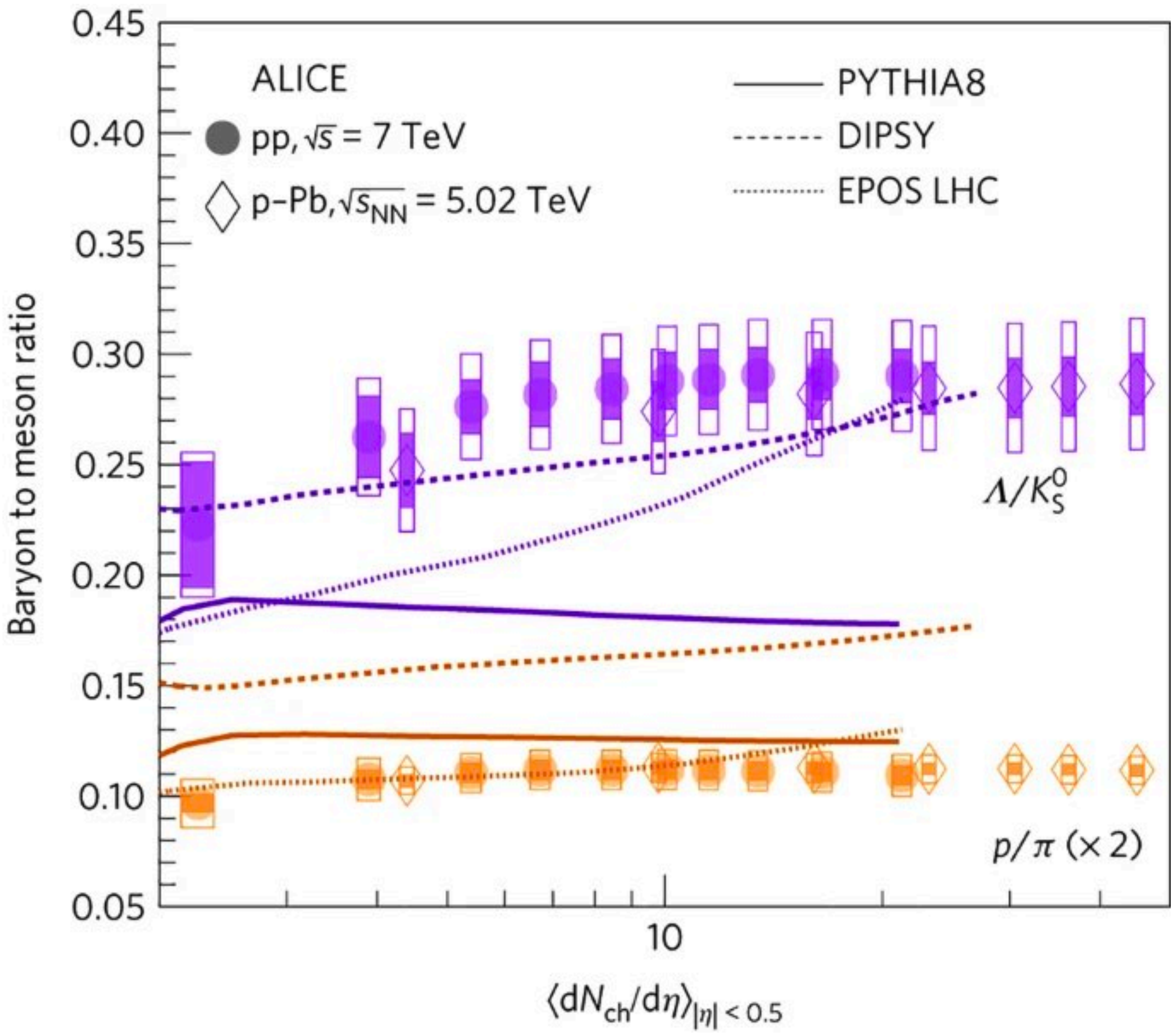

Results cannot be simultaneously reproduced by any of the MC models commonly used at the LHC. The closest one is DIPSY.

Strangeness enhancement in pp collisions in ALICE at $\sqrt{s} = 7$ TeV

In the figure: The yield ratios to pions divided by the values measured in the inclusive INEL > 0 pp sample, both for pp and p–Pb collisions

Observation: The observed multiplicity-dependent enhancement with respect to the INEL > 0 sample follows a hierarchy determined by the hadron strangeness.

Empirical Fit: The observed the observed strangeness hierarchy can be described reasonably well with the empirical formula of the following form:

$$\frac{(h/\pi)}{(h/\pi)^{pp}_{INEL>0}} = 1 + a\,S^b \log\left[\frac{\langle dN_{ch}/d\eta\rangle}{\langle dN_{ch}/d\eta\rangle^{pp}_{INEL>0}}\right] \quad (1)$$

S = Strange Quark content in the hadron

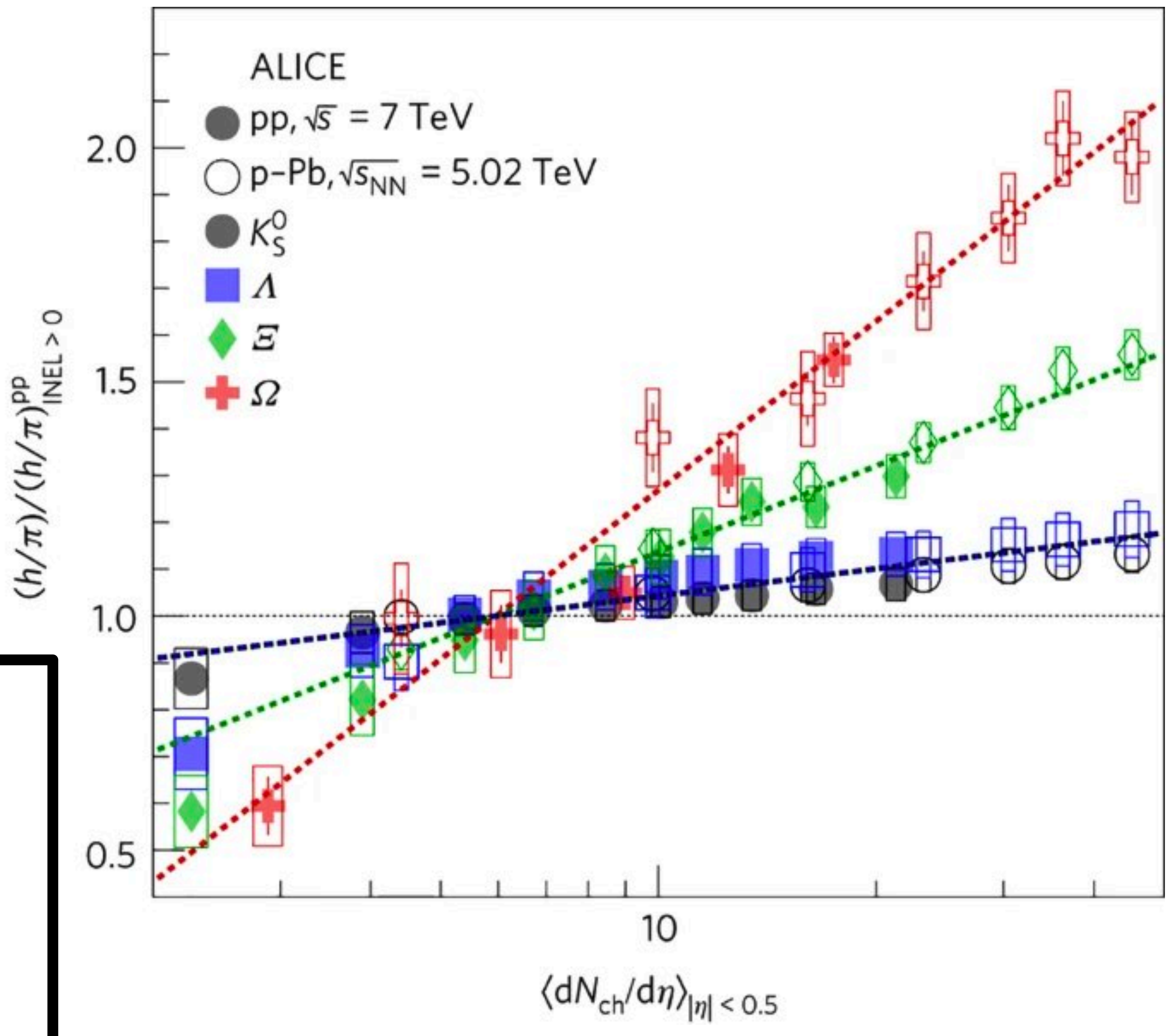

Summary

1. Strangeness enhancement is considered as a signal for the presence of QGP and was observed in relativistic heavy-ion collisions at RHIC and CERN.

2. Since pp collisions are considered as a benchmark for interpreting results heavy-ion collisions, the study of the possible presence of QGP in them is very crucial for interpreting results from the heavy-ion programs.

3. ALICE experiment at LHC can identify particles coming from pp collisions using its sophisticated detectors and analysis strategies.

4. Measurement of the yield of hyperons (Λ, K, Ω, Ξ) containing strange quarks produced in pp collisions were made with ALICE and compared with that of pions as a function of the multiplicity of the collision.

5. The yield ratios to pions were divided by the values measured in the inclusive $\text{INEL} > 0$ pp sample, both for pp and p–Pb collisions to study the evolution of the production of hyperons with multiplicity.

Conclusions

1. A significant enhancement of strange to non-strange hadron production is observed with increasing particle multiplicity in proton-proton collisions at ALICE.

2. The behaviour observed in proton-proton collisions resembles that of p–Pb collisions at a slightly lower centre-of-mass energy and that of Pb–Pb collisions high multiplicity.

3. The origin of enhanced strangeness production in hadronic collisions is apparently driven by the characteristics of the final state rather than by the collision system or energy and is not due to the difference in the hadron masses.

4. The commonly used Monte Carlo models like DIPSY, PYTHIA and EPOS cannot simultaneously reproduce the experimentally observed phenomenon

5. The observed multiplicity-dependent enhancement with respect to the INEL > 0 sample follows a hierarchy determined by the hadron strangeness.

Interpreting the result from heavy-ion collisions using the proton-proton collisions as a benchmark without a deconfined partonic medium formation requires a very careful revision.